الجمهورية الجزائرية الديمقراطية الشعبية

République Algérienne Démocratique et Populaire

وزارة التعليـــم العالـــــي و البحث العلمـــــي

Ministère de l'Enseignement Supérieur et de la Recherche Scientifique

المدرسة الوطنية المتعددة التقنيات

Ecole Nationale Polytechnique

Département de Génie Minier

Laboratoire Génie Minier

Doctoral Thesis in mining engineering

Application of Artificial Intelligence to the Prospecting of Pb-Zn Deposits in Algeria and Metallogenic Implications

Presented by: Selma REMIDI

Presented and defended publicly on (14/01/2026)

Composition of the jury :

President	Mr. Malek OULD HAMOU,	Professor (ENP)
Promoter	Mr. Abdelhak BOUTALEB,	Professor (USTHB)
Co-Promoter	Mr. Salaheddine TACHI	MCA (UBMA)
Examiner	Mr. Rezki AKKAL,	Professor (ENP)
Examiner	Mr. Lounis SAMI,	Professor UMMTO
Examiner	Mr. Saadia YSBAA,	MCA UMBB
Examiner	Mr. Sami YAHIAOUI	Professor (ENP)

ENP 2026

الجمهورية الجزائرية الديمقراطية الشعبية

République Algérienne Démocratique et Populaire

وزارة التعليـــم العالـــــي و البحث العلمـــــي

Ministère de l'Enseignement Supérieur et de la Recherche Scientifique

المدرسة الوطنية المتعددة التقنيات

Ecole Nationale Polytechnique

Département de Génie Minier

Presented by: Selma REMIDI

Doctoral Thesis in mining engineering

Application of Artificial Intelligence to the Prospecting of Pb-Zn Deposits in Algeria and Metallogenic Implications

Presented by: Selma REMIDI

Presented and defended publicly on (14/01/2026)

Composition of the jury :

President	Mr. Malek OULD HAMOU,	Professor (ENP)
Promoter	Mr. Abdelhak BOUTALEB,	Professor (USTHB)
Co-Promoter	Mr. Salaheddine TACHI	MCA (UBMA)
Examiner	Mr. Rezki AKKAL,	Professor (ENP)
Examiner	Mr. Lounis SAMI,	Professor UMMTO
Examiner	Mr. Saadia YSBAA,	MCA UMBB
Examiner	Mr. Sami YAHIAOUI	Professor (ENP)

ENP 2026

الجمهورية الجزائرية الديمقراطية الشعبية

République Algérienne Démocratique et Populaire

وزارة التعليـــم العالـــي و البحث العلمـــي

Ministère de l'Enseignement Supérieur et de la Recherche Scientifique

المدرسة الوطنية المتعددة التقنيات

Ecole Nationale Polytechnique

Département de Génie Minier

Presenté par: Selma REMIDI

Thèse de Doctorate en Génie Minier

Application de l'Intelligence Artificielle à la Prospection des gisements de Pb-Zn en Algerie et Implications Metallogeniques

Presenté by: Selma REMIDI

Présentée et soutenu pbliquement le (14/01/2026)

Composition des member de jury :

President	Mr. Malek OULD HAMOU,	Professor (ENP)
Promoteeur	Mr. Abdelhak BOUTALEB,	Professor (USTHB)
Co-Promoteur	Mr. Salaheddine TACHI	MCA (UBMA)
Examinateur	Mr. Rezki AKKAL,	Professor (ENP)
Examinateur	Mr. Lounis SAMI,	Professor UMMTO
Examinatrice	Mr. Saadia YSBAA,	MCA UMBB
Examinateur	Mr. Sami YAHIAOUI	Professor (ENP)

ENP 2026

ملخص

في السياق العالمي الحالي الذي يتميز بالطلب المتزايد على المعادن الأساسية، أصبح التنقيب عن المعادن الأولية استراتيجية عالية المخاطر و تتطلب استثمار هام للتنويع الاقتصادي في الجزائر. الهدف الرئيسي من هذه الدراسة هو الحد من عدم اليقين المتعلق بالاستكشاف من خلال تحديد ورسم خرائط للتعرف عن موقع تواجد معادن الرصاص والزنك (Pb–Zn) غير المكتشفة في شمال شرق الجزائر. يشكل هذا العمل أول تطبيق شامل لمختلف أساليب النمذجة التنبؤية لرسم خرائط احتمالية المعادن (MPM) في هذه المنطقة، بناءً على المعطيات الجيولوجية السابقة و المحددة لشروط تكوين المعادن مثل الحركة التكتونية بهدف تطوير وتوجيه آلاستثمارات المستقبلية.

ولتحقيق هذه الغاية، تم تطوير نموذج عمل متعدد المعايير لنظم المعلومات الجغرافية لمقارنة طريقين مختلفتين للنمذجة. تم استخدام الأساليب القائمة على المعرفة، بما في ذلك عملية التحليل الهرمي (AHP) والمنطق الضبابي (FUZZY LOGIC)، لترجمة الخبرة الجيولوجية والنماذج المعدنية (المصدر – الصرف – المكمن) إلى تنبؤات مكانية. وبالتوازي مع ذلك، تم تنفيذ مناهج تعتمد على البيانات باستخدام خوارزميات التعلم الآلي المتقدمة، مثل الغابة العشوائية (RF) وآلة تعزيز التدرج الضوئي (LightGBM) والشبكات العصبية التلافيفية (CNNs). تم تحسين هذه النماذج من خلال طريقة مجموعة التراص، مما يسمح بدمج العديد من المتعلمين من أجل التقاط العلاقات الجيولوجية المعقدة وغير الخطية بشكل أفضل.

وقد خضعت النماذج للتحقق الدقيق باستخدام مجموعة شاملة من مؤشرات الأداء الإحصائية. وأظهرت النتائج أن النماذج المبنية على الخبرة، وخاصة Fuzzy Logic، تظل موثوقة للتحقق الجيولوجي، بدقة تصل إلى 78.27%. ومع ذلك، أثبت نموذج مجموعة التكديس المبني على البيانات أنه الأكثر كفاءة، حيث وصل إلى دقة ملحوظة بلغت 97.67% ومساحة تحت المنحنى (AUC) بلغت 0.983. تحدد الخرائط النهائية لـ MPM بشكل فعال المناطق ذات الإمكانات العالية، لا سيما على طول حزام الصهارة الساحلي والممرات الهيكلية الرئيسية للمجال الخارجي. وبالتالي توفر هذه الدراسة أداة قوية لدعم القرار لاستكشاف التعدين، مما يحسن بشكل كبير تحديد الأهداف وإدارة الموارد في الجزائر.

الكلمات المفتاحية: رسم خرائط الإمكانات المعدنية (MPM)، الرصاص والزنك (Pb-Zn)، الذكاء الاصطناعي، متعدد المعادن، الجزائر، التعلم الآلي، التعلم العميق.

Résumé :

Dans le contexte mondial actuel marqué par une demande croissante en métaux de base, l'exploration minière est devenue une priorité stratégique à haut risque et à forte intensité capitalistique pour la diversification économique de l'Algérie. L'objectif principal de cette étude est de réduire l'incertitude liée à l'exploration en identifiant et cartographiant le potentiel non découvert en plomb-zinc (Pb–Zn) dans le Nord-Est algérien. Ce travail constitue la première application exhaustive de diverses approches de modélisation prédictive pour la cartographie de la prospectivité minérale (MPM) dans cette région, en s'appuyant sur son cadre tectono-sédimentaire et magmatique complexe afin d'orienter les futurs investissements miniers.

À cette fin, un cadre SIG multicritère rigoureux a été développé pour comparer deux philosophies de modélisation distinctes. Les approches basées sur la connaissance, notamment le Processus Hiérarchique Analytique (AHP) et la logique floue, ont été utilisées pour traduire l'expertise géologique et les modèles métallogéniques (Source–Drain–Piège) en prédictions spatiales. Parallèlement, des approches basées sur les données ont été mises en œuvre à l'aide d'algorithmes avancés d'apprentissage automatique, tels que Random Forest (RF), Light Gradient Boosting Machine (LightGBM) et les réseaux de neurones convolutifs (CNN). Ces modèles ont été optimisés par une méthode d'ensemble de type Stacking, permettant d'intégrer

plusieurs apprenants afin de mieux capturer les relations géologiques complexes et non linéaires.

Les modèles ont été soumis à une validation rigoureuse à l'aide d'un ensemble complet d'indicateurs statistiques de performance. Les résultats montrent que les modèles basés sur l'expertise, en particulier la logique floue, demeurent fiables pour la validation géologique, avec une précision de 78,27 %. Toutefois, le modèle d'ensemble Stacking basé sur les données s'est révélé être le plus performant, atteignant une précision remarquable de 97,67 % et une aire sous la courbe (AUC) de 0,983. Les cartes finales de MPM délimitent efficacement des zones à fort potentiel, notamment le long de la ceinture magmatique côtière et des couloirs structuraux majeurs du Domaine Externe. Cette étude fournit ainsi un outil robuste d'aide à la décision pour l'exploration minière, améliorant significativement la définition des cibles et la gestion des ressources en Algérie.

Mots-clés : CPM, Pb-Zn, Intelligence Artificielle, Polymétalliques, Potentielle minier, Algérie,

Abstract

In the current global context of increasing demand for base metals, mineral exploration has become a high-risk and capital-intensive strategic priority for Algeria's economic diversification. The primary objective of this study is to reduce exploration uncertainty by identifying and mapping undiscovered Lead–Zinc (Pb–Zn) mineral potential in Northeast Algeria. This research represents the first comprehensive application of multiple predictive modeling approaches for Mineral Prospectivity Mapping (MPM) in the region, capitalizing on its complex tectono-sedimentary and magmatic framework to support informed mining investment decisions.

To achieve this objective, a robust multi-criteria GIS-based framework was developed to compare two distinct modeling paradigms. Knowledge-driven approaches, including the Analytic Hierarchy Process (AHP) and Fuzzy Logic, were employed to translate expert geological knowledge and metallogenic concepts (Source–Drain–Trap) into spatial predictions. In parallel, data-driven models were implemented using advanced machine learning algorithms, namely Random Forest (RF), Light Gradient Boosting Machine (LightGBM), and Convolutional Neural Networks (CNN). These models were further enhanced through a Stacking ensemble strategy, integrating multiple learners to better capture complex and non-linear geological relationships.

All models were rigorously validated using a comprehensive set of statistical performance metrics. The results indicate that expert-based models, particularly Fuzzy Logic, remain reliable for geological interpretation, achieving an accuracy of 78.27%. However, the data-driven

Stacking ensemble model outperformed all other approaches, attaining an exceptional accuracy of 97.67% and an Area Under the Curve (AUC) of 0.983. The final MPM outputs successfully delineate high-prospectivity zones, notably along the coastal magmatic belt and major structural corridors of the External Domain. This study provides a robust decision-support framework for mineral exploration, significantly improving target prioritization and resource management strategies in Algeria.

Keywords: MPM, Pb-Zn, Artificial Intelligence, Polymetallic, Mineral Prospectivity, Algeria, Machine Learning, Deep Learning.

Acknowledgement

First and foremost, I would like to express my sincere gratitude to my supervisor, Professor Abdelhak Boutaleb, and my co-supervisor, Dr. Salaheddine Tachi, for their continuous support, guidance, and encouragement throughout this research. Their expertise and patience played a vital role in the realization of this work.

I also wish to extend my heartfelt thanks to the members of the defense jury:

- Professor Malek Ould Hamou (ENP), President of the jury
- Professor Rezki Akkal (ENP)
- Professor Sami Yahiaoui (ENP)
- Professor Lounis Sami (UMMT)
- Dr. Saadia Ysbaa (MCA, UMBB)

Their careful reading, constructive comments, and valuable insights have greatly enriched this thesis.

I am also deeply grateful to Dr. Abderraouf Seffari (CRAAG) for his generous support and guidance, and to Mr. Hasnaoui Yacine for his precious help and involvement during the critical phases of my research.

To all my colleagues, professors, and the staff at ENP and beyond ; thank you for creating such a motivating and collaborative environment.

Finally, my warmest thanks go to my family and friends for their unwavering support, patience, and belief in me throughout this long journey.

Dédicace

À ma chère famille,

À ma mère, dont l'amour, les prières et les sacrifices ont été le socle de tout ce que j'ai pu accomplir.
À mon père, pour son soutien et sa présence indéfectible tout au long de mon parcours académique.
À mes sœurs — Asma, Houda et Amine — pour leur appui constant et leurs encouragements précieux.

Votre présence, votre confiance et votre affection m'ont portée tout au long de ce chemin.

Je dédie également ce travail à la mémoire de mon petit ange Amira, qui repose au paradis.

Ce travail est autant le vôtre que le mien.

Avec tout mon amour,
Selma

إذا غامرتَ في شرفٍ مرومِ فلا تقنعْ بما دونَ النجوم

فطَعنٌ في عُلى مجدٍ وسَيرٌ إلى نَيلِ العُلى بغيرِ لومِ

Table of Contents

List of tables

List of figures

Abbreviations list

AHP: Analytic Hierarchy Process

AI: Artificial Intelligence

AUC: Area Under the Curve

CNN: Convolutional Neural Network

CR: Consistency Ratio

DL: Deep Learning

FNN: Feed-forward Neural Network

FN: False Negative

FP: False Positive

FR: Frequency Ratio

FPR: False Positive Rate

GIS: Geographic Information System

LGBM: Light Gradient Boosting Machine

ML: Machine Learning

MPM: Mineral Prospectivity Mapping

MVT: Mississippi Valley-Type

OMK: Kabylian Oligo-Miocene

Pb Zn: Lead Zinc

RF: Random Forest

ROC: Receiver Operating Characteristic

TN: True Negative

TNR: True Negative Rate (equivalent to Specificity)

TP: True Positive

TPR: True Positive Rate (equivalent to Recall or Sensitivity)

VMS: Volcanogenic Massive Sulfide

General Introduction

General Introduction:

This PhD thesis investigates the application of both classical and data-driven approaches for mineral potential prediction for lead-zinc deposits in northeast Algeria. It outlines a comprehensive approach from data collection and preparation to model development, evaluation, and interpretation.

Recent technological advances have transformed mineral exploration by improving analytical precision and enabling the prediction of mineral potential in unexplored areas. In response to resource depletion and the high cost of traditional exploration, mineral prospectivity mapping (MPM) has emerged as an effective multi-criteria, GIS-based approach. MPM integrates geological information as spatial layers to model and delineate prospective zones through quantitative spatial analysis

Recent technological advances have transformed mineral exploration by improving analytical precision and enabling the prediction of mineral potential in unexplored areas. In response to resource depletion and the high cost of traditional exploration, mineral prospectivity mapping (MPM) has emerged as an effective multi-criteria, GIS-based approach. MPM integrates geological information as spatial layers to model and delineate prospective zones through quantitative spatial analysis.

The geological framework of northern Algeria, particularly its northeastern sector, is characterized by a complex tectono-sedimentary, magmatic, and metamorphic evolution spanning from the Precambrian to the Quaternary. This region has been the subject of extensive scientific inquiry aimed at deciphering the kinematics and geodynamic development of the Maghrebides mountain chain. Numerous studies (Michard et al. 2006; Romagny et al. 2020; Leprêtre et al. 2018; Peucat, Mahdjoub, Drareni 1996; Mahdjoub, Choukroune, Kienast 1997; Seffari et al. 2023; Afalfiz 1990; Boutaleb et al. 2000; Benali 2007; Kolli 1997a) have significantly contributed to unraveling the intricate geological development of the region and understanding the processes governing mineral occurrences. These investigations have highlighted the pervasive distribution of various mineralizations, including Pb, Zn, and Cu, predominantly within eastern northern Algeria. The spatial distribution and genesis of these mineralizations are intimately linked to episodes of tectonic activity, magmatic processes, and sustained hydrothermal fluid circulation.

Algeria, like many regions globally, has experienced significant exploitation of its heavy metal reserves Pb, Zn, Cu, Ag, and Fe, over the past decade. Situated within the Alpine chain, Algeria's northern regions are shaped by geodynamic interactions between the Eurasian and African superblocks. The northern domain, encompassing the Tellian Atlas, the High Plateaus,

and the Hodna chain, is rich in mineralization. These deposits are often trapped within rocks and fractures caused by syn-sedimentary faults, which control paleogeography and play a crucial role in the spatial distribution of mineralization(Haddouche et al. 2016; Ysbaa, Nedjai, et al. 2019; Ysbaa, Haddouche, et al. 2019; Ysbaa et al. 2020).. Hydrothermal fluids, often precipitated from magmatic sources and facilitated by compressional tectonic movements, are recognized as key drivers of these mineralizing processes.

Available lithological and structural maps, metallogenic data, and geological reports were carefully processed, classified, and digitized to ensure effective integration into both knowledge-driven and machine-learning-based models. The resulting mineral prospectivity maps provide a robust delineation of areas with high Pb–Zn potential, offering valuable guidance for future targeted exploration. By combining established geological knowledge with advanced spatial analysis and predictive modeling, this study enhances mineral prospectivity mapping in northeastern Algeria and contributes to a more efficient and sustainable approach to base-metal resource exploration

This thesis represents a pioneering contribution to mineral prospectivity mapping in northeastern Algeria, demonstrating that data-driven machine learning and ensemble models significantly outperform classical GIS-based, knowledge-driven approaches by effectively capturing complex, non-linear relationships controlling Pb–Zn mineralization. Its originality lies in providing one of the first large-scale, performance-based integrations and comparisons of advanced ML techniques with classical MPM methods using a comprehensive and well-constrained regional dataset.

To achieve these objectives, this thesis is structured into 5 main chapters after this introduction:

- **Chapter 1 – Literature Review:**Overview of MPM methods, from traditional approaches to knowledge-driven (AHP, Fuzzy Logic) and data-driven machine learning techniques.
- **Chapter 2 – Geological Setting:**Description of the geological framework of northeastern Algeria and data preparation related to Pb–Zn mineralization.
- **Chapter 3 – Structural Analysis:**Spatial analysis of faults and lineaments using Fry analysis and rose diagrams to assess structural controls on mineralization.
- **Chapter 4 – Data and Methods:** Integration of geoscience data in GIS and implementation of knowledge-driven and machine learning models for MPM.
- **Chapter 5 – Results:** Presentation and validation of mineral prospectivity maps using statistical and spatial performance metrics.
- **Conclusion:** Comparison of methods and discussion of implications for future mineral exploration.

Chapter 1: Literature Review

1. Introduction:

MPM is a critical process in mineral exploration that involves quantifying and mapping the likelihood of mineral deposits at specific locations. This field has evolved significantly with advancements in data analysis techniques, transitioning from traditional knowledge-driven approaches to more sophisticated data-driven methods. The integration of geological, geophysical, geochemical, and remote sensing data has become essential for creating accurate prospectivity maps.

MPM can be broadly categorized into two main approaches: knowledge-driven and data-driven methods. Knowledge-driven approaches rely on expert knowledge of mineral systems and geological processes to identify potential areas for mineralization. In contrast, data-driven methods leverage statistical and machine learning algorithms to analyze large datasets and identify patterns indicative of mineral deposits. Recent advancements in machine learning and deep learning have further enhanced the capabilities of MPM. Techniques such as random forests, support vector machines, and convolutional neural networks have been applied to improve predictive accuracy and handle complex, high-dimensional datasets. Additionally, ensemble methods and hybrid models have emerged as powerful tools for integrating diverse algorithms and datasets, offering more robust and reliable predictions.

The state-of-the-art in MPM also includes innovative applications of transfer learning, self-supervised learning, and reinforcement learning, which address challenges like sparse labeled data and complex decision-making processes in exploration strategies. Furthermore, the integration of three-dimensional (3D) modeling techniques has improved the ability to identify deep-seated ore bodies, providing a more comprehensive understanding of subsurface structures.

This chapter aims to provide a comprehensive overview of the current state of MPM, highlighting recent advancements, challenges, and future directions in this rapidly evolving field.

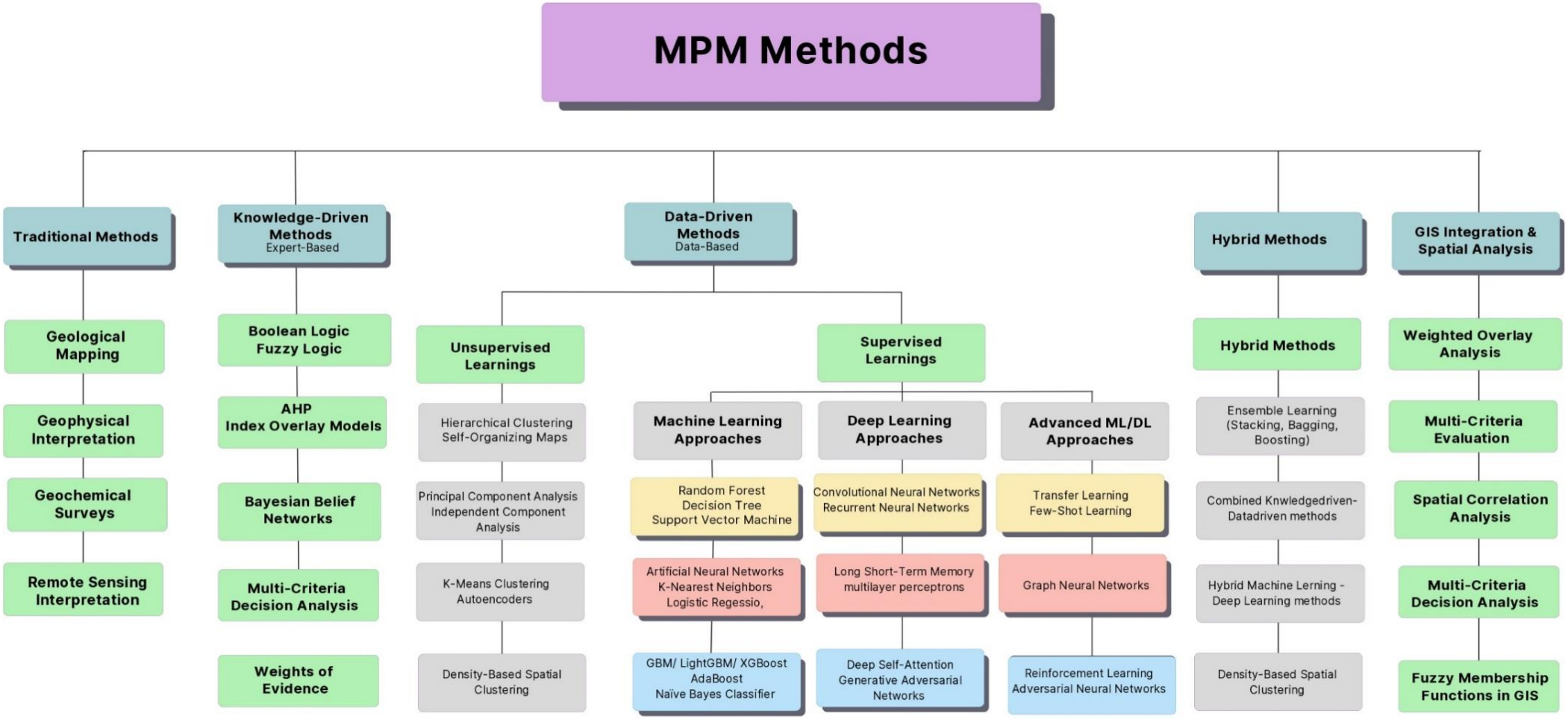

Figure 1: state of art of all MPM methods

2. Traditional approaches :

Traditional MPM methods have evolved from basic statistical correlation techniques to more sophisticated spatial analysis frameworks. Early studies relied on simple bivariate correlation methods (e.g., logistic regression) to determine mineralization potential. Over time, multivariate techniques, such as principal component analysis (PCA) and discriminant analysis, improved prediction accuracy (Bonham-Carter 1994; Carranza 2008)

Traditional MPM methods rely on statistical models to analyze geological, geochemical, and geophysical data for mineral (Agterberg, Bonham-Carter, Wright 1990; Geoffroy, Wignall 2012; Zhao 1992). Techniques such as singularity theory and geochemical anomaly mapping have been widely used to predict ore deposits (Cheng 1999, p. 1; 2007; Cheng, Zhao 2011; Chen, Cheng 2016). For instance, geochemical data has been analyzed using advanced statistical methods to identify meaningful signatures for mineral prediction (X. Wang et al., 2007; G. Wang et al., 2011; Hao et al. 2014; Tian et al. 2018; Grunsky & Caritat 2019; Tian et al. 2023; J. Wang & Zuo 2019). These approaches identify geochemical signatures linked to mineralization, forming the basis for exploration targeting. However, their ability to capture complex, nonlinear geological patterns is limited. To address this, probabilistic frameworks like weights of evidence (Behera, Panigrahi 2022; Fu et al. 2021; Nwazelibe, Unigwe, Egbueri 2023) have been employed to quantify spatial relationships between geological features and mineral occurrences Structural analysis further aids in delineating favorable zones by assessing fault structures and tectonic controls Analysis (Holyland, Ojala 1997; Smith, Gardoll 1997; Liu, Sousa Jr., Gopinath 2000) .

The limitations of traditional MPM methods are particularly pronounced when dealing with high-dimensional datasets and complex geological settings. In Pb-Zn exploration, these limitations can lead to missed opportunities or inefficient exploration strategies. For instance, traditional methods may fail to fully account for the interplay between multiple geological factors that influence mineralization, such as fault structures, geochemical signatures, and tectonic controls. This can result in prospectivity maps that do not accurately reflect the potential for Pb-Zn deposits in areas with complex geological histories. As a result, there is a growing need for more advanced, data-driven approaches that can better handle these complexities and improve predictive accuracy.

3. Knowledge driven methods :

The researches of (Shabani et al. 2022; 2022; Rahimi et al. 2024; Zhang, Zhou 2015) Integrate expert knowledge with fuzzy logic to combine multiple evidential maps and assess mineral prospectivity. Expert-Knowledge Driven (EKD) methods in mineral prospectivity mapping rely on expert judgment to integrate various geological, geochemical, and geophysical datasets (Ali Hosseini, Abedi 2015; Ma et al. 2020; Senanayake et al. 2023).

These methods are particularly useful in less-explored regions where data-driven approaches are less feasible. Hybrid approaches, such as combining the Analytic Hierarchy Process (AHP) with fuzzy logic, leverage both expert knowledge and the ability to handle imprecise data (Najafi, Karimpour, Ghaderi 2014; Rahimi et al. 2020; 2024; Ziaii, Pouyan, Ziaei 2009). Another hybrid method integrates Best Worst Method (BWM) with Technique for Order Preference by Similarity to Ideal Solution (TOPSIS) to evaluate and prioritize exploration targets based on multiple criteria (Forson et al. 2024). Case-Based Reasoning (CBR) involves combining spatial and attribute features to represent mineralization cases, identifying similar cases to predict mineral prospectivity based on historical data (He 2012). The Mineral Systems Approach identifies key geological processes involved in mineral formation and translates these concepts into mappable proxies for exploration targeting (Sri Suryani, Sibaroni, Heriawan 2016; Sadeghi et al. 2019). Additionally, techniques like evidential belief functions (Mohammadpour, Bahroudi, Abedi 2021; Maleki et al. 2022)and weights of evidence (Behera, Panigrahi 2022; Fu et al. 2021; Nwazelibe, Unigwe, Egbueri 2023) are used to integrate uncertain data and quantify spatial relationships between geological features and mineral occurrences functions. The AHP is also utilized to structure decision-making and evaluate the relative importance of different factors through pairwise comparisons, aiding in the prioritization of exploration targets (Feizi, Karbalaei-Ramezanali, Tusi 2017; Nouri et al. 2013).

Expert-Knowledge Driven (EKD) methods have contributed significantly to MPM by leveraging expert judgment to integrate diverse datasets. However, these methods are inherently subjective and may struggle to capture complex geological relationships. This subjectivity and limited adaptability to new data underscore the need for more objective and dynamic approaches. Consequently, data-driven methods, such as machine learning, offer a promising complement to EKD techniques, potentially enhancing the accuracy and efficiency of mineral exploration by handling large datasets and identifying nuanced patterns.

4. Data-Driven Methods

Data-driven methods have transformed MPM by leveraging statistical models and machine learning (ML) algorithms to analyze large, complex datasets and identify prospective areas.

4.1. Machine learning methods :

Machine learning (ML) has significantly enhanced MPM by leveraging advanced algorithms to analyze complex datasets and identify prospective areas.

Logistic regression, one of the earliest statistical approaches in this field, has been widely applied since the 1980s for predicting mineral occurrences (Chung, Agterberg 1980; Carranza, Hale 2001a; Harris, Pan 1999; Chen et al. 2011; Xiao et al. 2022; Wang et al. 2024) . Over time, advancements in computational power have enabled the adoption of more sophisticated ML techniques. Among these, artificial neural networks (ANNs) have gained prominence for their ability to model nonlinear relationships and process high-dimensional data (Brown et al.

2000; Harris, Pan 1999; Köhler et al. 2021; Porwal, E J M Carranza, Hale 2003; Rigol-Sanchez, Chica-Olmo, Abarca-Hernandez 2003). Similarly, support vector machines (SVM) have been effectively used for classification tasks in mineral exploration due to their robustness in handling complex datasets (Abedi, Norouzi, Bahroudi 2012; Cardoso-Fernandes et al. 2020; Yongliang, Wu 2017; Zuo, Carranza 2010).

Recent developments have introduced ensemble methods such as random forests , which excel at reducing overfitting and improving predictive accuracy by combining multiple decision trees (Carranza, Laborte 2015a; Xiang et al. 2020; Li et al. 2021; Behnia et al. 2023). Isolation Forests have also been employed to detect anomalies in geochemical datasets, aiding in the identification of potential mineralization zones (Chen, Wu 2018; Shuai Zhang et al. 2022; Saremi et al. 2024). Furthermore, gradient boosting algorithms like XGBoost have emerged as powerful tools for MPM due to their efficiency and ability to handle imbalanced datasets (Elbegue, Allek, Zeghouane 2022; Lin et al. 2023; Lu et al. 2023; Bigdeli, Maghsoudi, Ghezelbash 2024). Additionally, techniques such as gradient boosting machine (GBM), AdaBoost and LightGBM have been utilized for their speed and performance in handling large datasets (Fan et al. 2022; Tongfei Li et al. 2024; Zhao et al. 2022). These machine learning methods are particularly effective at capturing complex relationships within geological data, offering a robust framework for mineral exploration.

ML models can uncover subtle patterns and anomalies indicative of mineral deposits. However, despite their advantages, these methods often require large amounts of high-quality training data and careful feature engineering to ensure reliable predictions.

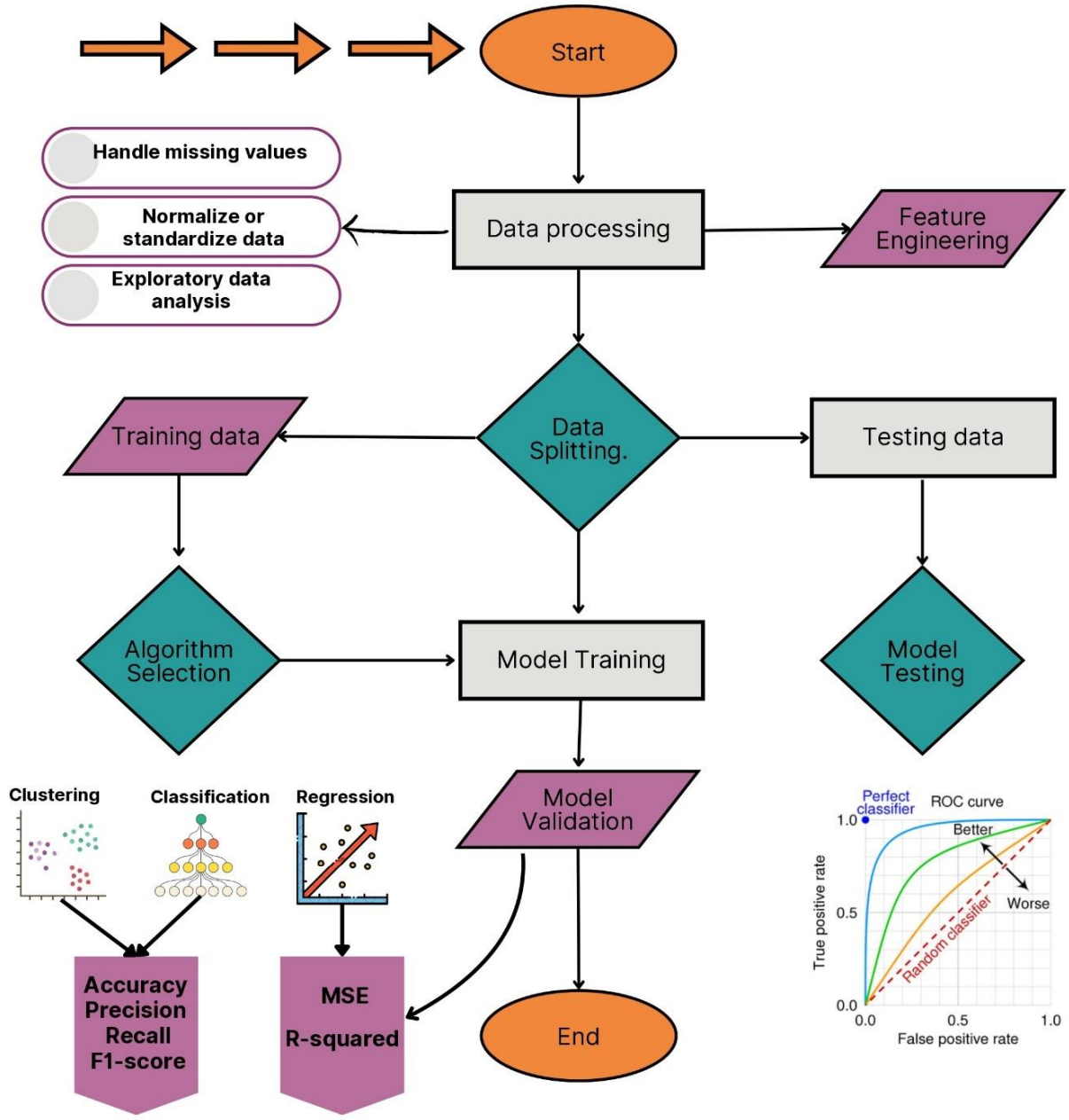

Figure 2: Machine Learning Supervised Algorithm

4.2. Unsupervised methods:

Unsupervised learning methods are particularly useful in mineral prospectivity mapping when dealing with unlabeled data, which is common in underexplored or poorly documented regions. These methods are employed to uncover hidden patterns, relationships, or anomalies in large

geospatial datasets without relying on predefined labels or training samples. For example, clustering techniques like self-organizing maps (SOM) are effective for grouping geospatial data into clusters with similar characteristics, such as geochemical or geophysical signatures, which can indicate prospective areas for mineralization (Bigdeli, Maghsoudi, Ghezelbash 2022; Chen et al. 2023; Engle et al. 2022). Similarly, dimensionality reduction methods like autoencoders are used to compress high-dimensional data into latent representations, enabling the identification of subtle patterns or anomalies that may not be evident in raw datasets (Chen et al. 2019; Xie et al. 2023; Yang et al. 2022).

Anomaly detection methods, such as one-class support vector machines (OC-SVM), are particularly valuable for identifying outliers in geochemical and geophysical data, which often act as proxies for mineral deposits. These methods excel in scenarios where positive samples (e.g., known mineral occurrences) are scarce and the majority of the dataset consists of unlabeled or background samples (Chen, Wu 2017; Yongliang, Wu 2017). Additionally, unsupervised learning is instrumental in automating the traditionally labor-intensive process of manual data filtering and feature selection. For instance, SOMs have been successfully applied to gridded geophysical datasets to delineate exploration targets without relying on preprocessed geological maps or expert-driven spatial proxies, as demonstrated in studies targeting rare earth element (REE) deposits in India (Aranha, Porwal 2022).

These methods are particularly advantageous in unexplored terrains where geological knowledge is limited or absent. By leveraging the inherent structure of the data itself, unsupervised learning provides a robust and time-efficient alternative to traditional knowledge-driven approaches. Furthermore, integrating unsupervised techniques with supervised models can enhance predictive performance by using the clusters or anomalies identified as inputs for further classification tasks. This makes unsupervised learning a critical component of modern MPM workflows, especially in regions with abundant unlabeled data but minimal historical exploration records.

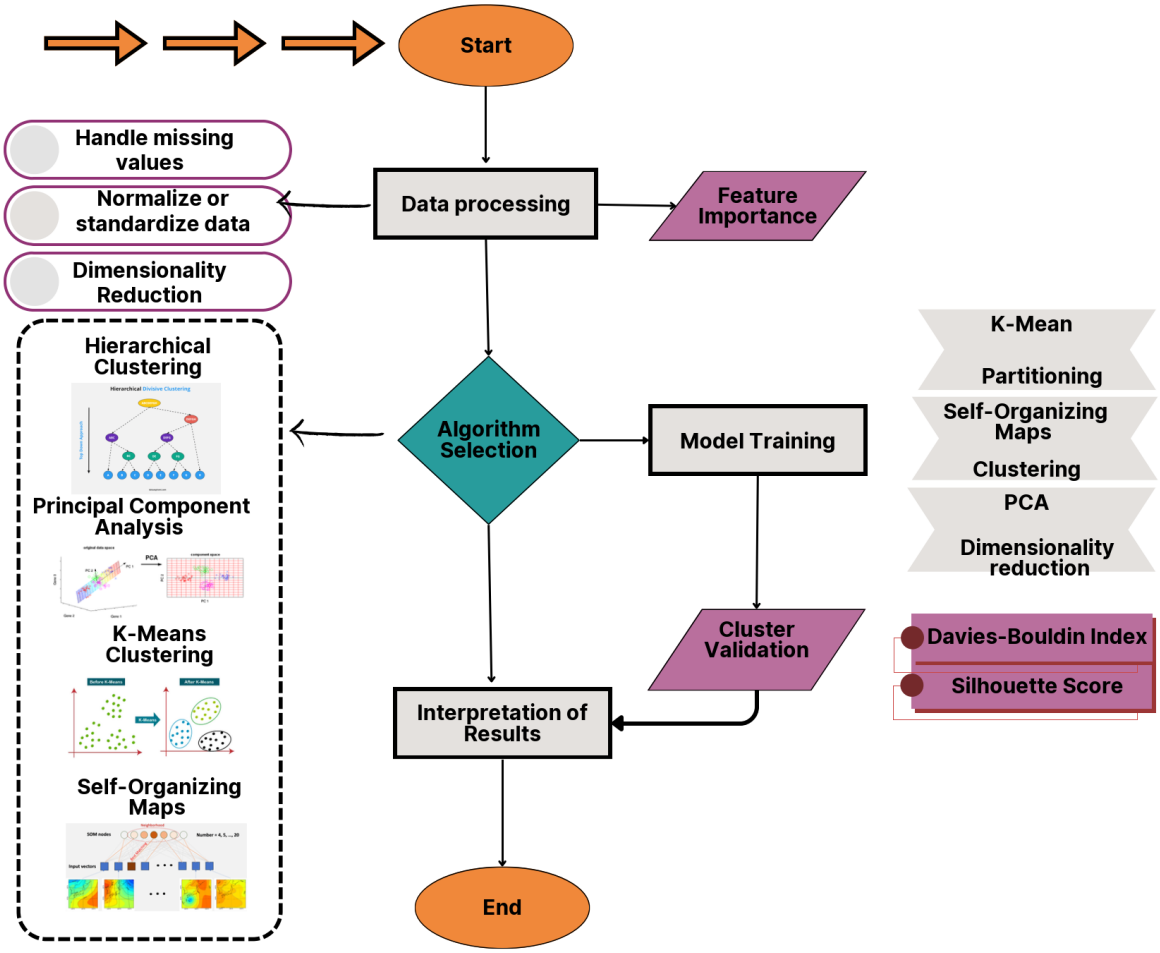

Figure 3: Machine Learning Unsupervised Algorithms

4.3. Deep Learning based approaches

The advent of deep learning has further revolutionized mineral prospectivity mapping, particularly in the analysis of complex, high-dimensional datasets. Convolutional Neural Networks (CNNs) have shown exceptional promise in processing image-based data, such as remote sensing and geophysical imagery, enabling the identification of subtle spatial features associated with mineralization (Shin et al. 2016; McMillan et al. 2021; Cheng Li et al. 2024; Yang, Zuo 2024). These networks are particularly effective for tasks like detecting alteration zones or structural features in satellite imagery, which are critical for mineral exploration. Multilayer Perceptrons (MLPs), on the other hand, have been employed for their ability to model complex relationships in high-dimensional datasets, making them suitable for integrating diverse geochemical, geological, and geophysical data **)** (Deng et al. 2021; Otele et al. 2021; Skabar 2007; Zhong, Deng, Yu 2021).

Generative Adversarial Networks (GANs) have emerged as a powerful tool for data augmentation and synthetic data generation, addressing the challenge of limited labeled datasets

in MPM. By generating synthetic samples that mimic real-world data distributions, GANs enhance training datasets and improve model robustness datasets (Farahbakhsh, Maughan, R. Dietmar Müller 2023a; Jordão et al. 2022; Lin, Zuo 2024; Wu et al. 2023; Zhang, Zuo 2021). Autoencoders have been widely applied for feature extraction and anomaly detection, compressing high-dimensional data into latent representations to identify subtle patterns indicative of mineralization **Autoencoders** (Chen et al. 2019; Zhang et al. 2021; Yang et al. 2022; Zuo et al. 2022; Xie et al. 2023; Mirzabozorg, Abedi, Yousefi 2024). These methods are particularly useful for detecting geochemical anomalies or rare mineralization signatures.

Recurrent Neural Networks (RNNs) and their variant Long Short-Term Memory (LSTM) networks have been applied to time-series analysis of geophysical data, such as seismic or magnetotelluric surveys. These models excel at capturing temporal dependencies and integrating sequential information to identify patterns linked to mineral (Appiah-Twum, Xu, Sunkari 2024; Singh, Ray, Sarkar 2018; Wang, Li, Zuo 2024; 2024; Wang, Zuo 2022). Additionally, deep self-attention mechanisms have been utilized to capture internal relationships between various evidence layers while accounting for spatial heterogeneity in geological data (Yin, Zuo, Sun 2023). This approach enhances the interpretability of models by identifying key features driving prospectivity predictions.

Despite their transformative potential, deep learning methods face challenges related to computational cost, the need for large labeled datasets, and extensive hyperparameter tuning. However, their ability to process diverse data types and capture complex nonlinear relationships makes them indispensable for modern MPM workflows. Future research could focus on integrating deep learning with traditional or machine learning methods to create hybrid frameworks that balance interpretability with predictive accuracy.

4.4. Transfer Learning & Few-Shot Learning

Transfer learning has emerged as a powerful technique in MPM, enabling the adaptation of pre-trained models to refine predictions in regions with limited labeled geological data. This approach leverages knowledge gained from well-documented areas (e.g., brownfields) and applies it to underexplored or poorly documented regions (e.g., greenfields) data (Li et al. 2020; Li, Liu, Chen 2023; Shin et al. 2016). For instance, transfer learning can utilize pre-trained models developed for remote sensing tasks, such as satellite imagery analysis, and fine-tune them to predict mineralization potential in new geological settings. By incorporating geological constraints and domain-specific knowledge, transfer learning not only improves predictive accuracy but also reduces uncertainties in MPM (Lauzon, Gloaguen 2024). This method is particularly effective when data is sparse or when the target region differs significantly from the source domain.

Few-shot learning addresses the challenge of sparse labeled datasets by leveraging meta-learning techniques that enable models to make accurate predictions with minimal training samples (Kong et al. 2025; Li, Sun, Qiao 2025; Zhou et al. 2023)**.** This approach is particularly valuable in mineral exploration, where acquiring labeled data is often expensive and time-consuming. Few-shot learning algorithms focus on learning generalized representations that can adapt quickly to new tasks with very few examples, making them highly suitable for greenfield exploration scenarios.

4.5. Self-Supervised and Semi-Supervised Learning

Self-supervised learning has gained traction in MPM as it enables models to extract meaningful representations from vast unlabeled geological datasets. By designing pretext tasks (e.g., predicting missing parts of geophysical maps or reconstructing geochemical patterns), self-supervised methods reduce reliance on labeled data while capturing complex spatial and geochemical relationships (Kumari et al. 2023; Miao et al. 2024). These representations can then be fine-tuned for downstream tasks such as mineral prospectivity prediction, enhancing model performance in data-scarce environments.

Semi-supervised learning bridges the gap between supervised and unsupervised approaches by leveraging a small set of labeled geological samples alongside a large corpus of unlabeled data tasks (Li, Sun, Qiao 2025; Li, Chen, Wang 2024; Tao et al. 2022; Wang, Zuo, Xiong 2020). This technique uses the labeled data to guide the learning process while extracting additional information from the unlabeled dataset, improving both predictive accuracy and generalization. For example, semi-supervised methods have been successfully applied to integrate sparse geochemical data with extensive remote sensing imagery, enabling more reliable prospectivity mapping in underexplored regions.

4.6. Reinforcement Learning & Adversarial Learning

Reinforcement learning optimizes geological exploration strategies by refining decision-making through reward-based learning (Kumar, Dimitrakopoulos 2022; Shi, Zuo, Zhou 2023). In this context, exploration strategies are treated as sequential decision-making problems, where the algorithm learns to maximize rewards by identifying high-potential areas for further investigation. This approach is particularly useful for designing efficient exploration campaigns by balancing risk and reward.

Adversarial learning enhances model robustness against noise and uncertainty in geospatial data. Techniques such as adversarial neural networks improve prediction reliability by

generating synthetic adversarial examples during training to test the model's resilience (Lin, Zuo 2024; Saranathan, Parente 2021). These methods are especially valuable in mineral exploration, where datasets often contain significant noise due to measurement errors or incomplete sampling.

4.7. Ensemble Methods

Ensemble methods have become a cornerstone in mineral prospectivity mapping due to their ability to improve predictive accuracy and model robustness by combining multiple algorithms. These methods can be categorized into bagging, boosting, and stacking, each with distinct mechanisms and applications. Bagging involves training models independently on bootstrapped subsets of the data and then aggregating their predictions, as seen in Random Forest, which is widely used for handling high-dimensional datasets and reducing overfitting (Hajihosseinlou, Maghsoudi, Ghezelbash 2023; Yin, Li 2022). Boosting, on the other hand, sequentially trains models to correct the errors of their predecessors, with algorithms like XGBoost being particularly effective in improving prediction accuracy by combining weak learners into a strong ensemble (Farhadi et al. 2024; Giri et al. 2024). Stacking combines predictions from multiple base models using a meta-model, allowing for the fusion of heterogeneous classifiers with complementary strengths (Hajihosseinlou, Maghsoudi, Ghezelbash 2024; Yousefi et al. 2024). This approach has been used to integrate RF, SVM, and MaxEnt for MPM, resulting in more accurate predictions compared to individual models. By leveraging these ensemble techniques, researchers can enhance model robustness, reduce instability caused by individual biases, and optimize feature selection, ultimately leading to more reliable prospectivity maps. The future of ensemble methods in MPM is promising, with potential advancements in hybrid frameworks that combine ensemble techniques with deep learning architectures to further enhance predictive performance.

4.8. Hybrid Models

Hybrid models combine different machine learning algorithms or integrate machine learning with traditional statistical or knowledge-driven approaches to enhance predictive performance. For instance, genetic algorithm–support vector machine (GA-SVM) models have been used to optimize feature selection and improve the spatial correlation between geological features and mineral occurrences (Du et al. 2021; Oliveira et al. 2023). Similarly, hybrid neuro-fuzzy systems and ensemble approaches have been developed to balance interpretability with predictive power, making them suitable for complex geological settings (Afzal et al. 2022; Xiao et al. 2022). These models leverage the strengths of each component algorithm, such as the

adaptability of machine learning and the domain-specific insights of traditional methods, to produce more accurate and geologically meaningful predictions.

3D Mineral Prospectivity Mapping

The shift towards three-dimensional (3D) MPM has significantly enhanced the ability to identify deep-seated ore bodies. This approach integrates 3D geological, geochemical, and geophysical data to create comprehensive subsurface models that provide valuable insights into the spatial distribution of mineralization (Li et al. 2019; Wang et al. 2011b; Xiang et al. 2020). For example, return-risk analysis frameworks combined with machine learning have been applied to imbalanced datasets for mapping Cu-Au deposits in complex terrains (Gao et al. 2024; Peng et al. 2023) . These methods allow exploration teams to visualize ore-forming processes in three dimensions, improving targeting accuracy in regions with limited surface expressions of mineralization.

Moreover, advanced techniques like voxel-based modeling enable the integration of diverse data types into a unified framework, facilitating better understanding of subsurface structures and their relationships with mineral deposits (Xiao et al. 2021; Zhang et al. 2020). By incorporating depth-related variables such as fault density or stratigraphic entropy into predictive models, researchers can identify prospective zones at greater depths than traditional two-dimensional approaches allow. This transition to 3D mapping represents a critical advancement in modern exploration workflows, enabling more efficient allocation of resources in complex geological settings.

This expanded section highlights the strengths of ensemble methods and hybrid models while emphasizing the transformative potential of 3D mineral prospectivity mapping in modern exploration efforts.

5. State-of-the-Art in Mineral Prospectivity Mapping Using Metallogenic Factors

Metallogenic factors play a critical role in the ore formation process by controlling the spatial and temporal distribution of mineral deposits and providing insights into the geological, geochemical, and structural conditions that favor mineralization. These factors include ore-controlling structures, fluid pathways, host rock characteristics, and geotectonic settings, which collectively influence the concentration of metals into economically viable deposits. For example,(Wei et al. 2020) demonstrated the importance of integrating metallogenic factors such as fault systems, stratigraphic units, and hydrothermal alteration zones to model Mississippi Valley-Type (MVT) Pb-Zn deposits in China. Similarly, (Zhang et al. 2019)

highlighted how metallogenic models incorporating multi-scale datasets—such as structural features and geochemical anomalies—enhanced the prediction of gold deposits in the Wulong district. Metallogenic models also provide a conceptual framework for understanding ore-forming processes, as reviewed by (Pohl 2022) , who emphasized their significance in linking mineral systems to exploration strategies. Furthermore, studies like (Leach et al. 2001; 2005; 2010) explored sediment-hosted lead-zinc deposits, showing how metallogenic factors such as fluid migration pathways and tectonic settings control mineralization over geological time. (Kesler et al. 1996) further contributed by analyzing Na-Cl-Br systematics in fluid inclusions from MVT deposits in the Appalachian Basin, offering constraints on solute origins and migration paths critical for understanding metallogenic processes.

These factors not only guide exploration but also improve predictive accuracy by identifying critical controls on ore genesis, making them indispensable in modern MPM workflows.

6. Applications of Machine Learning Across Geosciences

The application of machine learning (ML) extends beyond mineral exploration to address a wide range of challenges across geosciences, showcasing its versatility in handling complex, nonlinear, and large datasets. In geochemical modeling, ML has been used to predict element distributions, identify geochemical anomalies, and model ore-forming processes (X. Wang et al., 2007; G. Wang et al., 2011; Tian et al., 2023). Similarly, geophysical data interpretation benefits from ML algorithms for subsurface mapping, anomaly detection, and identifying potential mineralization zones using seismic, magnetic, and electromagnetic data (Abd-AlHai et al. 2023; Bencharef et al. 2022; Ogungbemi et al. 2022). In mineralogical analysis, ML techniques such as convolutional neural networks (CNNs) have been applied to classify mineral phases and analyze hyperspectral imagery for mineral identification (Rubo et al. 2019; Jooshaki, Nad, Michaux 2021; Mustafa et al. 2022). Beyond resource exploration, ML plays a critical role in environmental studies, including climate modeling, groundwater contamination assessment, and air quality (Voukantsis et al., 2011; Sajedi-Hosseini et al., 2018; Andrée et al., 2019). For instance, it has been employed to model flood susceptibility by integrating topographic, hydrological, and climatic data (Hasnaoui et al. 2024) . In landslide susceptibility mapping, ML integrates datasets such as digital elevation models (DEMs), lithological maps, and satellite imagery to predict landslide-prone areas with high accuracy. Techniques like support vector machines (SVMs) and artificial neural networks (ANNs) have been successfully applied in regions like Japan and India to assess landslide risks with accuracies exceeding 90% (Mojaddadi et al. 2017). In structural geology, ML algorithms are used to analyze fault networks, predict fracture distributions, and model tectonic deformations (Schaaf, Bond 2019; Ogungbemi et al. 2022). These applications highlight the ability of ML to tackle diverse geoscientific problems with high precision.

In addition to these fields, ML has been applied to archaeological prospection for detecting buried structures using geophysical data and remote sensing imagery (Oonk, Spijker 2015; Albrecht et al. 2019; Gattiglia 2025). It also plays a role in oceanography, where algorithms are used for water quality monitoring and detecting harmful algal blooms (Andrée et al. 2019; Sadaiappan et al. 2023). Furthermore, soil erosion modeling leverages ML techniques like random forests and gradient boosting machines to predict erosion risks based on topographic and climatic variables(Bouguerra et al. 2023; Sahour et al. 2021).

The growing adoption of ML in geosciences demonstrates its ability to process vast datasets efficiently while addressing nonlinear relationships and uncertainties inherent in geological systems. With advancements in computational power and algorithmic development, the potential applications of ML continue to expand across diverse geoscientific domains.

Chapter 2: Geological Setting of the Northeastern Algeria

1. Introduction :

Northern Africa is bordered by a young Alpine orogenic system known as the Tello-Rif or Maghrebides belt (Durand Delga 1980; Michard et al. 2006). This belt links, on its eastern side, the Apennines via the Sardinia Channel, northern Sicily (Peloritani Mountains), and the Calabrian Arc (Mascle et al., 2004), while on its western side it connects the Betic Cordilleras through the Gibraltar Arc and the Alboran Sea basement (Comas et al. 1999; Frizon De Lamotte, Michard, Saddiqi 2006; Durand Delga 1980).

Algeria itself is geologically diverse, comprising two primary domains: the southern Saharan domain and the northern Atlas zone. The Saharan region is characterized by extensive Precambrian basement outcrops in the Hoggar and Eglab massifs, which are overlain by the relatively young sedimentary cover of the Saharan platform. In contrast, the northern Atlas zone forms a structural boundary that includes both the Saharan Atlas from the High Atlas in Morocco to the Tunisian Atlas; and the more intricate Tellian Atlas, which features a series of mountain chains interspersed with the central High Plains that transition into the Hodna chain and the Oran High Plains (fig. 4).

The Maghrebides chain, comprising thrust sheets emplaced onto the African platform, further subdivides into distinct geological domains: the Kabylian, Flysch, and Tellian units, the latter being entirely overlain by the Numidian Neritic formation. Field observations and laboratory analyses reveal that northeastern Algeria is built from a complex stack of geological units specifically, the internal, flysch, and external zones; formed during the convergence between Africa and Europe in the peri-Mediterranean Alpine event. This orogenic phase induced significant crustal deformation, magmatism, and hydrothermal fluid circulation (Jolivet, Faccenna 2000; Faccenna et al. 2004; Rosenbaum, Lister 2004; Seffari et al. 2023). creating fractures, faults, and magmatic intrusions that served as conduits for mineralizing fluids. These processes resulted in the formation of ore deposits enriched in both base and precious metals, which have been further exposed by subsequent tectonic uplift and erosion.

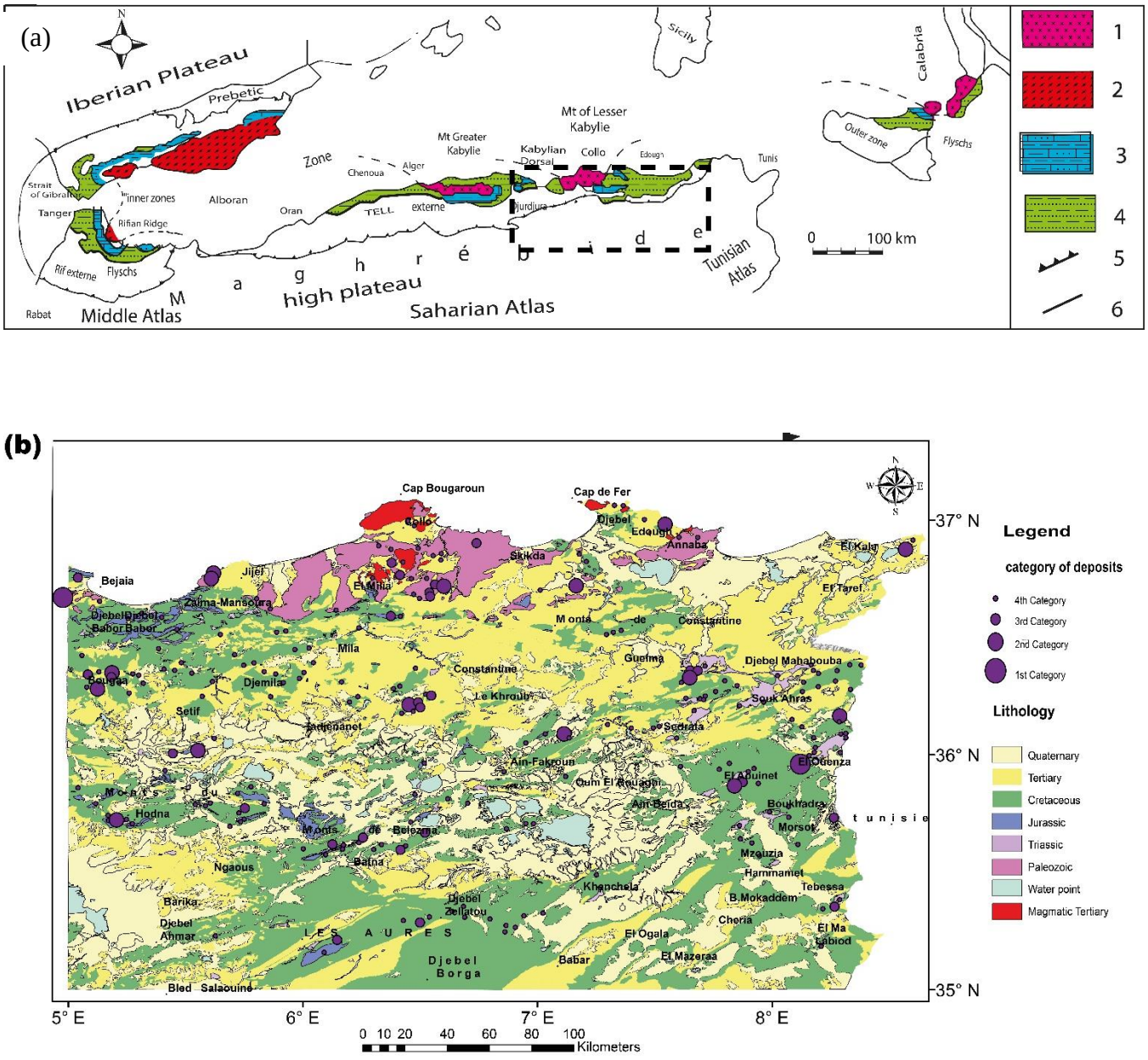

Figure 4: : Illustration of the structure of Alpine orogenesis in the context of the western Mediterranean (Durand-Delga, 1980). (1) Ancient Kabyle, Peloritani, and Calabrian massifs and their cover; (2) Ancient Betico-Rifian massifs (Paleozoic and Permo-Triassic); (3) Peri-Mediterranean Mesozoic ridge (Betic, Rifian, Kabyle, and North-Sicilian); (4) Cretaceous and Nummulitic Flyschs; (5) Front limits of the Alpine nappes; (6) Abnormal contacts between Alpine nappes.

2. Regional Geology

The study area is located in northeastern Algeria and encompasses various geological formations known as the Maghrebides, which are part of the peri-Mediterranean Alpine orogenic belt. This mountain chain is relatively young in formation and extends over 2,000 kilometers.

The **Kabylian domain** is composed of the Kabylian basement and the Kabylian dorsal. The Kabylian basement consists of pre-Triassic metamorphic rocks and is located in northeastern Algeria. The basement of these massifs is characterized by large southward thrusts and is divided into two main units: the upper and lower complexes.

2.1. The Tellian Atlas

The **Tellian Atlas** is part of the peri-Mediterranean Alpine orogen, a ring-shaped mountain chain extending over 2,000 km from the Atlantic Ocean to the Ionian Sea. In North Africa, it stretches approximately 1,500 km from Bizerte (Tunisia) to Rabat (Morocco) and has geological equivalents in both countries. This mountain system is subdivided into two main domains, forming the **Maghrebides belt**, which is further divided into:

The Internal Domain (Northern Zone)

The External Domain (Southern Zone)

2.2. The Internal Domain

The internal domain includes the Kabylian region and the Edough Massif (Annaba) and is composed of:

- Crystalline basement (metamorphic rocks)
- Unmetamorphosed Paleozoic formations

The basement of "Petite Kabylie" extends from Texenna to the Filfila region and is composed of a series of thrust sheets, ranging from lower to upper nappes. This geological structure presents a complex stratigraphy with distinct lithological units. (Thiébaut 1951; Durand Delga 1969; 1980; Bossière 1980; Bouillin et al. 1984; Mahdjoub 1994; Saadallah 1992).

In the Texenna region, located in the southwest of "Petite Kabylie", the basal unit consists of khondalites and kinzigites, which are interbedded with leptynites containing garnet-bearing pyroxenites, gabbros, and amphibolites. Above this sequence, a layer of kinzigites follows, which has undergone local migmatization and is intruded by garnet-biotite granite, indicating a high-grade metamorphic evolution. (Arab et al. 2016; Durand Delga 1969; Gélard 1979; Raoult 1974)

The central part of the region is primarily composed of paragneiss, which in some areas exhibits migmatitic textures. Moving upward, the upper sequence is characterized by an alternation of quartzitic sandstones and metapelites, with interbedded marble lenses. This flysch-like formation also includes volcanic rocks, marbles, micaschists, quartzites, and amphibolites, forming a diverse lithological assemblage. According to (Afalfiz 1992; 1990; Afalfiz, GUY,

SEMROUD 1998), this sequence is associated with polymetallic mineralization, suggesting a significant metallogenic potential.

The terminal series consists of blue marbles, chloritoschists, sericitoschists, graphitic schists, porphyroids, and arkoses. This unit is equivalent to the so-called satin series or phyllites, which also appear in the Beni Afeur units (Infra-Silurian). The satin series was historically considered the basement of the Paleozoic (Silurian), and the Beni Afeur unconformity was first described by Durand Delga in 1952.

2.2.1. The kabylian dorsal

The “Kabylian Dorsal” is a key component of the internal domain of the Maghrebides. This geological formation developed during the peri-Mediterranean Alpine orogeny, resulting from the collision of the African and Eurasian plates (Durand Delga 1969)., as well as the Alboran plate, during the Mesozoic and Cenozoic eras.

In this study, the “Kabylian Dorsal” is considered to occupy an external position relative to other units of the internal domain of the Maghrebides (see Fig. 4). It is composed of a complex set of tectonic slices, ranging in age from the Permo-Triassic to the Eocene, and is characterized by the predominance of carbonate formations. The Liassic sedimentary sequence allows for the differentiation of three distinct units within the Dorsal: internal, median, and external, which are superimposed yet distinct in their stratigraphy and lithology.

The stratigraphic sequence of the “Kabylian Dorsal” consists of three main units:

1. The Permo-Triassic series, characterized by continental red detrital facies, including conglomerates, sandstones, and red clays, often associated with evaporite deposits. This unit is also referred to as the Kabylian Triassic or Permo-Triassic with "verrucano" facies.
2. The Liassic to Eocene series, predominantly composed of carbonate rocks, reflecting a marine sedimentary environment during this time.
3. The Eo-Oligo-Miocene molassic formations, which mark the transition to a foreland basin setting, recording the final phases of the Alpine orogenic evolution in the region.

2.2.2. The Kabylian Oligo-Miocene (OMK)

The Kabylian Oligo-Miocene (OMK), as described by (GERY et al. 1981)in Djebel Aït Aissa Mimoun (Great Kabylie), presents a well-defined stratigraphic sequence that reflects significant geological processes. At its base, it consists of alluvial cone conglomerates, which have been dated to the Upper Oligocene (Raoult 1974). These deposits are overlain by microconglomerates, indicative of a fluvial to shallow marine environment, formed due to sedimentary transport from the nearest hinterland (Gélard 1979)

In Petite Kabylie, the OMK is characterized by micaceous sandstones interbedded with continental-derived conglomerate lenses, likely transported by gravity flows into a marine

setting .Similar successions have been identified by (Arab et al. 2016) in regions such as Chakfa (Jijel), Tamalous, Oued Z'hor, and Ouled Atia (Collo region). These deposits indicate a dynamic sedimentary environment influenced by both fluvial and marine processes.

At the base of the OMK sequence in Petite Kabylie, (Arab et al. 2016) documented the presence of breccias composed mainly of basement materials, also observed in Laazib (Chekfa, Jijel province). In the Tamalous region, fluvial channels filled with rounded conglomeratic clasts of centimeter-scale size have been identified. These deposits closely resemble those found in Aït Aissa Mimoun (Great Kabylie), as described by (Bouillin 1977) and (Durand Delga 1969). The fluvial channels are embedded within reddish sandstones with low-angle cross-stratification, which transition into ripple structures toward the upper layers.

Further evidence of sediment transport and deposition is seen along the Oued Z'hor coastline, where , (Arab et al. 2016) reported basement-derived conglomerates in direct contact with the gneissic basement. The overlying fluvial deposits exhibit a gradual fining-upward sequence, transitioning from coarse conglomerates to medium-grained massive sandstones with horizontal stratification, reflecting a shift from high-energy fluvial deposition to more stable conditions.

At the top of the OMK sequence, siliceous facies such as radiolarites and diatomites, occasionally interbedded with marly layers, mark the transition from continental to shallow marine environments, ultimately evolving into deeper pelagic sedimentation during the late Oligo-Miocene. This progression highlights the complex interplay of tectonics, sedimentation, and paleoenvironmental changes that shaped the OMK deposits in the Kabylian region.

2.3. The Flysch Domain

The Maghrebian flysch formations are composed of deep-sea deposits dating from the Cretaceous to Paleogene periods. These deposits stretch for approximately 800 kilometers along the coastal zones, from Mostaganem to Bizerte in Tunisia. Formed by turbidity currents, the flysch deposits are divided into two main groups. (Raoult 1969)

2.3.1. Mauritanian Flysch

The Mauritanian flysch, described by (Gélard 1979), is found in the internal part of the flysch domain. These deposits extend from the Berriassian-Valanginian to the Oligocene and consist of a thick sequence of proximal deposits. The series is characterized by alternating beds of clay, limestone, and sandstone. The earliest deposits are proximal, located in the internal flysch domain, and are made up of alternations of argillaceous, limestone, and sandstone layers. These begin with red radiolarites from the Dogger-Malm and transition into conglomeratic levels from the Paleocene. These deposits are sourced from the internal domain, indicating that material was transported from this region.

2.3.2. Massylian Flysch

The Massylian flysch, located in the external part of the flysch domain, is distinguished by its distal series. It consists of a succession of layers, including a pelito-quartzitic series from the Albo-Aptian, followed by a pelito-microbreccia series from the Upper Cretaceous, as described by Raoult (1969). These distal deposits reflect a shift toward deeper marine conditions, with fine-grained sediments transported farther from the source area.

These flysch formations provide valuable insights into the tectonic and sedimentary processes that shaped the Maghrebian region during the Cretaceous and Paleogene periods, offering a detailed record of deep-sea environments and the dynamic interactions between land and sea during these geological epochs.

2.4. The External Domain

The external domain, located between the internal zones and the pre-Atlas foreland, it is represented by the Tellian series, the allochthonous foreland series, and the autochthonous Atlas foreland series (Bouillin 1977; Durand Delga 1969; Kieken 1962; Vila 1980).

The external domain, located between the internal zones and the pre-Atlas foreland, includes schistose autochthonous units found in the coastal Oran massifs, Cheliff, Dahra-Boumaad, Blida, and Babors. It also features intra-Tellian autochthonous units, such as the Bibans and Ouarsenis (Amrouna) massifs, and Tellian nappes, which are allochthonous thrust sheets from the Early Miocene. Additionally, it includes the Southern Tellian Foredeep, a Miocene basin that accommodated the Tell nappes over the pre-Atlas foreland.

2.4.1. The Tellian Series

The Tellian series consist of thick sequences dominated by marls, which are thought to have originated from the Tellian trough (Vila 1980). After examining very southern Tellian series, J.V. Vila subdivided them into three main units: Ultra-Tellian units, Tellian units sensu stricto, and the Peni-Tellian series with Nummulites, which roughly correspond to the paleogeographic boundaries of the Cretaceous, Paleocene, and Eocene.

- **Ultra-Tellian Units**: These were defined at Kef Sidi Driss and Djebel Bousbaa (Guelma region) (Raoult 1969; Vila 1980). Typical formations include the Lower Cretaceous with clear marl-limestone sequences containing Ammonites (Valanginian to Vraconnian), Middle Cretaceous with Rotalipores, a Senonian marly and micritic sequence rich in microfaunas of Globotruncana and Heterohelicids, and an Eocene with three main layers: black marls with yellowish balls (Danian-Paleocene), Ypresian-Lutetian lower formed by black flint limestones, and dark marly upper Lutetian.
- **Tellian Units Sensu Stricto**: Defined by (Vila 1980) these units correspond to the Meso-Tellian series in (Durand Delga 1969) nomenclature . Characterized by a Lower Cretaceous rich in terrigenous sediments, the intercalations of neritic facies remain moderate from the Upper Cretaceous to the Oligocene.
- **Peni-Tellian Series and Meridional Units with Nummulites: The** term "Peni-Tellian" was created to refer to a series located on the southern slope of Djebel Zouaoui

in the Chattabah massif near Constantine. These series likely represent a transition between the neritic facies of Constantine and the deeper northern facies with Biban affinities (Kazi-Tani 1986) . The Peni-Tellian series are primarily composed of neritic facies from the Upper Cretaceous to Oligocene and show strong affinity with the southern foreland. The Meridional units with Nummulites are only found in the southern confines of the Constantine neritic mass and consist exclusively of Senonian and Eocene formations rich in Nummulites

2.4.2. The Allochthonous Foreland Series

According to (Vila 1980), the allochthonous foreland series can be classified into three main groups:

a) The Southern Sétifian Organization

The Sétifian series exhibit a uniformly subsiding platform character. However, their southern part shows significant variations, indicating a transition towards the more southern autochthonous Hodna domain to the west (Djebel Tafourer).

b) The Constantinois Organization

This organization includes the neritic Constantinois series to the north and the Sallaoua series to the south. . (Durand Delga 1969; GLACON 1952; Savornin 1920)

- **The Neritic Constantinois Series**: These series constitute the main limestone massifs of the Constantinois neritic domain, characterized by thick carbonate formations indicative of a subsiding platform. The limestone massifs in the southern part do not extend beyond the Turonian and terminate with an anomalous contact. No Eocene formations are stratigraphically associated with the Constantinois neritic series (J.M. Vila, 1980).
- **The Sallaoua Units**: These units are marked by argillaceous-marly sedimentation throughout the Cretaceous. The Djebel Djaffa illustrates transitional facies between the southern Constantinois neritic series and the northern Sallaoua series (Blayac 1912; David 1956).

c) The Algero-Tunisian Organization

This structural unit is specific to the Algero-Tunisian border region and northern Tunisia. It exhibits sedimentation patterns similar to those of the Tellian nappes or the northern Sallaoua-type series.

2.5. The Atlas Foreland

The Atlas foreland extends from west to east, encompassing the Hodna Mountains, the Batna Mountains, and the Aurès Massif. This region is characterized by thick Mesozoic series, with sedimentation remaining relatively uniform, marked by subsiding platform facies invaded by sandstone deposits from the Berriasian to the Albian (Delfaud, 1974; Guiraud, 1973; Vila, 1980).

- **The Aurès Massif**: As the eastern extension of the Saharan Atlas, this massif is structured by large, relatively regular folds oriented northeast-southwest. These features, first described by (Lafitte 1939), were outlined during a Post-Lutetian tectonic phase that led to the massif's emergence.
- **The Batna-Bellezma Mountains**: Located east of the Hodna Mountains, these structures have been extensively studied (Bellion 1972; Bureau 1973; Vila 1980). They are shaped by broad anticlines, with steeply inclined southern flanks and more gently dipping northern flanks.
- The following figure show the main geological domains of the study area

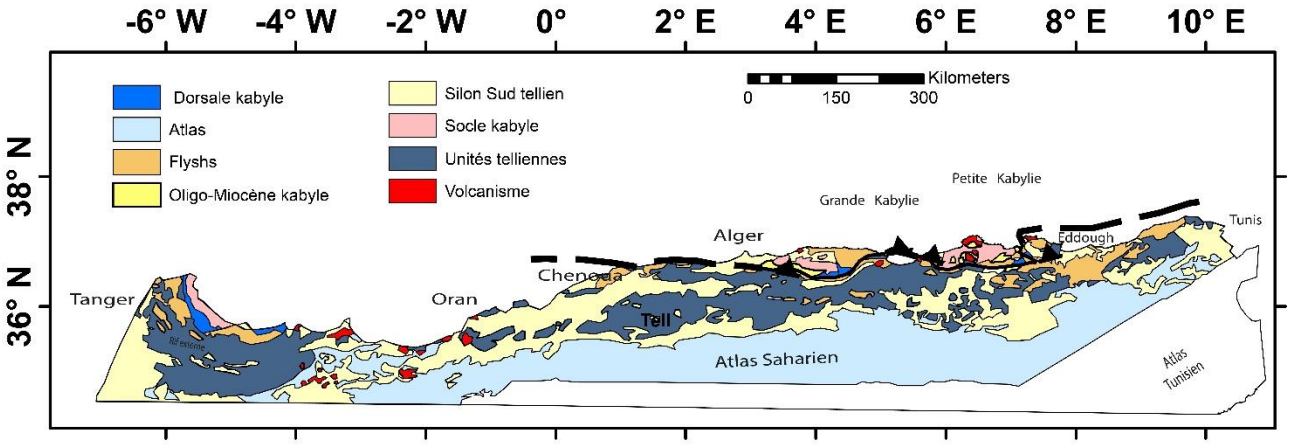

Figure 5: Structural map of the Tell-Rif belt (Vila 1980; Domzig 2007)

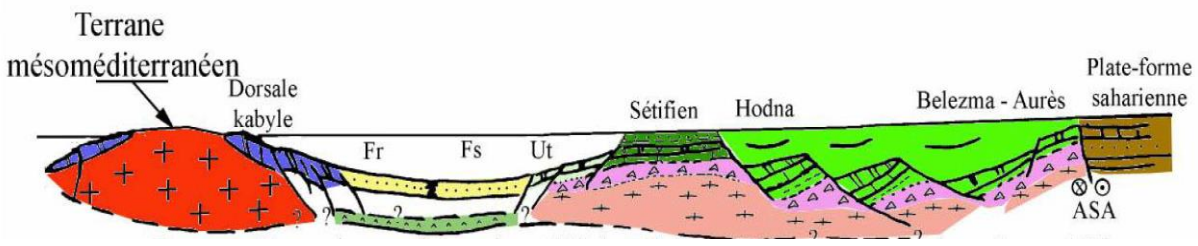

Figure 6:Schematic N-S palinspastic cross-section of the tectono-structural domains of Northeastern Algeria (Guiraud 1973; Vila 1980; Kazi-Tani 1986; Bouillin, Durand-Delga, Olivier 1986)

3. Mineralization and Main Pb-Zn Deposits of Northeastern Algeria

Northern Algeria belongs to the Mesogean Alpine province, which extends across the Betic Cordillera in southern Spain and northern Morocco. This province hosts a large number of Pb-Zn and polymetallic mineralizations.

In northern Algeria, an ancient Hercynian basement outcrops in the massifs of Grande and Petite Kabylie, the Edough, and within the horsts of the High Plateaus domain. The main mineralizations include stratabound Mississippi Valley-Type (MVT) Pb-Zn deposits, polymetallic vein-type deposits of epithermal or mesothermal, , as well as peri-granitic deposits within the basement (skarns, greisen, etc.).

3.1. Alpine Metallogenic Phases:

The alpine metallogenesis contributed in the formation of three groups of deposits

- **Around 17 Ma:** Formation of polycyclic skarns, enriched in elements such as tungsten and tin, associated with Burdigalian leucogranites.
- **Around 16 Ma:** Development of polymetallic mesothermal veins containing Cu, Zn, Pb, Bi, Ag (and occasionally Au), characterized by zoned propylitic alteration. These veins are both spatially and temporally linked to Langhian microgranite intrusions.
- **Around 15 Ma:** Emergence of typical epithermal mineralizations related to peraluminous rhyolitic magmatism. Within the mesothermal veins, synchronous epithermal parageneses evolve, delineating a secondary mineralization cycle driven by thermal recharge of the hydrothermal system. Antimony mineralization manifests primarily as berthierite–stibnite, sometimes followed by a later stage marked by auriferous arsenopyrite.

3.2. Internal domain

In northern Algeria, an ancient Hercynian basement outcrops in the massifs of “Grande Kabylie“ and Petite Kabylie, in the Edough area, and within the horsts of the Hauts Plateaux domain. The primary mineralizations include stratiform Mississippi Valley-type (Pb-Zn) deposits; polymetallic vein-type mineralizations that are epithermal, mesothermal, or porphyry in nature; and peri-granitic deposits in the basement (such as skarns and greisen).

The Hercynian orogeny played a crucial role in the formation of several ore deposits in Achab Tiri-Azarez-Bou M’lih, within Petite Kabylie. These deposits contain Pb, Zn, and Ba, as well as Pb, Zn, and Cu, and are hosted within metamorphic formations composed of carbonates and siliciclastic rocks. These deposits likely date back to the late Precambrian, forming an integral part of the mineralization history of the Kabylides.

These crystalline massifs **Kabyle basement** along the Mediterranean coast and experienced significant sedimentary gaps during the Triassic and Secondary periods, accompanied by notable volcanic activity from the Oligocene to the Pliocene, particularly during the Miocene. Mineralizations in this domain include polymetallic vein-type deposits, ranging from epithermal to mesothermal, as well as porphyry, skarn, and Mississippi Valley-Type (MVT) Pb-Zn deposits.

According to (Afalfiz 1990) these mineralizations are closely linked to meta-carbonate units within the upper Kabylian basement. These units serve as a transitional zone between schist

formations and the gneissic complex, which constitutes the metamorphic basement of Petite Kabylie.

3.3. The Tellian domain:

The autochthonous Tellian domain is the northernmost unit, surrounding the Kabyle basement massifs. It underwent significant deformation during the Cretaceous, characterized by thrusting and southward imbrications. This domain hosts polymetallic mineralizations (Pb-Zn-Cu-Hg) occurring as vein-type deposits, with epithermal to mesothermal affinities, as exemplified by the Oued El Kebir deposit.

The pre-Saharan intermediate domain of the Aïn M'Lila massif and its margins features neritic facies from the Juarassic and Lower Cretaceous. Pb-Zn mineralizations, predominantly of the MVT type, are mainly concentrated along the massif's borders, as observed in the Ain Kahla and Kherzet Youssef deposit.

The pre-Saharan domain of the Eastern Atlas is influenced by two main tectonic trends (NW-SE and WSW-ENE) and features Triassic and Mio-Pliocene diapirism. The main mineralizations are concentrated in Lower Cretaceous reefal highs, particularly near Triassic diapirs, as seen in the Mesloula deposit.

3.4. Foreland Regions

Between the allochthonous foreland and the Atlas foreland, mineral deposits are primarily hosted in carbonate sedimentary sequences rich in lead (Pb), zinc (Zn), with occasional copper (Cu), barium (Ba), and fluorine (F). These deposits exhibit Mississippi Valley-Type (MVT) characteristics (Boutaleb 2001; Leach et al. 2001) and are linked to hydrothermal fluids circulating along fractures in sedimentary basins. They share mineralogical traits with fault-related deposits in similar geological settings. These deposits have historically contributed up to 80% of Algeria's lead and zinc production and are mainly found in Mesozoic and Cenozoic intracontinental basins of the High Plateaus and the Saharan Atlas.

The total estimated production exceeds 20 million tones of combined Pb-Zn, distributed over a 1,000 km belt stretching from the Algerian-Moroccan to the Algerian-Tunisian border. Along this belt, several mining districts can be identified, including El Abed-Deglène-Ghar Roubane to the west, the Saida-Takhameret block, the Ouarsenis, the Constantinois neritic domain, the Sétifien-Hodna, the Belezma-Aurès, and the Diapiric Zone in the east.

From a metallogenic perspective, these deposits are considered epigenetic, with mineralization processes occurring primarily during the Eocene (Boutaleb et al., 1999). The mineralizing fluids were both saline and warm, driven by basin conditions. Given their economic significance, these deposits remain a prime target for exploration programs, focusing on both known sites and adjacent occurrences to identify similar Pb-Zn mineralizations.

3.4. Magmatic Activity Along the Algerian Coast

The northern Algerian coastline experienced extensive magmatic activity from the Oligocene through the Quaternary, which resulted in the emplacement of granitoid intrusions and a range of volcanic rocks—from acidic to basic compositions, predominantly andesitic (Maury et al. 2000; Ouabadi 1994).. This activity is intrinsically linked to the geodynamic evolution of the western Mediterranean and the peri-Mediterranean Alpine chains, whose tectonic framework was formed by the closure of the Tethys Ocean following the collision of the African and European plates. This orogenic process created two tectonic provinces: the Alpidic branch, which includes the Betic Cordillera and the Alps, and the Dinaric branch, comprising the Calabro-Sicilian Arc, the Apennines, and the Maghrebides.

From Béjaia to Annaba—and across regions such as Amizour, El Aouana (Bosch et al. 2014; Bruguier et al. 2017; Fernandez et al. 2016; 2020), Collo and the area is dominated by plutonic rocks, notably granitoids and diorites, intercalated with volcanic units like andesite, dacite, and rhyolite (Laouar et al. 2018; Ouabadi 1994; Seffari et al. 2023) . Two main pulses of magmatic activity have been recognized: the first at approximately 22 million years ago, and the second between 16 and 13 million years ago (Abbassene 2016; Belanteur 2001; Bellon 1976; Benali 2007; El Azzouzi et al. 2003). These events were critical in shaping regional mineralization, with deposits showing strong spatial and temporal links to Neogene magmatism.

Mineralization related to these magmatic phases is categorized into two types: proximal deposits, closely associated with granitoid intrusions (e.g., Boudoukha), and peripheral deposits found near magmatic bodies, such as at Ain Barbar and Kef Oum Teboul. Unlike typical carbonate-hosted vein systems, these mineralizations are primarily composed of sphalerite and galena, often accompanied by barite and occasional enrichments in copper and silver—with some veins recording silver levels exceeding 100 g/t. These characteristics underscore the economic potential of the deposits, particularly where resource sizes exceed one million tones or the concentration of valuable metals is notably high (Afalfiz, GUY, SEMROUD 1998; Aissa 1982; Boutaleb et al. 2000; Marignac, Djamel-Eddine 2017; Ysbaa et al. 2020). The following table summerise the main deposits of each metallogenic district (tab. 1).

Table 1: Main Pb-Zn Deposits: Metallogenic Framework of Northeastern Algeria

Domain	Region	Geological Age	Geological Description	Mineralisation	Important Deposits
Coastal Volcanic Manifestations	Coastal (implied)	Meso–Cenozoic	—	VMS-type mineralizations associated with volcanism	Oued Amizour, Oued El Kebir, Boussoufa, Tifaraouine
Internal Domain	Petite and Grande Kabylie	Ante-Alpine, Late Precambrian	Carbonate metamorphic formations	—	Tiri, Azaraz, Boumlih, Achab, Oued Bibi, Oued Z'hor
External Domain	South Sétif	—	Autochthonous to parautochthonous terrains	Epigenetic (sphalerite, galena, pyrite)	Khoukdéma, Aanini, Aïn Sedjra, Kef Semmah, Aïn Roua, Zdim, Gustar, Djebel Sekrine, Koudiet El Bassour, Braou, Skaken
	Hodna	Jurassic and Lower Cretaceous	Folded domain	MVT type (sphalerite, galena, pyrite)	Kherzet Youcef, Chabet El Hamra, Tartaout (East & West), Gustar, Sekkaken, Koudiat Taga, Dra Sfa, Braou, Djebel Zdimm, Kef El Djebas, Draa El Maiz, Draa Boutouil, Ain Kahla, Ain Raffah (North & South), Foural, Anza, Bahloul, Gouzi, Chaabet El Hamra, Kef Omar, Tamtart, Tebesbes, Rasfa, Kef Essanar, Soubella, Abiane
	Belezma	Jurassic, Lower Cretaceous, and Miocene	Fissure fillings in carbonate rocks of various orientations	Sphalerite, pyrite, and galena	El Merouana, Tizourit, Boukendouch, Djebel Mhasseur

	Monts des Aures and Batna	Cretaceous and Miocene	Carbonate rocks	Baryte and galena	Ichmoul, Ain Mimoun, El Hrig and de Taghit, Tiouknine, Djebel Fedjoudj, Dra El Ahmar, Bou Aoun, Djendeli (Cu), Djebel Mogref, Mekouche, Hadjar Mekouch, Chellala, Ain Bougdaa, Tenoun Kenine
	Neritic Constantinois (Algero-Tunisian border, Ghar Roubane)	Jurassic, Lower Cretaceous, and Miocene	Autochthonous to parautochthonous terrains	Epigenetic (sphalerite, galena, pyrite)	Djebel Debbagz, Ain Arko
Diapiric Zone	Diapiric Zone	Aptian–Albian	Carbonate rocks	Siderite and galena	El Khenga, El Ouasta, Essoubaa, Mkhiriga, Petit Boudjaber, M'Zeita, Boukhadra, Mesloula, Mezouzia, Ouenza, Hamimat, Aon Mimoun, Kef Oum Teboul, Ain Mimoune, Ain Barbar

3.5. Economic Importance of the main Pb Zn Deposits

Mineralized systems in northeastern Algeria offer significant economic potential and play a crucial role in the region's mining industry. Miocene volcanic-associated deposits, formed during a period of intense magmatic activity, provide a substantial contribution to the national reserves of Zn-Pb and other valuable metals. These systems not only highlight the complex interplay between tectonic processes and magmatism but also serve as key targets for exploration and economic development.

These polymetallic deposits are classified into five metallogenic classes based on their economic significance (Boutaleb et al. 2023). The most valuable deposits are those related to magmatic processes, For example, the Oued Amizour volcano-plutonic complex, discovered by ORGM in 1990, hosts Algeria's largest Zn-Pb deposit. This deposit is estimated to contain 53 million tones of ore, representing 40% of the country's Zn-Pb reserves, and approximately 3.5 million tones of metal, including 2.8 million tones of Zn and 0.7 million tones of Pb (Graïne, Marignac 2001; Gravelle 1959; Semroud 1993). West of this complex, the El Aouana region features the Oued El Kebir deposit, with an estimated 11.5 million tones of ore, while the Boussoufa deposit further west is believed to exceed 13 million tones of Zn-Pb-Cu ore, although precise grades remain uncertain (Benali 2007; Satouh 2007). Following these are stratabound-type mineralizations hosted in carbonate rocks formed by high-temperature, metal-rich fluids migrating along tectonically induced structures during the late Langhian phase are analogous to the Miocene deposits in the Edough region (Aissa 1982; Marignac, Djamel-Eddine 2017) are found in the Hodna Basin, Belezma, and parts of the diapiric regions. These Mississippi Valley-type deposits have historically contributed up to 80% of national Pb-Zn production, with reserves reaching 27 million tones.

. Mineralizations associated with volcanic rocks, often exceeding 1 million tones in reserve and sometimes containing valuable by-products such as silver or copper, also hold significant economic interest. In contrast, deposits without a direct volcanic association generally have a lower economic importance. Finally, the smallest deposits, such as those in the metamorphic basement like Achab Tiri, exhibit reserves below 3 million tones of ore averaging 2.19% Pb and 2.78% Zn, further underscores the exploration promise of the area (Boutaleb, Aissa, Kolli 2023) (see Tab. 02).

Table 2: geological reserves of the main Pb Zn deposits in Northeaster Algeria

District / Zone	Gisement / Occurrence	Type / Composition	Resources / Data
	Achab	Pb–Zn–Ba (polymetallic)	1.23 Mt; 1.92% Pb; 1.66% Zn; 105 g/t Ag
	Tiri	Pb–Zn–Ba	2.87 Mt; 2.27% Pb; 3.37% Zn; 94 g/t Ag

Metemorphic basement (kabylie)	Boudoukha	Zn–Pb–Cu–Ag	3.808 Mt; 1.04% Pb; 5.84% Zn; 0.34% Cu
	Aïn Barbar	Cu–Pb–Zn–Ag–Au	1.86 Mt; 4.30% Zn; 1.20% Cu; 1.4% Pb
	Filfila	Cu (±Sn)	4,156,794 t; 2.87% Cu (119,300 t Cu; 20,300 t Sn?)
	Karezas	WO_3	581 t (>0.7%)
	Kef Oum Theboul	–	–
	Sidi Kamber	–	–
Épi-/Mésothermaux	Oued Amizour	Pb–Zn	30 Mt; 5.5% Zn; 1.4% Pb (11 Mt: 10.9% Zn; 3% Pb)
	Oued El Kebir	Cu–Pb–Zn–Ag–Au	11.525 Mt; 2.63% Pb; 2.09% Zn; 0.7% Cu; 86 g/t Ag
	Bou Soufa	Cu	35,070 t; 1.57% Cu
	Bauchitan	Cu	652,000 t; 1.14% Cu (of which 86,000 t at 3.65% Cu)
Domaine Externe Districts polymétalliques / MVT (Tellien & Atlas Tellien)	Djebel Taya	Pb–Zn–As–Sb–Hg–Ba	–
	Koudiat Stah (Bou Cherf)	Pb–Zn–Cu–Hg–Sb (MVT)	–
	Aïn Kébira	Pb–Zn–Cu (MVT)	~10 occurrences (~100–150 t each)
	Boukhdema (Guergour)	Zn (MVT)	8.38 Mt; 4.89% Zn; 2.32% Pb
	Aïn Sedjra (Guergour)	Zn (MVT)	36,000 t; 10.47% Zn; 1.47% Pb
	Kef Semmah (Guergour)	Zn (MVT)	2 Mt; 5% Zn
	Aïn Roua (Guergour)	Zn (MVT)	–
	Amalou (Guergour)	Zn (MVT)	–
	Anini (Guergour)	Fe (MVT)	6.75 Mt; 55% Fe
	Zn–Pb Boukhdéma	Zn–Pb	7.7 Mt; 5.25% Zn; 2.52% Pb
	Zn–Pb Aïn Sedjra	Zn–Pb	800,000 t; 11.99% Zn; 1.25% Pb
	Djebel Felten	Pb	76,000 t Pb
	Kherzet Youssef	Zn–Pb (MVT)	1.6 Mt; 18% Zn; 3.6% Pb (resources)

District Hodna–Bélezma (Hauts Plateaux)	Chaabet El Hamra	Zn–Pb (MVT)	4.8 Mt; 6.4% Zn
	Aïn Kahla	Zn–Pb (MVT)	7 Mt; 3.97% Zn; 1.79% Pb
	Djebel Gustar	Zn–Pb (MVT)	91,500 t Pb + Zn
District de Batna (MVT Zn–Pb)	Tenoun Kenin	Pb–Zn–Sb	Former small mine (data not provided)
	Messouda	Pb–Zn	Former small mine (data not provided)
	Merouana	Pb–Zn	Former small mine; probable: 1,000 t Zn (6.8%)
	Djebel Hanout	Pb–Zn	Former small mine (data not provided)
	Aïn Arko	Pb–Zn	Former small mine (data not provided)
	Chellala	Zn–Pb	–
	Aïn Boughda	Pb–Zn–Sb	–
	Haout Kebir	Pb–Zn–Sb	–
	Theniet Fourar	Pb–Zn–Sb	–
District d'Hammam N'Bails	Hammam N'Bail	MVT Pb–Zn–Sb	2.4 Mt; 1.5% Pb; 5.3% Zn; 3.4% Sb
District des Diapirs (Aptien para-récifal, Atlas Tunisien, MVT) District des Diapirs	Mesloula	Pb–Zn–Ba–F–Ag (MVT)	–
	Bou Jaber	$BaSO_4$, CaF_2, Pb–Zn	7.2 Mt; 20% $BaSO_4$; 9% CaF_2; 5% Pb–Zn
	Ouenza–Boukhadra	Fe (hematite–siderite)	87 Mt; 48% Fe
	Ouasta	Pb–Zn (MVT)	–
District Aurès / Atlas Saharien	Djebel Ichmoul	Pb–Ag–Ba–Zn (MVT)	1.24 Mt; 4.04% Pb; 1.1% Zn; 38.13% Ba

4. Tectonic Controls on Mineralization

The mineralization in northeastern Algeria is fundamentally governed by its structural framework, which has evolved through multiple orogenic events. The Alpine orogeny, in particular, played a decisive role in shaping the region's tectonic setting through the collision of the African and Eurasian plates. This process generated extensive fault systems, shear zones, and fold structures, especially in the Kabylian and Tellian regions. These tectonic features

created efficient pathways for hydrothermal fluids to migrate and deposit economically significant metals such as lead, zinc, and copper. In Kabylia, compressional tectonics are intimately linked to magmatic intrusions, which in turn have fostered skarn-type mineralization along the contact zones between intrusives and carbonate sediments. The resulting polymetallic deposits underscore the complex interplay between deformation, magmatism, and fluid flow in the region (Faccenna et al. 2004; Jolivet, Faccenna 2000; Rosenbaum, Lister 2004; Seffari et al. 2023).

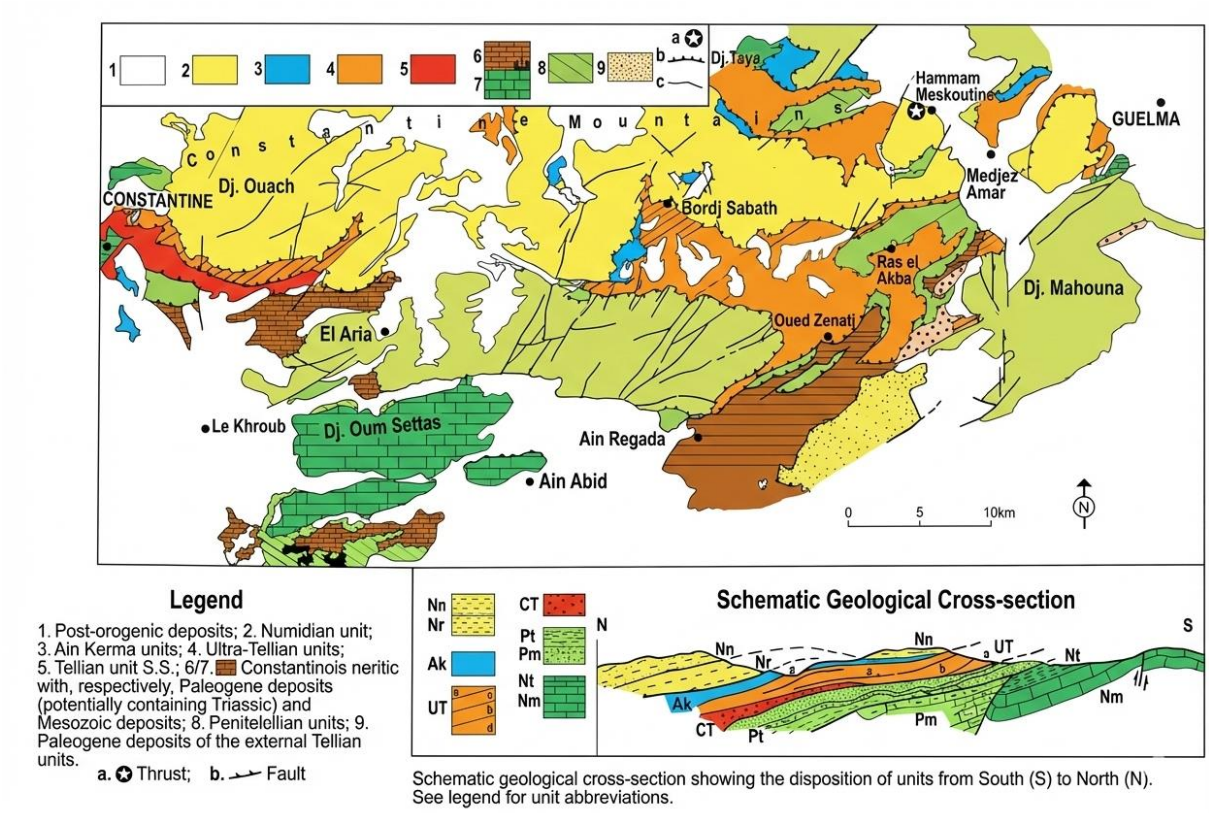

Schematic geological cross-section showing the disposition of units from South (S) to North (N). See legend for unit abbreviations.

Figure 7: Structural map of the oriental tell from Constantine to Guelma

4.1. Structural Trends and Exploration Implications

Distinct structural trends further influence the spatial distribution of mineral deposits in northeastern Algeria. Pb-Zn mineralization within the Tellian Chain follows prominent orientations—E–W, NE–SW, and NW–SE—which correspond to subsiding basins and synclinal folds identified through both field observations and gravimetric studies (Boutaleb 2001; Boutaleb, Aïssa 1999). In the Hodna and Belezma regions, ore bodies are closely associated with deep NW–SE lineaments that appear to control hydrothermal fluid pathways. Similarly, in the Batna-Aurès region, the Tébessa Mountains, and diapiric provinces, mineralized zones are concentrated along intersections of NE–SW and NW–SE faults and folds, which likely acted as conduits during hydrothermal activity in the Jurassic and Cretaceous periods. Recognizing these structural trends is critical for exploration, as they help delineate areas with enhanced potential for economically viable deposits (Haddouche et al. 2016; Ysbaa, Haddouche, et al. 2019; Ysbaa et al. 2020).

5. Metallogenic context of northeast Algeria :

The formation of mineral deposits in the Tellian chain is controlled by geodynamic processes and follows a polyphased evolution. Sulfides precipitated during major metallogenic events linked to tectono-sedimentary or magmatic episodes, reflecting the distinct characteristics of different paleogeographic domains. Pb-Zn deposits, classified based on their host rocks, morphological and structural characteristics, and paragenesis, are grouped into five major categories corresponding to key metallogenic events.

- **Mineralization associated with the metamorphic basement** in Kabylie is primarily linked to the Hercynian orogeny, which played a key role in forming deposits such as Achab Tiri, Azarez, and Bou M'lih in Petite Kabylie (Aissa 1997; Kolli 1997b; Boutaleb et al. 2000). while later Eo-Alpine events influenced similar deposits in Grande Kabylie (Marignac, Zimmermann 1983)where the crystalline massifs host mineral deposits that occur as both vein-type in gneiss and schists and stratiform deposits within carbonate formations, enriched in Ba, F, Pb, Zn, Fe, and Cu (Kolli 1997b). Among these, the Oued Bibi deposit, hosted in dolomitic carbonates, stands out for its high lead and zinc content, along with significant silver enrichment, making it a priority for further exploration (Bolfa 1948)

- **Mineralization associated with magmatism.:** this type of mineralization is Volcanogenic massive sulfide (VMS), it is associated with Miocene magmatic activity (Benali 2007) ,these mineralizations are located in stress relaxation zones are closely linked to Neogene tectonic contexts, including extensional phases, detachment faults, contemporary magmatic activity, and associated hydrothermal circulation. These processes are particularly evident in the volcano-plutonic regions along the Algerian coast, where hydrothermalism plays a key role in ore formation. Major occurrences include the deposits of Oued El Kébir, Boussoufa, and Oued Amizour, as well as the pyrite masses in central Petite Kabylie and the Edough Massif. (Belanteur 2001; El Azzouzi et al. 2003; Laouar et al. 2018; Lekoui et al. 2018)
- **Mineralization unrelated to volcanic activity** specifically, low- and high-sulfidation types linked to late-stage volcanism and epithermal processes (Aissa 1997; 1998) appears to result from constraints that facilitated the flow of hot mineralizing fluids. These fluids were channeled into favorable structures formed by vertical tectonics during the Fini-Langhian phase, a mechanism similar to that observed in the Miocene deposits of the Edough region (Aissa et al. 1995). Notably, only a few vein deposits have demonstrated significant economic potential, with reserves exceeding one million tones.
- **Mineralization with spatial links to volcanism:** This group comprises polymetallic deposits of medium to potentially high temperature, forming in quartz carbonate veins

that occur in conjunction with Neogene magmatic activity along the Algerian coast. Deposits either hosted by granitoid rock, such as those at Bou-Doukha or found in their vicinity (e.g., Aïn Barbar and Kef Oum Teboul) exhibit paragenetic features that differ from those exclusively contained within carbonate sequences, which are typically characterized by sphalerite and galena with a baryte gangue.

- **Stratabound-Type Mineralization:** Epigenetic mineralization occurs in carbonate formations such as Nérétique Constantinois, Sétifien-Hodna, Belezma-Aurès, and areas associated with diapirism, comparable to Mississippi Valley-Type (MVT) deposits (Boutaleb et al. 2000; Leach et al. 2005). The Pb-Zn ± Cu ± Ba ± F deposits, along with vein-type mineralization, have historically accounted for up to 80% of Algeria's Pb-Zn production. These deposits are primarily concentrated in the Mesozoic-Cenozoic basins of the Hauts Plateaux and the Saharan Atlas, spanning over 1,000 km, with an estimated total production exceeding 20 Mt of Pb-Zn. The mineralization is epigenetic and polyphased, with the main event occurring during the Eocene. Mineralizing fluids are hot and saline, originating from basin environments. These deposits represent a key focus for exploration programs targeting Pb-Zn resources, particularly in known mining districts and nearby occurrences.

Chapter 3: Spatial Analysis of Structural Controls on Mineralization

1. Introduction:

This chapter focuses on the spatial analysis of fault structures and their relationship with known mineralization occurrences across the study area of northeastern Algeria, which has been divided into five distinct geological zones: the neritic Constantine, Hodna and South Setif, diapiric zone, littoral magmatism, and Monts of Aurès. Utilizing GIS-based spatial analysis tools, the distribution patterns of identified fault networks are examined within each zone to understand their density, orientation, and proximity to known mineral deposits. This investigation aims to elucidate potential structural controls on mineralization, exploring the spatial associations between fault systems, which can act as conduits for ore-forming fluids, and the documented locations of mineral occurrences within each of the defined geological domains. The findings of this spatial analysis provide critical insights into the structural framework influencing mineralization and contribute to a more refined understanding of the region's metallogenic evolution, laying the groundwork for subsequent prospectivity modeling efforts.

2. Fry method

Fry analysis is a geometric method of spatial autocorrelation used to study the spatial distribution and relationships of point data, such as mineral deposits (Fry 1979). It involves analyzing the distances and orientations between points to identify patterns, trends, and potential geological controls(Smith, Gardoll 1997; Wang, Zuo, Zhang 2015; Zheng et al. 2020). Originally designed for strain analysis, Fry analysis is widely applied in mineral exploration to assess mineralization trends associated with linear structures

2.1. Rationale for Using Fry Analysis in the Northeast Algeria Pb-Zn Study

Fry analysis was chosen for this study to investigate the spatial distribution and structural controls of Pb-Zn mineralization in northeast Algeria, a region characterized by carbonate-hosted deposits (Boutaleb 2001; Ysbaa et al. 2020). Given the large scale of our study area and the diverse mineralization styles observed, this method provided a systematic approach to assessing spatial relationships with geological structures, helping us identify key ore-controlling factors such as faults, fractures (Vearncombe, Vearncombe 1999). Its ability to reveal preferred ore body orientations linked to regional tectonics made it particularly valuable for understanding mineralization patterns. Additionally, Fry analysis complemented other geostatistical techniques by offering detailed geometric insights into deposit distribution, enhancing our interpretation of metallogenic processes at both regional and deposit scales (Carranza 2009).

The objectives of these analyses is to illustrate exploratory spatial data analysis of mineral deposit point patterns were to:

(i) establish if the spatial intensity of gold mineralisation significantly varied across each study region;
(ii) investigate any spatial clustering of gold mineralisation at different scales; and
(iii) in case of a significant regional linear spatial heterogeneity, identify likely major metallogenic controls on the spatial distribution of the orogenic gold mineralisation.

2.2. Methodological Steps

We divided the study area into five main mineral districts where ore accumulation is more distinct. To analyze the spatial relationships of the Pb-Zn deposits, we applied the Fry method. This involved assessing the distances and orientations between pairs of deposits by plotting them on a Fry diagram. The analysis allowed us to identify spatial patterns such as clustering and alignment, providing insights into the structural controls and tendencies of mineralization within the study area.

The objectives of these analyses were to conduct an exploratory spatial data analysis of Pb-Zn deposit point patterns in northeast Algeria, specifically to:

(i) determine whether the spatial intensity of Pb-Zn mineralization significantly varies across the five identified mineral districts;

(ii) investigate the presence of spatial clustering or alignment of Pb-Zn deposits at different scales;

(iii) in the case of significant regional linear spatial heterogeneity, identify the likely major structural or metallogenic controls influencing the spatial distribution of the carbonate-hosted Pb-Zn mineralization.

2.3. Structural and Spatial Anisotropy Analysis

Fry analysis is particularly useful at both regional and deposit scales. At the regional scale, it helps assess distribution patterns of mineralization and their relationship with controlling structures (Fry 1979). At the deposit scale, it provides insights into ore zone characteristics like spacing, directionality, high-grade zones, and grade distribution. The method is effective in identifying directional anisotropy and multiple preferred orientations at different scales, making it an alternative to variography for directional studies (Carranza 2009; Vearncombe, Vearncombe 1999).

Spatial Analysis of Structural Controls on Mineralization

To complement the Fry analysis and further investigate directional controls on mineralization, we constructed rose diagrams for both Pb-Zn deposits and faults. For deposits, the rose diagram quantified the azimuthal distribution of their spatial alignment, revealing dominant directional trends that may correlate with regional tectonic structures. For faults, the rose diagram mapped their strike orientations to identify principal structural trends in the study area. By comparing these diagrams, we assessed whether deposit alignment patterns align with fault orientations, providing insights into potential structural pathways for mineralizing fluids. This dual analysis enabled us to evaluate whether fault systems exerted a primary control on the spatial distribution of Pb-Zn mineralization, addressing objective (iii) by linking observed linear heterogeneity to geological drivers the results are shown in figure 8, 9

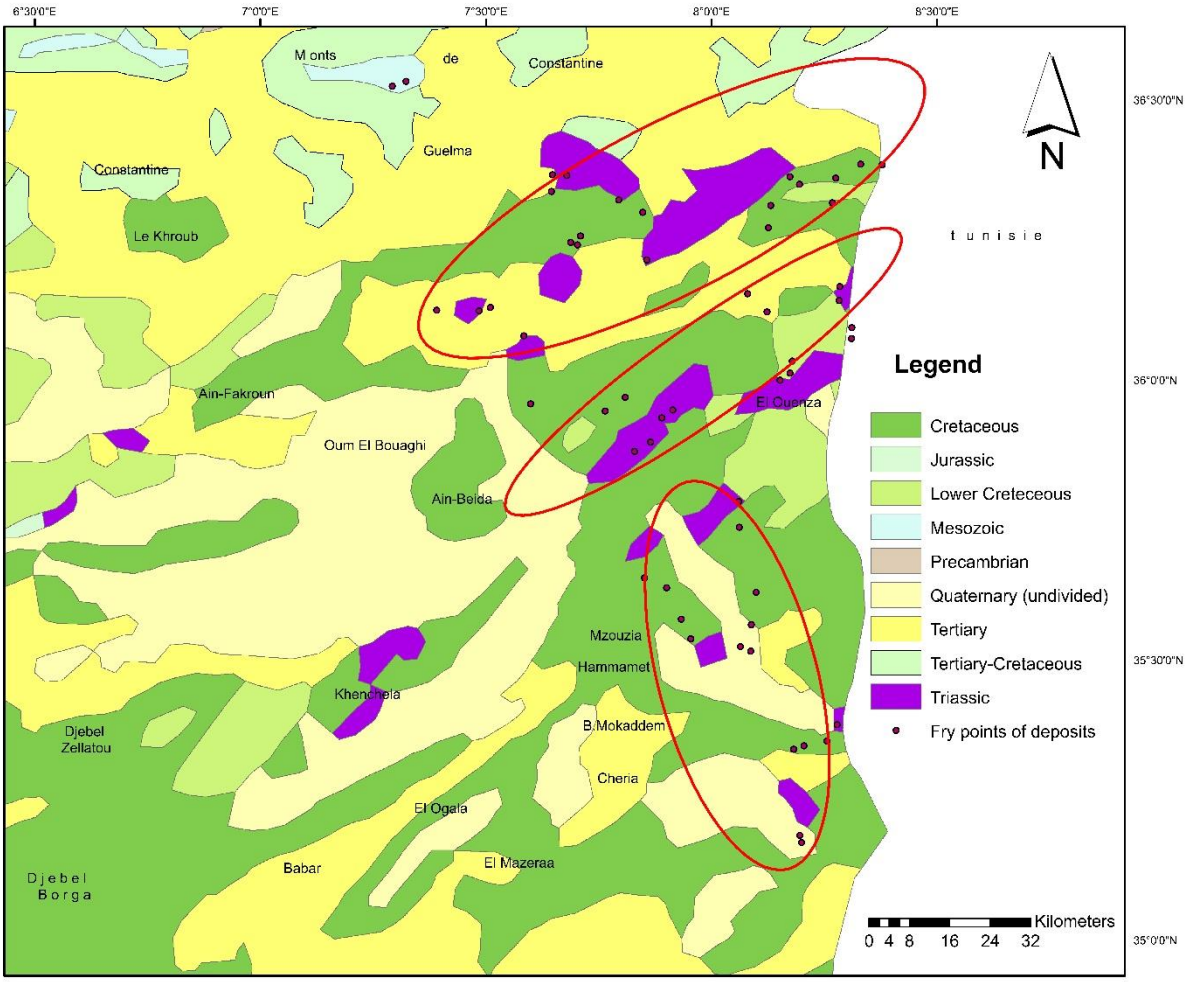

Figure 8: Spatial Distribution of Pb-Zn Deposits and Fry Points within the Diapiric Zone.

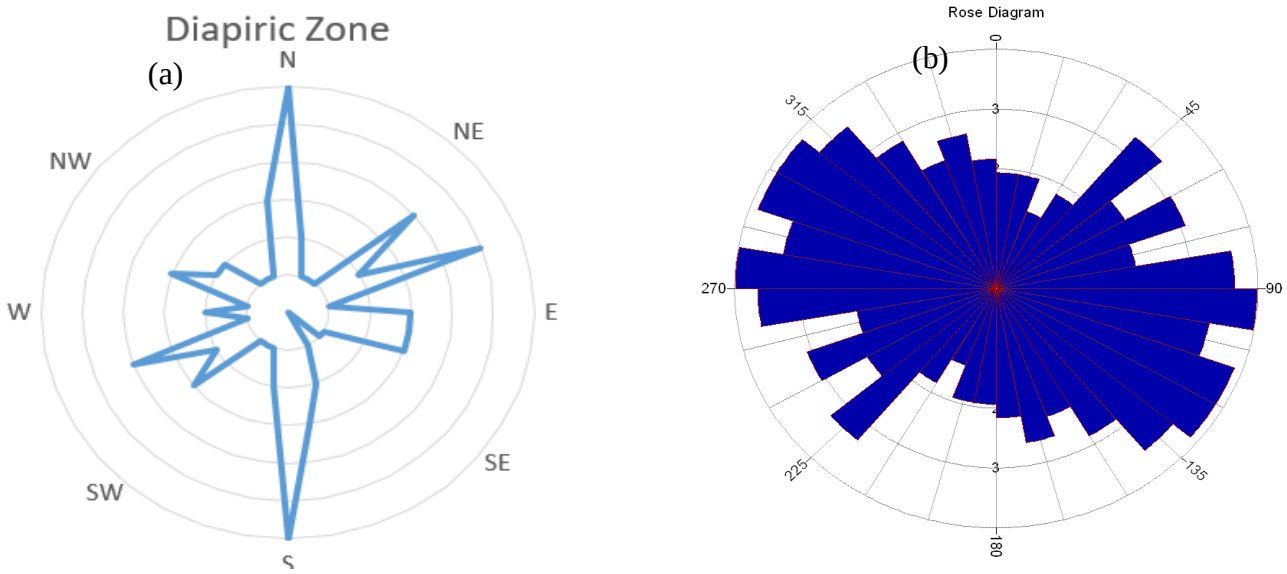

Figure 9: (a) Polar Histogram of Fry Analysis Point Trends, (b) Rose Diagram of Fault Orientations within the Diapiric Zone.

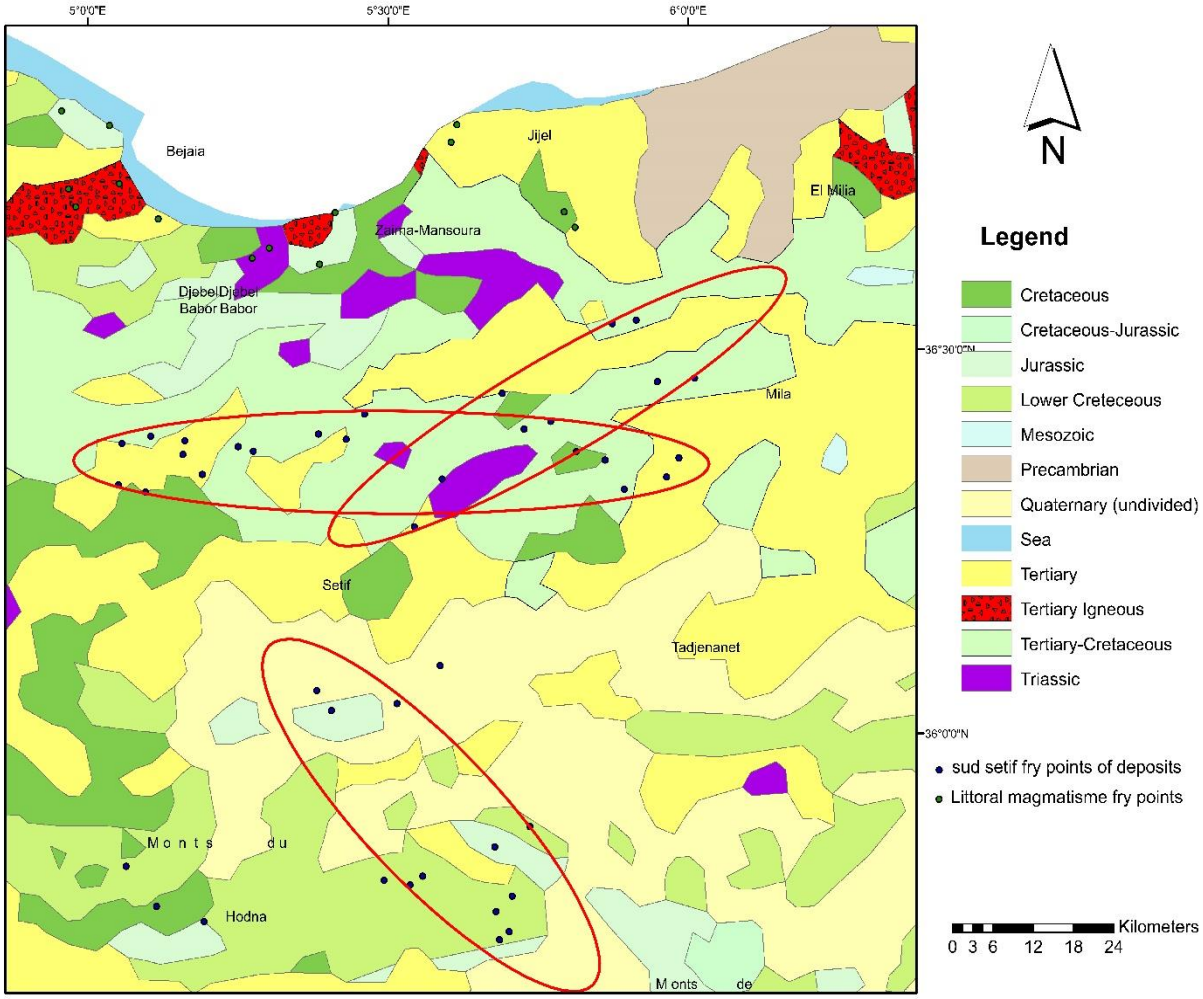

Figure 10: Spatial Distribution of Pb-Zn Deposits and Fry Points within the South setifian and littoral magmatism

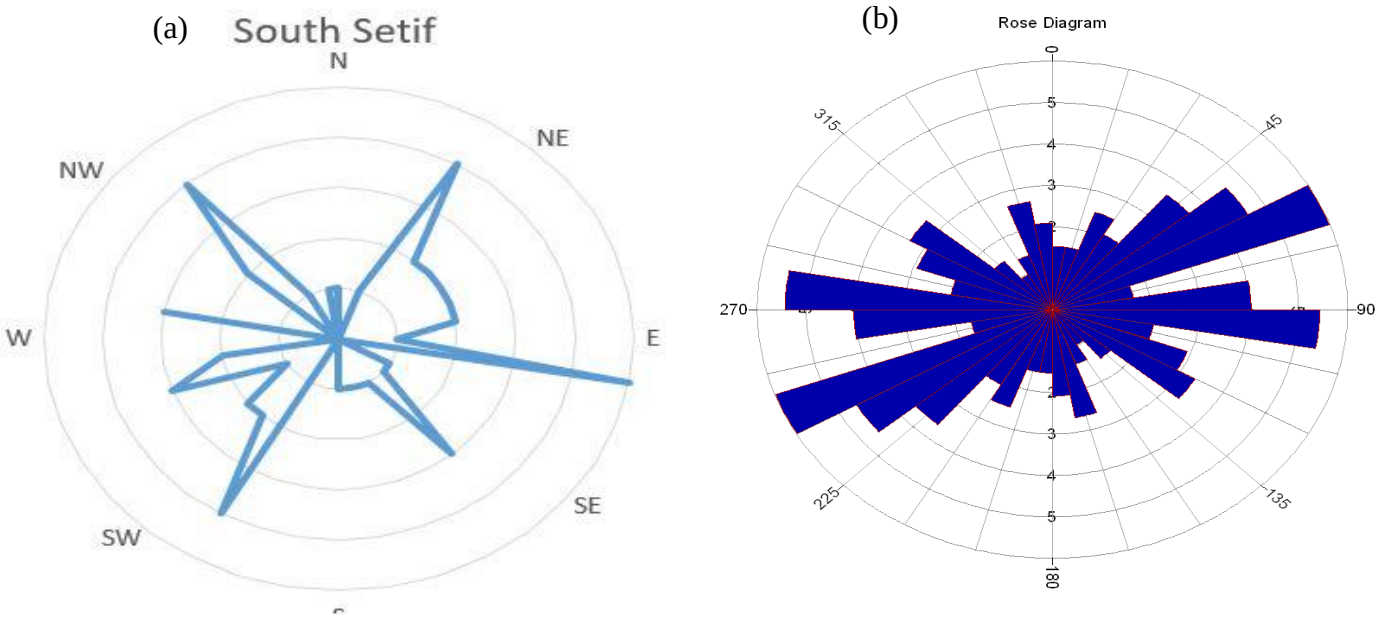

Figure 11: (a) Polar Histogram of Fry Analysis Point Trends, (b) Rose Diagram of Fault Orientations within the South Setifian and Hodna region

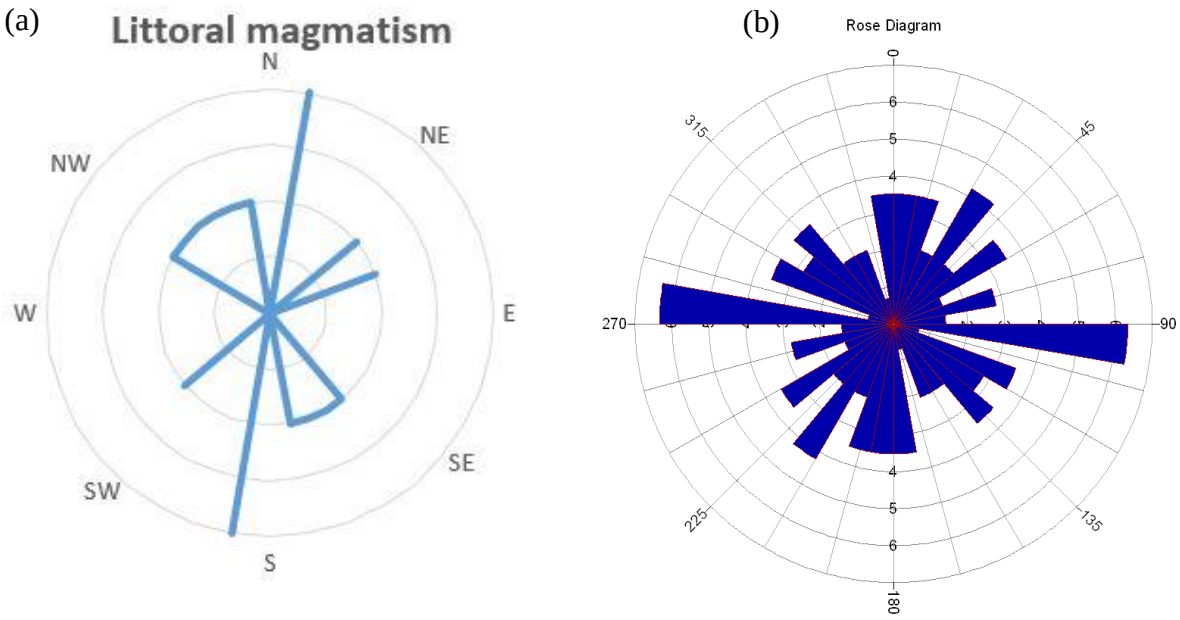

Figure 12: (a) Polar Histogram of Fry Analysis Point Trends, (b) Rose Diagram of Fault Orientations within the Littoral magmatism region.

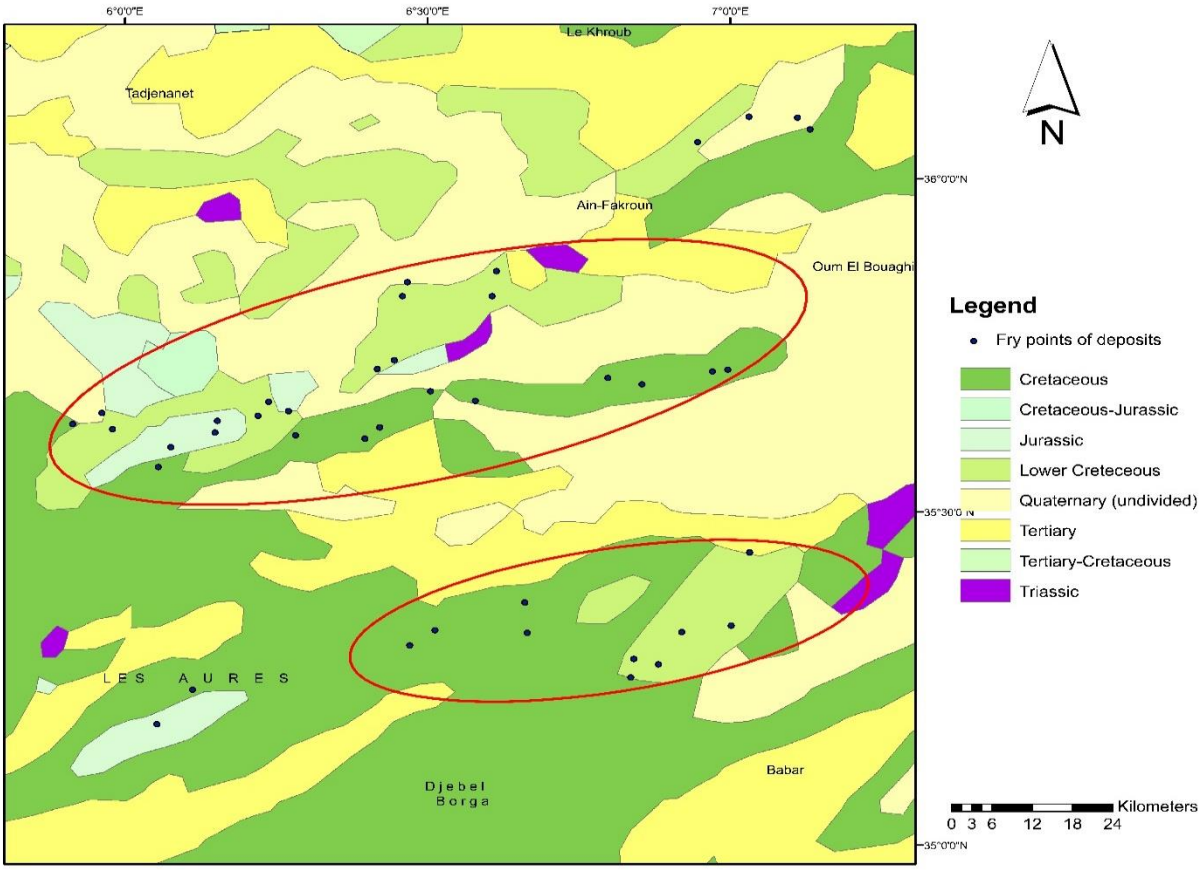

Figure 13: Spatial Distribution of Pb-Zn Deposits and Fry Points within the Mounts of Aures

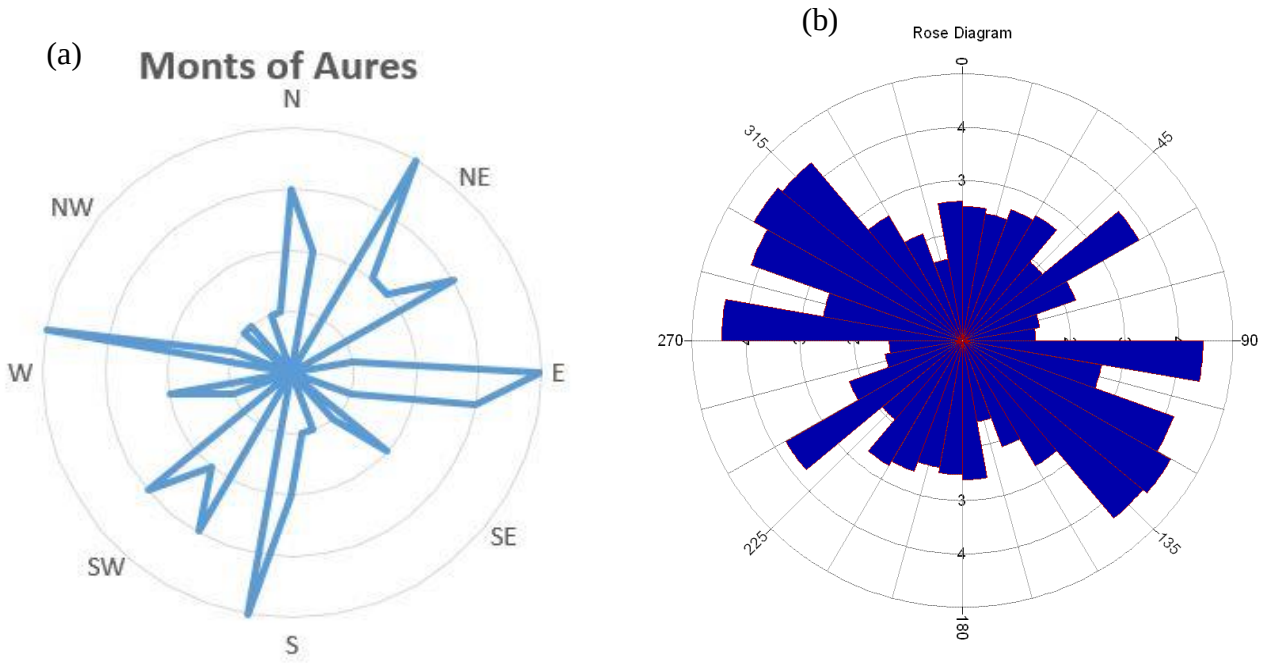

Figure 14 : (a) Polar Histogram of Fry Analysis Point Trends, (b) Rose Diagram of Fault Orientations within the Mount of Aures .

2.4. Applications and Interpretation

Rose Diagram Analysis of Faults and Mineral DepositsThe figures illustrate the Fry point analysis of mineral deposits across the five main mineral districts within the study area. This analysis was conducted to assess the relationship between tectonic structures and the spatial distribution of orebodies.

Coastal deposits: For deposits associated with magmatic activity, the Fry point patterns reveal a random distribution. This randomness can be attributed to the Neogene tectonic context, where related mineralization typically occurs in zones of stress release (such as extensional areas, detachment faults, active magmatic settings, and associated convective hydrothermal systems). These conditions are particularly evident in the volcano-plutonic regions along the Algerian coast, where hydrothermal processes have played a major role in ore formation. Notable examples include Oued El Kébir, Boussoufa, Oued Amizour, as well as the pyrite-rich massive sulfide deposits of central Petite Kabylie and the Edough massif (Boutaleb, Aissa, Omar 2023; Gravelle 1959; Kolli 1997c; Lekoui 2019).

The rose diagram displays a clear dominant N–S alignment in the spatial distribution of ore deposits associated with littoral (coastal) magmatism. Secondary orientations are observed in the NW–SE and NE–SW directions, though they are less pronounced; the N–S structural controls (e.g., large faults or tectonic lineaments) likely dominated the emplacement of the magmatic bodies and associated mineralization to a great extent. The secondary directions (NW–SE and NE–SW) may be explained as subsidiary fracture systems or cross-cutting faults that helped in fluid flow or ore accumulation. The orientation is consistent with Neogene extensional tectonics in the Algerian coastal regions, producing crustal thinning zones, magmatic rise, and hydrothermalism. These directions can also be coincident with detachment faults or strike-slip fault systems that were active during or after magmatic emplacement.

Diapiric zone : Fry point pattern analysis of the deposits in this zone reveals three distinct mineral groupings forming elliptical clusters. In the southern area, an elliptical arrangement oriented NE contains 15 deposits**,** suggesting a collapsed structure. In the northern part, two parallel elliptical patterns oriented NE–SW are observed. These spatial trends align with (Haddouche et al. 2016) findings, which emphasize the existence of significant regional structural corridors governing the distribution of mineralization, are consistent with these spatial trends. Specifically, Pb-Zn (±Ba) deposits are concentrated along NE-SW trending zones that border sedimentary basins that are subsiding. Major NE-SW faults, which are frequently intersected by NW-SE fault systems, are the usual locations for mineralization. Furthermore, deposits are frequently discovered on the flanks of anticlinal hinge zones. Ore occurrences hosted in Aptian limestones are spatially related in the diapiric zone.

Spatial Analysis of Structural Controls on Mineralization

Hodna and Southern Setif: Fry point analysis of the mineralized indices in the Hodna and southern Sétif area reveals three elliptical groupings, predominantly oriented SE. The rose diagram of fault trends highlights two preferred orientations: NW–SE and E–W. (Ysbaa, Nedjai, et al. 2019) whose interpretation of aeromagnetic and gravimetric data confirmed that the mineralized zones are closely associated with tectonic lineaments of the same orientations, supports these structural trends. The geophysical analyses further indicate that these deposits are located near or along major folded structures, which are attributed to a late Eocene compressional tectonic event.

Saharian atlas/ Mount of Aures: This region is characterized by two groups of mineralized zones forming elliptical clusters that are linearly associated and predominantly oriented E–W, closely following a major fault system. This alignment is confirmed by the rose diagram of fault distribution, which shows dominant trends in the E–W, NW–SE, and NNW–SSE directions. These structural trends reflect a complex tectonic regime marked by the presence of both dextral strike-slip faults and normal faults, suggesting a combination of horizontal shearing and vertical extension.

The E–W faults, in particular, appear to have played a major role in controlling the localization of mineralization, acting as pathways for hydrothermal fluids. The NW–SE and NNW–SSE orientations may correspond to older inherited structures or secondary fault systems that further influenced mineral deposition. This structural setting is consistent with the regional tectonic evolution of the Saharan Atlas, especially during post-Hercynian reactivation and Neogene tectonic phases, which favored fracturing, faulting, and the formation of mineralized zones along these corridors. (Boutaleb 2001; Kazi-Tani 1986; Sami 2011; Vila 1980; Ysbaa et al. 2020)

3. Conclusion

The spatial distribution analysis of Pb-Zn mineralization, based on Fry point patterns and rose diagram interpretation, has provided valuable insights into the geological controls governing polymetallic deposits across northeastern Algeria. The alignment and clustering of deposits observed in the Fry diagrams, when compared with the orientations of regional faults, reveal a strong correlation between mineralization trends and structural frameworks, particularly along major fault systems, fold axes, and thrust zones.

In the Sétifian–Hodna domain, composed primarily of Mesozoic and Tertiary autochthonous formations, mineralized bodies (e.g., Abiane, Aïn El Kahla, Chabet El Hamra, Kherzet Youcef, and Gouzi) predominantly follow NW–SE and E–W tectonic corridors. These deposits typically occur as vein-type, lenticular, or stratabound concentrations located along or adjacent to faults,

especially at the margins of subsiding sedimentary basins. This region, along with the Eastern Saharan Atlas, hosts epigenetic MVT-type (Mississippi Valley-Type) deposits, reflecting post-sedimentary hydrothermal emplacement controlled by extensional tectonics and tilted block fault systems (Haddouche, Boutaleb, Benhamoud 2015; Herkat 1999; Ysbaa, Nedjai, et al. 2019).

In the diapiric zone, mineralization occurs within Aptian limestones, spatially associated with Triassic salt structures and aligned with NE–SW to E–W trending faults (Perthuisot, Rouvier 1992; Rouvier 1990; Ysbaa, Nedjai, et al. 2019). These structural traps reflect deeper tectonic processes and fluid migration along long-lived lineaments.

The littoral zones, particularly along the volcano-plutonic massifs of northern Algeria (e.g., Oued Amizour, El Aouana, Edough, and Petite Kabylie), exhibit mineralization linked to Neogene extensional tectonics, magmatic intrusions, and associated hydrothermal convection systems (Benali 2007; Kolli 1997c; Leach et al. 2001; Semroud 1993). These settings are characterized by distensional faulting, detachment structures, and active magmatism, favoring ore concentration in zones of stress release.

Faults of N–S orientation are rare in the southeastern Constantinois, generally associated with younger Pliocene tectonic phases (Bles 1969; Bolfa 1948)

Overall, the study confirms that mineralization in northeastern Algeria is structurally controlled, with deposits typically located along the margins of tectonically and/or sedimentologically subsiding basins (Boutaleb et al. 2000; Touahri 1987). The integration of spatial analysis with structural geology not only improves our understanding of ore distribution but also aids in delineating new exploration targets in similar tectonic settings.

Chapter 4: Data & Methods

1. Introduction

This chapter details the methodological framework employed for mineral prospectivity mapping of Pb-Zn deposits in northeastern Algeria. The study integrates both knowledge-driven and data-driven approaches, leveraging the capabilities of Geographic Information Systems (GIS) for spatial data management and analysis. This section outlines the specific methodologies adopted, including the preparation of the multi-source geoscience datasets, the conceptual basis for each modeling technique, and the procedures for model implementation and validation.

These machine learning models analyze the statistical and spatial associations between known mineral deposits and the conditioning geological factors (predictor maps), allowing for the quantification of mineral potential in unexplored regions. The hybridization of expert knowledge and data-driven intelligence aims to maximize model robustness, reduce bias, and improve the generalizability of the mineral prospectivity outputs.

2. Data preparation:

This mineral prospectivity mappingstudy for Pb-Zn deposits in northeastern Algeria is lies in the compilation and preparation of a comprehensive spatial dataset encompassing critical geological factors associated with ore genesis. The dataset draws upon established geological knowledge, verified mineral occurrences, and relevant spatial information, thereby providing a scientifically robust foundation for a geologically informed analysis.

2.1. Data Sources and Collection:

The primary data sources for this study include geological maps, field survey data, and geological reports previously elaborated by the National Office of Geological Infrastructure (ONIG) and the Agency of the Geological Service of Algeria (ASGA) (as detailed in Tab. 03). The data collection process involved a meticulous selection of geological features considered pertinent to Pb-Zn mineralization in the study area. These features encompass both lithological and geodynamic factors, including but not limited to the features used in this study , it involves lithology of favorable host rocks (like carbonates), proximity to major fault systems, fault density, proximity to fold axes, proximity to thrust faults, geological age of key formation

Table 3: Source of the elaborated factors

Factor	Source
Lithology (age)	Assembly of interpretative geological maps of Algeria prepared by the National Agency for Hydraulic Resources (NAHR)1:200 000 (2008)
Thrust	Structural map of the Alpine Chain; Eastern Algeria and Algero-Tunisian borders1:500 000 by Villa (1978)
Faults	Assembly of interpretative geological maps of Algeria by the National Agency for Hydraulic Resources 1/200 000 (2008)
Economy	Map of Mineral Deposits in Algeria, Constantine North 1:500 000 by National Office of Geology (ONIG)
Folds	Assembly of interpretative geological maps of Algeria prepared by the National Agency for Hydraulic Resources 1/200,000 (2008)
Geothermal gradient map	Geothermal Gradient Map (remote sensing derived images) from United States Geological Survey (USGS, 2020).
Metallogenic map	Elaborated after (Boutaleb, Aissa, Kolli 2023) researchs

2.2. Data Processing and Integration into GIS:

The Geographic Information System (GIS), utilizing Arcmap software, served as the central platform for spatial data integration and analysis (Longley 2005). The methodology involved the digitization of various geological maps, each representing a distinct conditioning factor relevant to polymetallic mineralization. These digitized maps were transformed into individual, spatially referenced data layers within the GIS. Subsequently, a comprehensive database was constructed, where known Pb-Zn deposits were represented as point features, each overlaid with the corresponding values extracted from the thematic geological layers. This spatially integrated database, facilitated both the visualization of complex geological relationships and the development of the final predictive model for mineral prospectivity.

The dataset preparation involves collecting all relevant data related to geological features that may influence the ore formation;

- Labeling: identifying the known deposits from different geological maps, field surveys, geological reports; these deposits will be used as training samples

- Data collection: select all geological features associated with mineral potential such as lithology and geodynamic factors, digitalization of all the existing maps and numerical extraction of the values

- Data processing: remove the errors; complete the missing values by processing geostatistical interpolation and normalizing values

The following figure presents the normalized dataset, stored in CSV format and ready for use in machine learning applications

	A	B	C	D	E	F	G
1	catégorie	age	densité faille	distance faille	grad thérm	Plis	Chevauchement
2	1	0,25	0,197198803	0,118484208	0,630097251	0,237508094	0,021694414
3	0,25	0,25	0,456520656	0,009201312	0,753160615	0,833787267	0,214785946
4	0,25	0,25	0,438813048	0,032588445	0,751638454	0,821298931	0,227839737
5	0,25	1	0,592805766	0,019191901	0,739146134	0,749662743	0,223314338
6	0,75	1	0,444864066	0,020443812	0,7189978	0,709793114	0,262546523
7	0,25	0,5	0,060882117	0,213534177	0,711516933	0,743674068	0,147366632
8	0,25	0,25	0,572362458	0,019712012	0,75388532	0,997938389	0,024347064
9	0,25	0,25	0,414401215	0,005526818	0,753720743	1	0,024787843
10	0,25	0,5	0,274952651	0,010217824	0,755126278	0,877825746	0,050044999
11	0,25	0,5	0,39477383	0,000254388	0,763100903	0,901993822	0,033625923
12	0,25	0,5	0,189273279	0,014189046	0,768299548	0,923984013	0,037153013
13	0,25	0,5	0,215354843	0,031429674	0,779819929	0,879329087	0,081906989
14	0,25	0,25	0,252207788	0,024808633	0,780321437	0,874662339	0,108723871
15	0,25	0,25	0,216794226	0,069849967	0,785315303	0,8548923	0,096470539
16	0,25	0,5	0	0,347611767	0,772248027	0,901329766	0,158040741
17	0,5	0,5	0,0139866	0,209574851	0,781607732	0,868772486	0,129368284
18	0,5	0,5	0	0,551367843	0,782754827	0,783078644	0,061347475
19	0,25	0,25	0	0,468470305	0,791305113	0,733683581	0,006605233
20	0,25	0,5	0	0,413719724	0,796906414	0,699734865	0,009687687

Figure 15: Normalized Input Dataset for Machine Learning-Based Mineral Prospectivity Modeling

2.3. Training and validation deposits:

For the data driven methods; This study leverages a dataset meticulously prepared to capture the geological controls on ore formation. The labeling of data points involved the precise identification of known mineral deposits using a combination of geological maps, field observations, and comprehensive geological reports. The resulting dataset of 514 locations, encompassing both deposit and non-deposit instances, was strategically split into a training subset (385 points) as illustrated in figure 16 for model learning and a held-out testing subset (129 points) for unbiased performance evaluation. The selection of input features prioritized geological attributes directly implicated in mineral potential, including detailed lithological

descriptions and key geodynamic parameters. The acquisition of these features involved the digitization of relevant geological maps and the numerical extraction of associated spatial data. Prior to modeling, the data underwent thorough processing, including error correction, the application of geostatistical Kriging interpolation to address missing values, and normalization to standardize the feature scales for effective machine learning algorithm training**.**

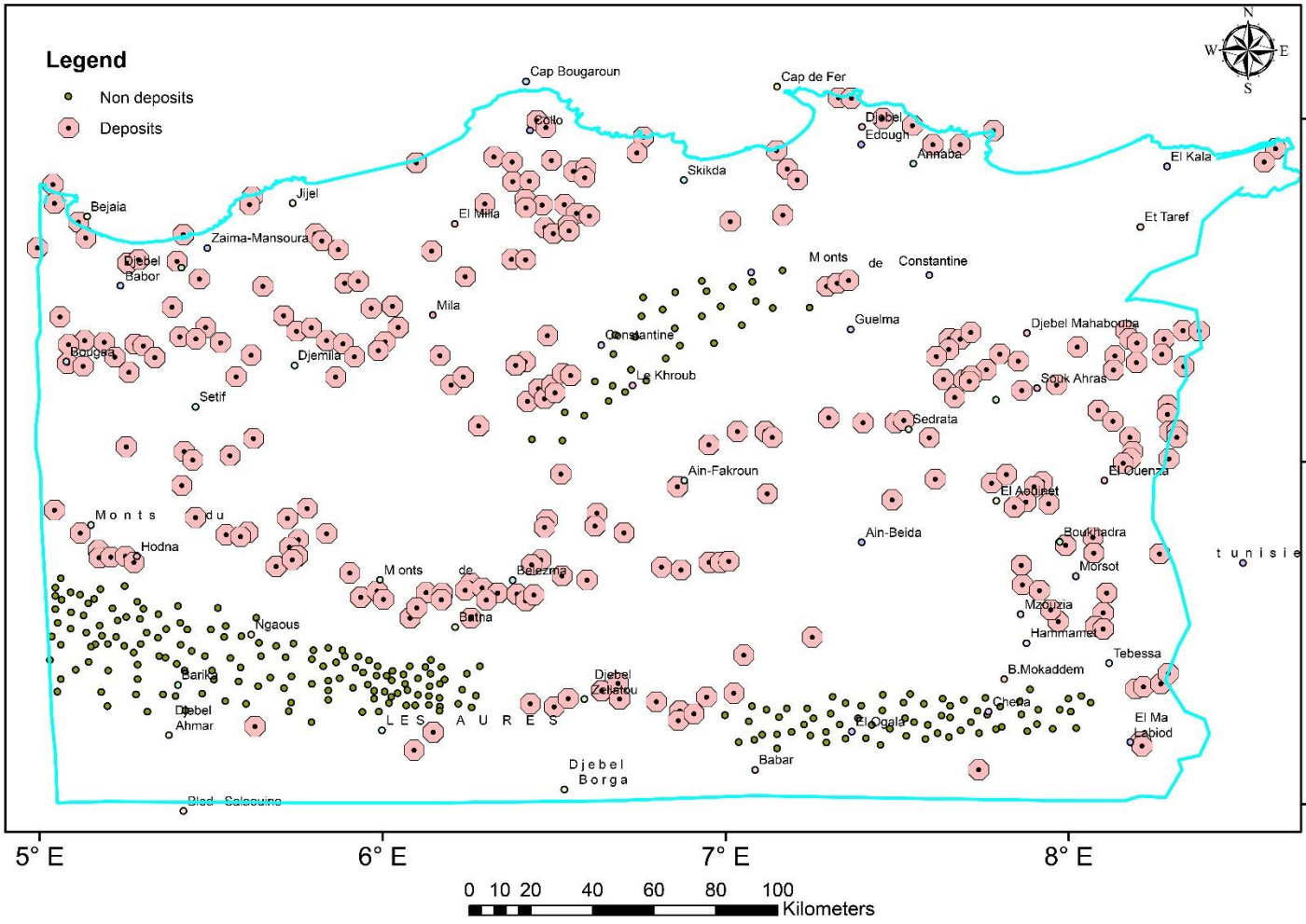

Figure 16: Map representing the distribution of Pb Zn deposits and non-deposit locations in the Northeast Algeria

2.4. Conditioning factors:

Polymetallic mineralization ore formation is a complex geological process intricately controlled by a confluence of several key conditioning factors. These factors, as highlighted by previous studies of (Wyborn, Heinrich, Jaques 1994; Blevin, Chappell, Allen 1996; Boutaleb 2001; Haddouche, Boutaleb, Benhamoud 2015; Sadeghi et al. 2019) can be broadly categorized as lithologic, geodynamic, geochemical, and metallogenic features. Understanding the individual roles and synergistic interactions of these controls is fundamental to unraveling the genesis of polymetallic deposits and effectively targeting prospective areas.

In the present study, the dataset was constructed based on key conditioning variables, including geological age, deposit type, metallogenic context, proximity to folds and faults, fault density, proximity to thrust zones, and geothermal gradient. Each of these factors is represented through a spatial predictor layer, reflecting the inherently geographic nature of mineral prospectivity analysis. The selection of the mappable exploration criteria has been meticulous, considering their role in the mineral accumulation process and the formation of polymetallic deposits. Correlations are established based on their proximity to major tectonic features, geological structures, and lithological features.

2.4.1. Lithological factors: They offer insights into the age of mineralization or the rocks hosting minerals. Each geological period is characterized by specific events related to the formation of ore deposits, and they have been classified according to their contribution to mineral occurrence as follows, from the strongest to the weakest influence: Cretaceous, Jurassic, Triassic, Paleozoic, Tertiary, Quaternary.

2.4.2. Economic factors: Economic factors play a crucial role in this MPM, with mineral occurrences classified into five distinct categories based on their estimated Pb-Zn ore reserves (Fig. 4). Category 0 denotes non-deposit locations. Categories 1 through 4 represent increasing levels of economic significance: Category 1 includes substantial deposits (>300,000 tons), Category 2 comprises medium-sized, exploitable deposits (30,000 - 300,000 tons), Category 3 encompasses artisanal or small-scale deposits (<30,000 tons), and Category 4 identifies mineral indices of potential metallogenic interest but with limited reserves (<1,000 tons). The resulting deposit category layer, derived from previous prospecting and geological reports (ASGA map summarized in Table 1), serves as a primary exploration criterion in our integrated numerical model, directly reflecting the economic potential of known mineralizations.

2.4.3. Geodynamic factors: Geodynamic factors encompass the structural and tectonic features that play a crucial role in the formation and localization of polymetallic mineralization. In this study, these factors are represented through several spatial predictor layers derived from geological and structural data, including faults, thrusts, folds, and their associated metrics (e.g., proximity and density).

- **Faults layer**: Faults, as illustrated in Figure 17a, are among the most prominent structural features influencing mineralization. Two predictor maps were derived from the fault dataset: the proximity to faults (Figure 18c), computed using Euclidean distance, and fault density (Figure 18b), which reflects the spatial frequency of faulting across the study area. The faults are predominantly oriented NW-SE in the Hodna and Belezma regions, and NE-SW/NW-SE in the Batna–Aurès and Tébessa Mountains, often intersecting or aligning with deep-seated tectonic structures and diapiric zones (Haddouche et al., 2016; Ysbaa et al., 2019). These structures are considered significant pathways for hydrothermal fluid migration and are therefore critical to the distribution of Pb-Zn mineralization.
- **Thrust Zones layer:** Thrusts are structural features resulting from intense compressive tectonic forces and are also included in the geodynamic analysis (Figure 17b). The

proximity to thrusts was used as a predictor layer. Thrust zones contribute to enhanced rock fracturing and increased permeability, thus facilitating the movement of ore-bearing fluids and creating favorable conditions for mineral deposition.

Folds layer: Folds, represented in Figure 17b, are considered another key geodynamic feature. A **proximity to folds** map (Figure 17d) was generated to evaluate their spatial relationship with known mineralized zones. Folds are significant for several reasons: they can act as conduits for hydrothermal fluids, enhance the permeability of host rocks, and create structural traps that concentrate ore minerals (Baratoux et al. 2005). Additionally, fold-related deformation can impact diagenetic processes and promote thermal gradients, which are essential in facilitating the transport and precipitation of Pb-Zn minerals (Evans, Fischer 2012)

4.4.5. Metallogenic factors: To incorporate the regional metallogenic context and genetic controls on Pb-Zn mineralization, known deposits and their formation conditions have been classified into five distinct types (Fig. 17c). This categorization, ordered from the weakest to the strongest perceived influence on mineral occurrence, includes: (1) Mineralization related to the metamorphic basement, (2) Mineralization associated with magmatism, (3) Mineralization spatially linked to volcanism, (4) Mineralization occurring independently of volcanic activity, and (5) Stratabound-type mineralization. This framework facilitates the evaluation of areas with geological characteristics analogous to known productive metallogenic settings.

- **Geothermal Gradient Map**: The geothermal gradient, illustrating the rate of temperature increase with depth (Fig. 17d), provides a crucial insight into subsurface thermal regimes, a key factor governing mineral formation. Elevated temperatures drive the circulation of hydrothermal fluids, particularly within fracture networks created by tectonic activity. As these hot, metal-bearing fluids ascend and cool, changes in temperature induce various crystallization phases and alter their chemical composition, ultimately leading to the precipitation and accumulation of ore minerals.

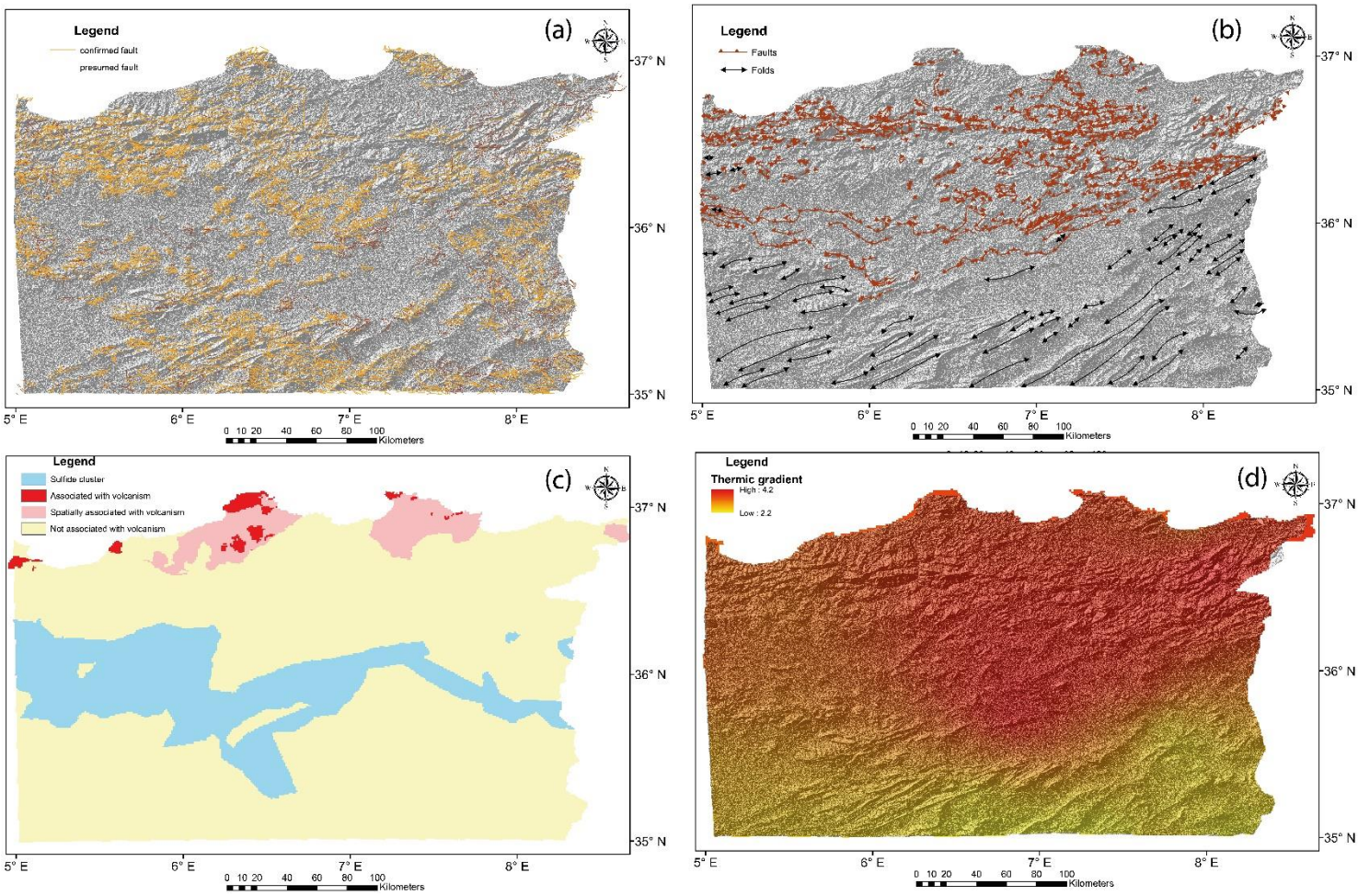

Figure 17: Conditioning factors for targeting criteria: (a) tectonic features for exploration targeting criteria confirmed faults and presumed faults, (b) Folds and thrusts, (c) Metallogenic formation , (d) Geothermal gradient map

2.5. Normalization of predictor maps:

To ensure equitable contributions from each conditioning factor in the subsequent analysis and to mitigate potential overfitting during model training, the raw data for each factor underwent a min-max normalization procedure, as described by Dogan et al. (2008). This method scales the original values (X) linearly to a standardized range between 0 and 1 using the equation:

$$X' = \frac{X - X_{min}}{X_{max} - X_{min}}$$

where X' represents the normalized value, and X_max and X_min are the maximum and minimum values observed for that specific conditioning factor across the dataset. Following normalization, the processed data for all conditioning factors, along with the binary classification labels (deposit/non-deposit), were integrated into a tabular format, ready for ingestion by the chosen binary classification algorithm. Representative sample maps illustrating the spatially distributed values of the normalized targeting criteria are presented in Figure 18

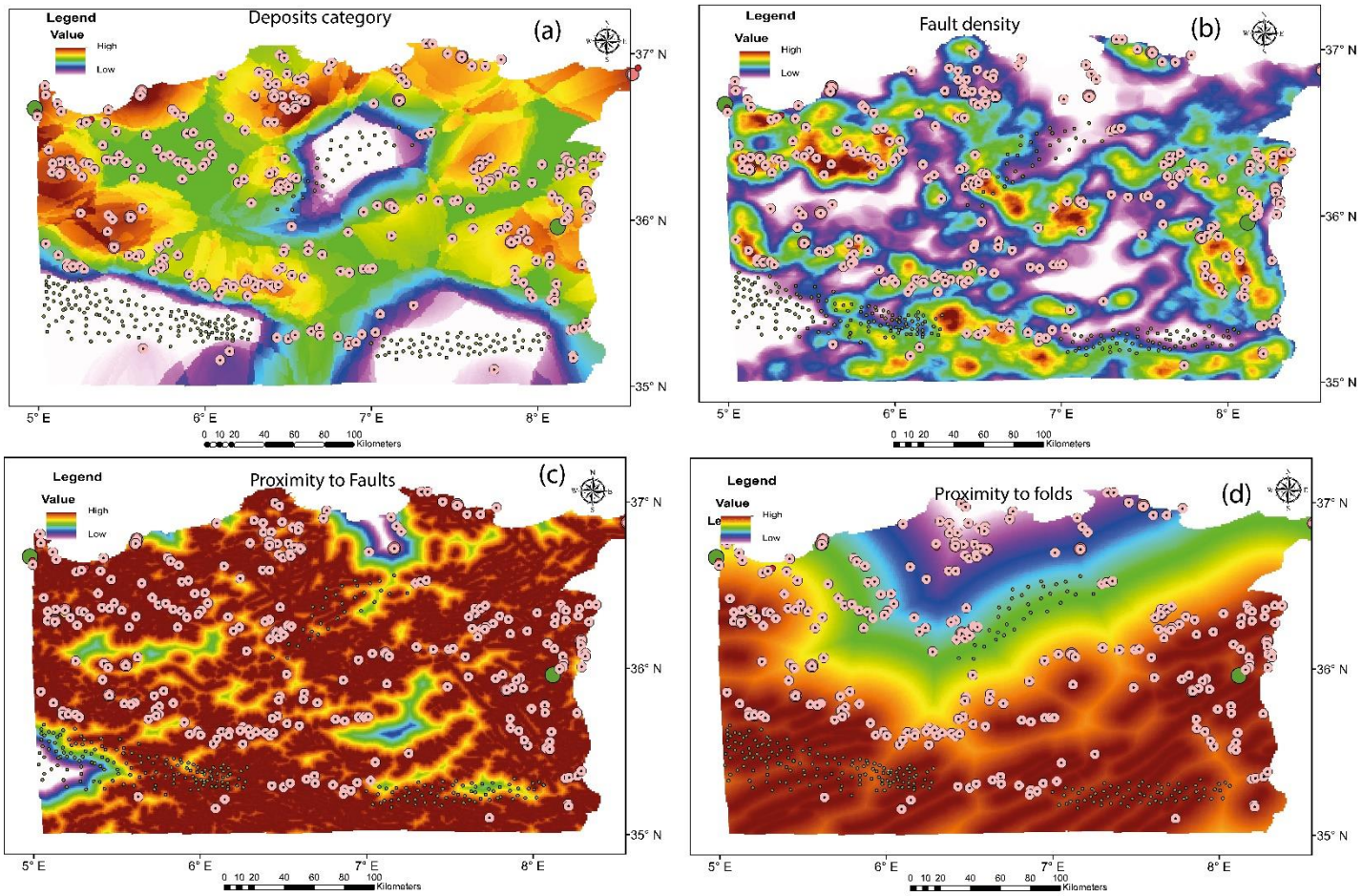

Figure 18: Maps representing normalized predictor maps

3. Knowledge-Driven Method:

Knowledge-driven methods in mineral prospectivity mapping leverage the accumulated expertise and understanding of ore-forming processes, geological controls on mineralization, and established metallogenic models to delineate potential target areas. These approaches rely on the explicit integration of expert knowledge, often formalized through rule-based systems or weighted combinations of evidence layers deemed significant for mineral deposit formation. Conceptual models of ore genesis typically guide the selection and weighting of these evidence layers and the geological characteristics observed in known mineralized districts. By directly incorporating expert judgment and established geological principles, knowledge-driven methods offer a transparent and interpretable framework for identifying prospective terrains, particularly in areas with limited data or where well-defined metallogenic models exist.

3.1. Analytical Hierarchy Process (AHP)

3.1.1. Over view of AHP:

- Provide a brief explanation of AHP as a multi-criteria decision-making tool.
- Highlight its suitability for integrating expert knowledge in MPM.

AHP is one of the most used methods in making decision with multiple criteria developed by saaty 1980 relies on transforming a problem as hierarchy of criteria and sub-criteria to evaluate and compare options, providing a structured and logical approach to decision-making.

it assesses a value that represents a performance degree for a mixt of quantitative and qualitative criteria structuring the problem to different values

The Analytic Hierarchy Process (AHP) is a structured approach to complex decision-making, where a problem is broken down into multiple interconnected components organized in a hierarchical format. At the top of this hierarchy lies the overall objective or main goal of the analysis. Directly beneath it are the key criteria or sub-goals that contribute to achieving this main objective. These can be further decomposed into more detailed sub-criteria if necessary, depending on the complexity of the problem.

At the lowest level of the hierarchy, a set of alternatives is introduced. These alternatives are evaluated with respect to how well they satisfy each criterion or sub-criterion. The evaluation is carried out through a series of pairwise comparisons, where elements are compared two at a time in terms of their relative importance or contribution toward the higher-level objective.

To quantify these judgments, AHP uses a predefined fundamental scale introduced by Saaty, which assigns numerical values to different levels of preference. The scale ranges from 1 (equal importance) to 9 (extreme importance), allowing decision-makers to express how much more one element is preferred over another in a given pairwise comparison. This process quantifies how much more one element contributes to the objective than another, allowing for a structured translation of qualitative preferences into numerical form.

Table 4: Scale of Relative Preference in AHP *(Saaty 1977)*

Level of Preference	Interpretation
1	Equal importance
3	Moderate importance
5	Strong importance
7	Very strong importance
9	Extreme importance

3.1.2. Pairwise Comparison Matrix and Consistency Evaluation

The mathematical properties of the matrix provide a means for evaluating the consistency of the judgments.

Matrix **A** is constructed where each element a_{ij} represents the relative importance of criterion i over criterion j.

3.1.3. Normalized Pairwise Matrix: Each element in the matrix is divided by the sum of its column:

n = number of criteria

W_i= the **i-th weight** from the normalized priority vector $\boldsymbol{Norm(a_{ij}) = \frac{a_{ij}}{\sum_{i=1}^{n} a_{ij}}}$

$\boldsymbol{\lambda_i}$= the **consistency ratio** for each criterion

Priority Vector (Weight Vector): calculate the average of each row in the normalized matrix:

$$W_i = \frac{1}{n}\sum_{ji} Norm(a_{ij})$$

Weighted Sum Vector: Multiply the original matrix A by the weight vector w:

$$P_i = \sum_{i=1}^{n} a_{ij} \,.\, W_j$$

Lambda max $\boldsymbol{\lambda_i = \frac{P_i}{w_i}}$ $\boldsymbol{\lambda_{max} = \frac{1}{n}\sum_{i=1}^{n} \frac{P_i}{w_i}}$

Consistency Index (CI) $\boldsymbol{CI = \frac{\lambda_{max} - n}{n-1}}$

Consistency Ratio (CR): To assess whether the level of inconsistency is acceptable, the Consistency Ratio (CR) is used: $\boldsymbol{CR = \frac{CI}{RI}}$

Table 5: Random Index (RI) Values for AHP

n	1	2	3	4	5	6	7	8	9	10
RI	0.00	0.00	0.58	0.90	1.12	1.24	1.32	1.41	1.45	1.49

Where RI is the Random Index, a reference value that represents the CI of a randomly generated matrix of the same order. A CR value less than 0.1 (10%) indicates that the judgments are sufficiently consistent to be used in the decision-making process.

- ✓ If **CR < 0.1** (or 10%) → Consistent and acceptable
- ✓ If **CR ≥ 0.1** → Inconsistent, revise pairwise judgments

3.1.4. MPM workflow for AHP method:

Generating a Mineral Prospectivity Map (MPM) with the Analytical Hierarchy Process (AHP) is based initially on collecting relevant exploration datasets (geological, geochemical, geophysical, structural, etc.) are compiled. Subsequently, a hierarchical framework of prospectivity criteria and sub-criteria, tailored to the target mineralization, is established. Expert knowledge is then employed to conduct pairwise comparisons between these criteria, quantifying their relative importance and normalizing the weights of each criterion. These derived weights are then applied to their corresponding spatial data layers within a GIS to produce the final prospectivity map, which is classified into zones of varying mineral potential (low to high). Finally, the map's predictive accuracy is assessed through validation against known mineral occurrences, to validate the generated model from AHP with the “real data".

3.2. Fuzzy Logic

3.2.1. Overview of the Fuzzy Logic:

Fuzzy logic is a branch of mathematics that enables computers to model the real world in a way that closely resembles human reasoning. It focuses on quantification and decision-making using language that accommodates ambiguity—terms such as *many*, *few*, *small*, *high*, or *dangerous*. It is particularly suited to situations where both the questions posed and the answers obtained involve vague or imprecise concepts.

In fuzzy logic, precise reasoning is considered a special case of approximate reasoning; everything is viewed as a matter of degree. Any logical system can, in theory, be extended into a fuzzy framework. In this context, knowledge is interpreted as a set of flexible or "elastic" constraints applied to a collection of variables. Inference then becomes the process of propagating these elastic constraints through the system (Sangalli 1996; Zadeh 1965).

3.2.2. Model prospectivity mapping using Fuzzy method

the domain of MPM, the identification of favorable locales for mineralization inherently involves the integration of diverse and often uncertain geoscientific datasets. These datasets, including lithology, structural features, geophysics, geochemistry, hydrology, and documented mineral occurrences, provide critical evidential layers for assessing mineral potential. Given the inherent vagueness and subjectivity associated with interpreting and combining such multi-

source information, fuzzy set theory offers a robust and flexible framework for handling uncertainty and representing the degree of favorability for mineralization based on the evidence presented by each data layer.

Modern geospatial analysis tools, particularly geographic information systems (GIS), provide the platform for implementing fuzzy logic-based approaches for the manipulation, analysis, and integration of these geoscientific datasets in mineral prospectivity modeling. These tools typically allow for a strategic separation of spatial and non-spatial attributes, which are then conveniently linked within relational database structures. The initial step in most data integration procedures involves analyzing the individual characteristics of each thematic map layer and examining their spatial relationships and contextual interdependencies.

Representing data for computational use involves translating real-world observations and expert knowledge into structured formats that follow logical and mathematical rules. This representation plays a central role in spatial data integration, as it dictates the types of combination rules that can be employed in the analysis. The manner in which spatial phenomena are modeled quantitatively directly influences the robustness and interpretability of the resulting maps (Carranza, Hale 2001b; Cheng, Agterberg 1999; Porwal, Emmanuel John Carranza, Hale 2003).

Fuzzy logic offers a unique advantage due to its capacity to integrate both quantitative measurements and qualitative knowledge. This includes observational insights, expert interpretations, and heuristic rules. In geological investigations where available data such as seismic profiles, borehole logs, geological maps, and remote sensing observations often contain varying degrees of uncertainty and subjectivity; fuzzy set theory provides a flexible and effective framework for aggregating diverse types of information into a consistent decision-support model.

3.2.3. General Workflow for Applying Fuzzy Logic in Mineral Prospectivity Mapping

- **Construction of a Geological Database**: This step involves compiling all relevant spatial and non-spatial data, including geological maps, geophysical datasets, borehole data, geochemical measurements, and satellite imagery.
- **Selection of Input Variables**: The most relevant evidential layers are chosen based on expert knowledge or data-driven selection criteria. Typical variables include distance to faults, geochemical concentrations, alteration zones, and lithological units.
- **Fuzzification of Input Data**: Crisp numerical values are transformed into fuzzy values that reflect degrees of membership in a defined set (e.g., low, moderate, high mineral potential). This is achieved using membership functions such as triangular, trapezoidal, or Gaussian functions.

Each raster layer was converted into a fuzzy membership raster using the **Fuzzy Membership** tool in ArcMap (**Spatial Analyst > Fuzzy Logic > Fuzzy Membership**). A suitable fuzzy

function (e.g., **Large**, **Small**, **Linear**, or **Gaussian**) was selected based on the expected influence of the factor:

- **Definition of Membership Functions and Rule Evaluation**: Appropriate membership functions are defined for each input layer, and expert-based or data-driven rules are formulated. For example: if the proximity to a fault is low and economic factor is high, then the mineral potential is considered high. (see table.06)

Table 6: Fuzzy Membership Functions for Geological Criteria

Criteria	G, Age	M, Factors	Econ, Factor	P, Fold	P, Fault	F, Density	P, Thrust	Geo, Grad,
Fuzzy membership function	Large	Large	Large	Small	Small	Large	Small	Large

- **Aggregation of Rule Outputs**: Once fuzzified, the standardized rasters were integrated using fuzzy overlay operators (e.g., Fuzzy SUM or Fuzzy GAMMA) to produce the final mineral prospectivity map. These operators allow for the combination of multiple factors while preserving uncertainty and gradual transitions between favorable and unfavorable zones.
- **Defuzzification (Optional)**: In cases where a crisp output is needed for classification or visualization, defuzzification methods can be applied to convert the fuzzy results back into a single numeric value.

The overall structure of knowledge driven methods is illustrated in figure 19

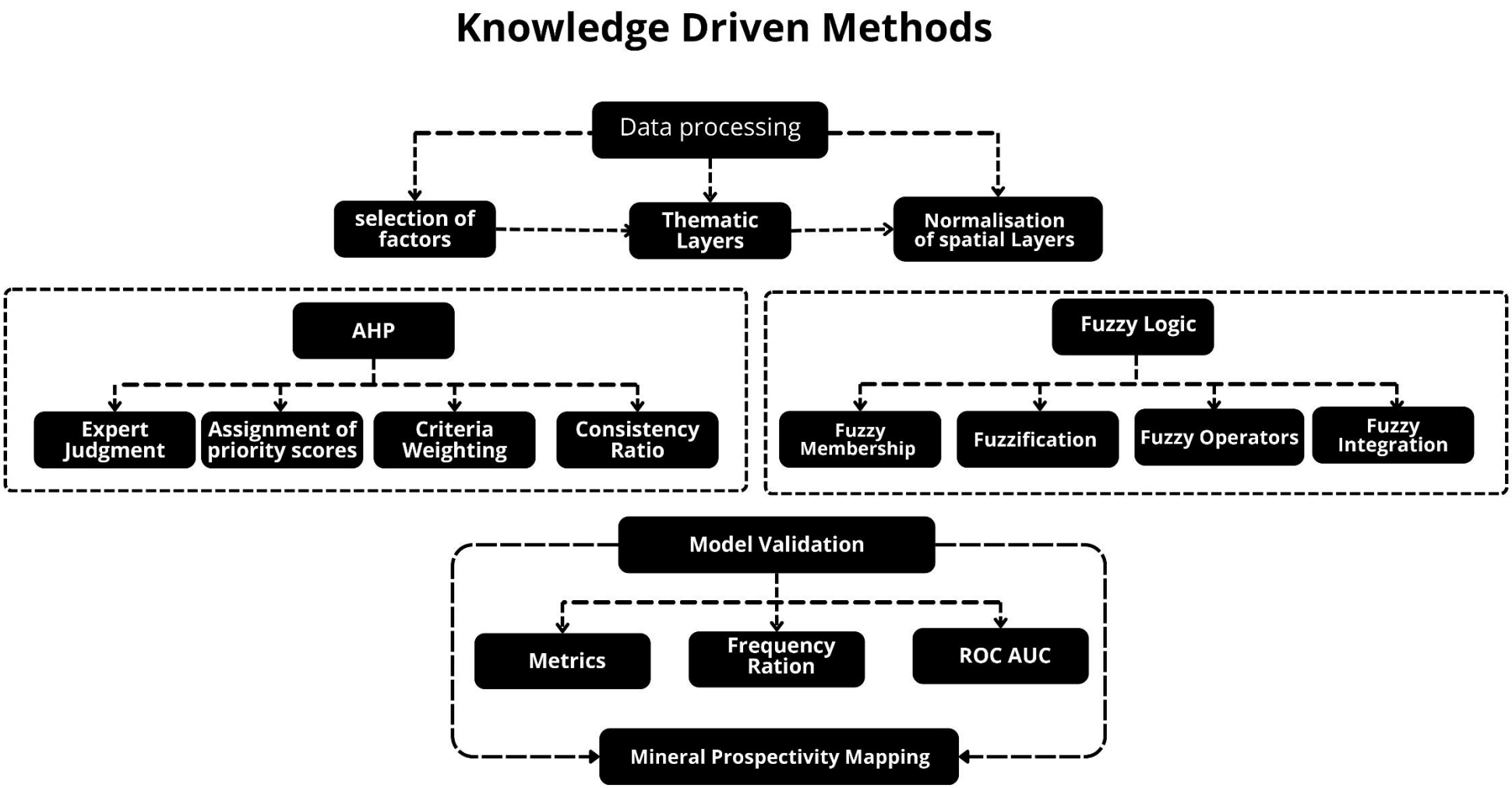

Figure 19: Work flowchart organizing MPM Knowledge driven methods

4. Data-Driven Algorithms: Machine learning Model selection

4.1. Introduction

Machine learning (ML) is a powerful tool for analyzing complex relationships within large datasets, identifying subtle patterns of mineralization that traditional methods may overlook. By learning from existing mineral deposit locations and their geological characteristics, ML algorithms can develop predictive models that can delineate prospective areas with enhanced accuracy and efficiency. This data-driven approach allows for a more quantitative and evidence-based assessment of mineral potential. ML is applied in multiple machine learning models (MPM) to handle different data types and complexities. This study uses ML algorithms to analyze a comprehensive spatial database of geological, geochemical, geodynamic, and metallogenic factors related to Pb-Zn mineralization in northeastern Algeria. The goal is to develop a robust predictive model that can identify new prospective zones, contributing to more efficient mineral exploration efforts.

In this study, multiple machine learning (ML) algorithms were employed to evaluate and compare their performance in modeling the influence of weighted geological and structural factors on mineral formation. The quality of the dataset, along with the spatial extent and complexity of the study area, played a pivotal role in guiding the selection of appropriate ML models for mineral prospectivity mapping. This chapter presents a comparative analysis of the selected ML algorithms based on their performance metrics and feature importance rankings. The objective is to identify the most influential predictors contributing to Pb-Zn mineralization and to visualize the resulting prospectivity maps across northeastern Algeria.

4.2. Machin learning algorithms:

The formation of mineral deposits, viewed through the lens of a metallogenic system, is a complex interplay of structural controls (thrusts, faults, and folds), fluid pathways, chemical reactions, and the mechanisms of mineral precipitation (Sun et al. 2019; Xu et al. 2021; Quanping Zhang et al. 2022). Understanding the geological elements that govern this intricate process is paramount for effective MPM. In this study, we leverage the power of machine learning to quantitatively assess the contribution of individual geological features in predicting mineral potential. By integrating a comprehensive numerical database with advanced algorithms, our goal is to generate a predictive map that not only highlights known mineral occurrences but also forecasts high-potential regions, even in underexplored areas(Farahbakhsh et al; 2023) .

To achieve this, we employed two distinct machine learning strategies to model mineral prospectivity: FNN and Stacking Ensemble Method (SEM).

We used a Feedforward Neural Network (FNN) as an independent predictive model. The architecture and hyperparameters of the FNN were carefully optimized through a dedicated process to maximize its predictive performance on the mineral prospectivity task. This allowed us to assess the capability of a non-linear model in capturing complex relationships within the geological data.

The Stacked Ensemble of Tree-Based and Convolutional Models was also implemented a powerful **stacked ensemble method** to combine the predictive strengths of multiple base models. Our ensemble comprises Random Forest, Light Gradient Boosting Machine (Light GBM) and Convolutional Neural Networks (CNN).

The selection of RF, Light GBM, and CNN as our base learners was driven by their complementary strengths in analyzing complex spatial datasets and enhancing predictive accuracy, which are particularly advantageous for mineral prospecting tasks:

- **Random Forest (RF):** Renowned for its effectiveness in integrating numerous geological predictor variables, RF utilizes an ensemble of decision trees. This aggregation approach inherently reduces overfitting and enhances the interpretability of feature importance, making it well-suited for handling the complex and often high-dimensional geological data relevant to mineralization.
- **Light Gradient Boosting Machine (Light GBM):** Building upon the principles of gradient boosting, Light GBM offers a highly efficient, fast, and powerful method for analyzing large datasets. Its ability to capture subtle and non-linear patterns within predictor maps is crucial for accurately delineating areas with potential mineral deposits.
- **Convolutional Neural Networks (CNN):** CNNs excel in spatial analysis by automatically learning hierarchical spatial dependencies and intricate patterns within grid-based data, such as the geological predictor maps used in this study. This capability is particularly vital in mineral prospecting, where spatial relationships between geological features often dictate mineralization patterns.

4.3. Feedforward Neural Network (FNN):

FNN is a foundational type of artificial neural network characterized by unidirectional information flow, moving sequentially from input through hidden layers to the output layer, without any feedback loops. As the simplest form of neural network, it serves as a precursor to more complex architectures like recurrent and convolutional networks. FNNs operate through a two-phase process: the feedforward pass, where input data is processed to generate an output, and backpropagation, where the network's internal connection weights are adjusted based on the prediction error to enhance model performance. Despite its relative simplicity, the FNN's versatility has led to its widespread application in diverse tasks such as pattern recognition, classification (Skabar 2003) regression analysis, and even more complex domains like image recognition and time series prediction.

4.3.1. Bayesian Optimization for Hyperparameter Tuning of the Feedforward Neural Network

Bayesian Optimization (BO) is a sophisticated yet efficient method for optimizing complex, often non-convex objective functions, particularly effective in continuous search spaces with a limited number of dimensions (typically under 20). Unlike traditional grid or random search, BO leverages a probabilistic surrogate model, commonly Gaussian Process Regression, to model the objective function. This surrogate model not only provides predictions but also quantifies the uncertainty associated with these predictions, guiding the intelligent selection of subsequent hyperparameter configurations to evaluate. Advanced BO strategies, such as parallel evaluations, multi-fidelity optimization, and robust handling of noisy data, further enhance its applicability in real-world scenarios (D. Li et al. 2022). Specialized acquisition functions, including Expected Improvement, Entropy Search, and Knowledge Gradient (Frazier 2018), are employed to balance exploration of uncertain regions and exploitation of promising areas within the hyperparameter space. Comprehensive tutorials and foundational concepts of BO are detailed in (Shahriari et al. 2016; Brochu, Cora, de Freitas 2010)

In this study, considering its efficacy in optimizing continuous parameters within a constrained search space, Bayesian Optimization was employed to fine-tune the critical hyperparameters of our Feed forward Neural Network (FNN). Specifically, the number of hidden layers, the number of neurons within each hidden layer, and the maximum number of training iterations were identified as having the most significant impact on the FNN's performance. Consequently, BO was strategically applied to explore the optimal configurations of these hyperparameters, aiming to maximize the predictive accuracy of the FNN for Pb-Zn MPM (see Tab. 07) for the optimized hyperparameter values). This targeted optimization ensures that the FNN is effectively trained to capture the complex relationships within our geological dataset.

Table 7: Hyperparameter Optimization Ranges with Optimal hyperparameters of FNN

Hyperparameter	Optimization range	Value
Batch Size	2; 32	26
Dropout	0; 0.9	0.114
Learning Rate	10^{-6}; 0	0.0065
Max Iterations	1; 100	39.0
Num Hidden Layers	1; 4	1.0
Num Layers	1; 4	2.0
Num Neurons	2; 32	19.0
Units per Layer	2; 32	16.0

4.4. Base models of the ensemble model learning:

4.4.1. RF :

RF, a powerful supervised machine learning algorithm originally introduced by (Breiman 2001), is adept at tackling both classification and regression tasks. Its strength lies in an ensemble learning approach, where multiple individual classifiers (decision trees) are combined to address complex problems and significantly enhance the overall model performance. RF employs two key randomization strategies that contribute to its robustness and ability to generalize: bootstrap aggregating (bagging) and random feature selection.

4.4.1.1. Bootstrap Aggregating (Bagging): Creating Diverse Training Sets

RF constructs an ensemble of decision trees by training each tree on a different subset of the original training data, a technique known as bootstrap aggregating, or simply "bagging" (Rodriguez-Galiano et al. 2012; Carranza, Laborte 2015b). In this process, for each tree, a bootstrap sample of the same size as the original training set is drawn with replacement. This ensures that each tree is trained on a slightly different perspective of the data, and importantly, any single data point can be included multiple times or not at all in a particular tree's training set.

4.4.1.2. Random Feature Selection: Enhancing Tree Diversity

During the growth of each decision tree within the RF, at each node, instead of considering all possible features to determine the best split, a random subset of the input features is selected. The algorithm then searches for the most informative split *only* within this randomly chosen subset. This introduces further diversity among the trees in the forest, reducing the correlation between their predictions and enhancing the ensemble's ability to generalize to unseen data.

4.4.1.3. Decision Tree Induction and Splitting Criteria

Each decision tree within the RF operates by recursively partitioning the feature space. Starting with the dependent variable at the root node, the tree aims to split the data into binary segments (leaf nodes) that exhibit greater homogeneity with respect to the target variable (dichotomy categorization). To determine the optimal split at each node, the algorithm evaluates all potential splits based on the chosen subset of features. The "best" split is selected by maximizing the purity of the resulting child nodes. RF utilizes various impurity measures to assess the quality of a split, including:

- **Gini Index:** For a node (t), the Gini index (G(t)) is calculated as:

$$\boldsymbol{G(t) = 1 - \sum_{i=1}^{c} P(i|t)^2}$$

C: the number of classes

p(i|t): the proportion of instances belonging to class (i) at node (t).

The split that results in the largest reduction in the weighted average Gini index of the child nodes is typically chosen.

Information Gain (related to Entropy): While often used in individual decision trees, RF implementations can also leverage information gain. Entropy (H(t)) at a node (t)is:

$$\boldsymbol{H(t) = -\sum_{i=1}^{c} P(i|t) log_2 P(i|t)}$$

Information gain is the reduction in entropy after a split.

- **Chi-Square:** This statistical test can be used to evaluate the significance of the split based on the distribution of classes in the child nodes compared to the parent node

4.4.1.4. Ensemble Prediction: Voting for Classification

For classification tasks, the RF classifier aggregates the predictions from all the individual decision trees in the forest. The final class prediction for a given input instance is determined by a **majority vote** among the predictions of all the trees. This ensemble approach reduces the risk of relying on the potentially biased prediction of a single tree, leading to more robust and accurate classification.

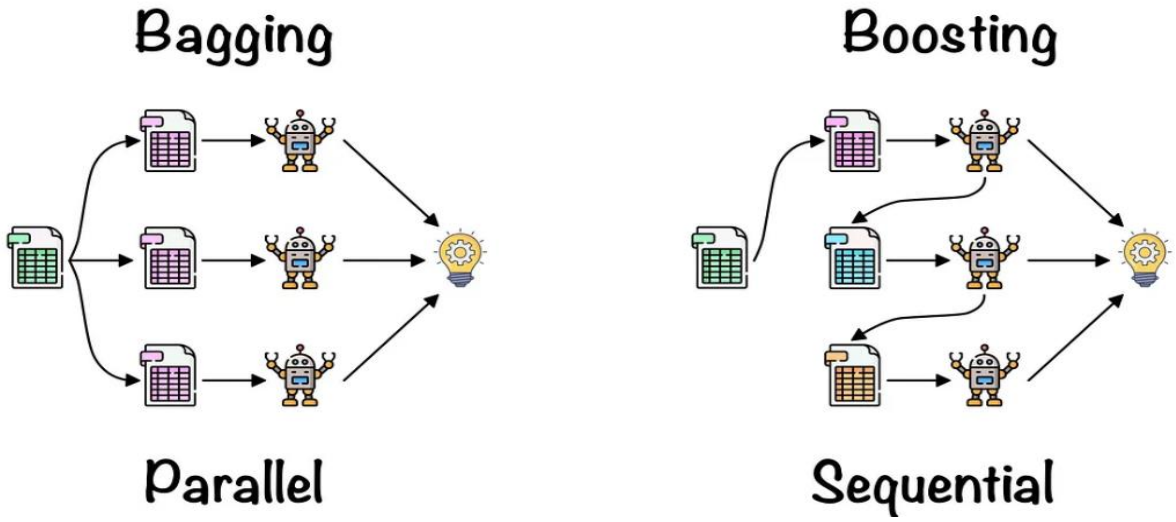

Figure 20: Random Forest architecture; Bagging and boosting (Dey, 2024)

4.4.1.5. Robustness Against Overfitting

A key advantage of the RF algorithm is its inherent ability to mitigate overfitting. The combination of training each tree on a different bootstrap sample and using a random subset of

features at each split ensures that the individual trees are diverse and less prone to memorizing noise in the training data. The aggregation of their predictions further smooths out individual tree errors, resulting in a more generalized and reliable model. Generally, increasing the number of trees in the forest tends to improve the model's accuracy and stability against overfitting.

4.4.2. Light GBM:

Light GBM algorithm was created by Microsoft. It is based on the boosting method known as the GBDT (Gradient Boosting Decision Trees), which combines decision trees to create a potent predictive model. it employs histogram-based method and a leaf-wise growth strategy for tree construction rather than the level-wise tree method, and makes Light GBM unique in its capacity to rapidly train high-performance prediction models. Unlike other machine learning methods that construct trees horizontally, Light GBM employs a leaf-wise strategy for developing decision trees. This approach results in a deeper and more complex tree structure with fewer nodes, thereby enhancing the accuracy of modeling nonlinear relationships and interactions among variables. In contrast, the Light GBM algorithm utilises histograms to partition floating-point eigenvalues into smaller bins. These bins are used to build a histogram, and the optimal segmentation point is determined based on the discrete values within the histogram. This strategy effectively reduces data storage and computational costs and is implemented using two algorithms, the light GBM algorithm provides a high accuracy and efficiency increase with data volume growth and a better loss reduction , it speeds up forecasting and reduces memory utilization.(Ke et al. 2017) This makes it a useful tool for machine learning tasks such as classification, regression, ranking, and others. Large datasets are frequently processed using Light GBM (Friedman 2001). It uses two novel techniques: Gradient-based One Side Sampling (GOSS) and Exclusive Feature Bundling (EFB).

These techniques address the weaknesses of the histogram-based algorithm that is the base of all GBDT (Gradient Boosting Decision Tree) frameworks. The Light GBM Algorithm's characteristics are formed by the two methodologies of GOSS and EFB. They work together to make the model work efficiently and to provide it a competitive advantage over alternative GBDT frameworks.

4.4.2.1. Gradient-Based One-Side Sampling (GOSS): The computation of information gain involves different data instances with different roles. Under-trained instances contribute more to the gain. GOSS keeps instances with large gradients and drops those with small gradients to maintain accuracy. This treatment can lead to more accurate gain estimation than uniformly random sampling, especially when the information gain value has a large range.(Si et al. 2017)

4.4.2.2. Exclusive Feature Bundling (EFB): High-dimensional data is sparse, allowing for a nearly lossless approach to reduce feature count. Many mutually exclusive features can be bundled into a single feature, reducing the complexity of histogram building. while feature is

bundled. As a result, the training framework's speed is increased without sacrificing precision.(Ke et al. 2017)

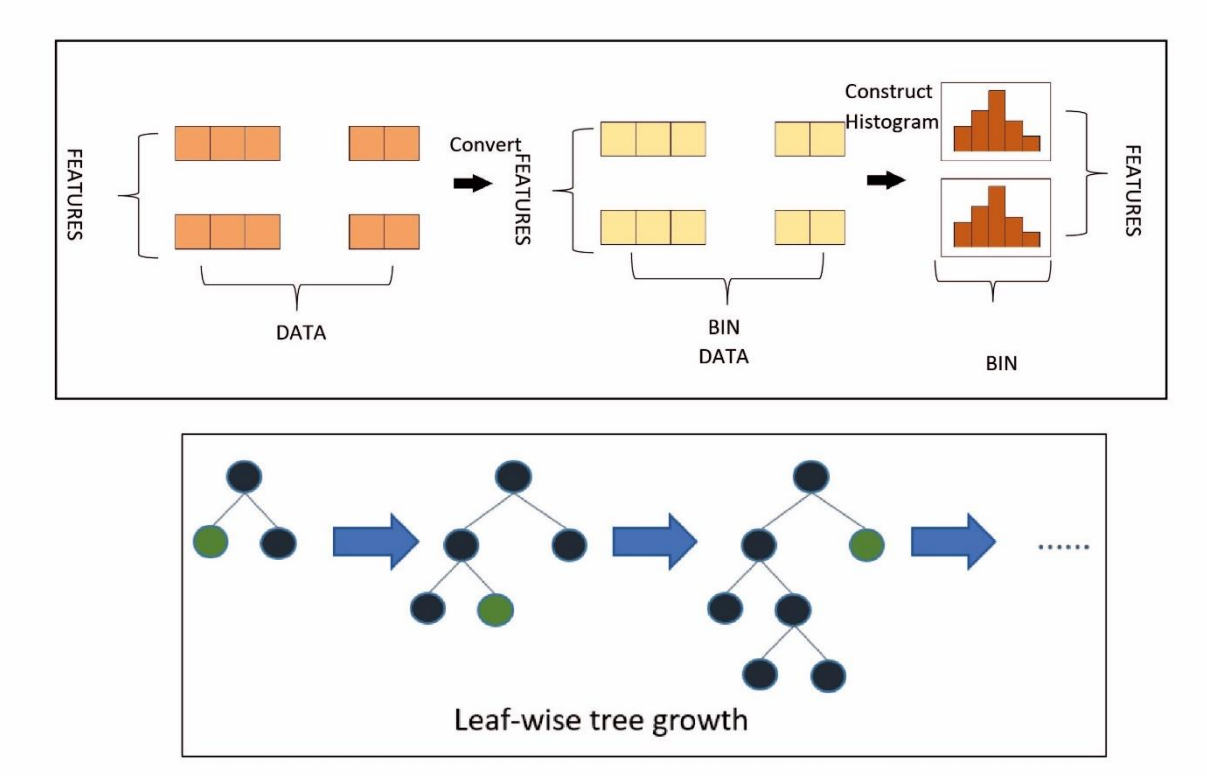

Figure 21: A Visual Representation of Light GBM Architecture

4.4.3. Convolutional Neural Networks (CNN):

Convolutional Neural Networks (CNNs) are a specialized class of artificial neural networks particularly adept at processing and analyzing spatial data, including visual information (Albawi et al., 2017; Dhillon & Verma, 2020; Shin et al. 2016). Their ability to automatically learn hierarchical spatial features makes them a powerful and efficient tool for enhancing predictive mapping in geological and mining applications, specifically within Mineral Prospectivity Mapping (Li et al., 2020; Li et al., 2021; Yang et al., 2021)

The architecture of a CNN is task-specific, designed to extract relevant features from input data. Typically, input data is processed through a series of convolutional layers, where learnable filters capture local spatial patterns. These layers are followed by non-linear activation functions and pooling layers, which progressively down-sample the feature maps while retaining the most salient information. Subsequent fully connected layers then integrate these high-level features for the final prediction. To mitigate overfitting, dropout layers can be incorporated. The network's performance during training is quantified using a chosen loss function.

Data & Methods

In this study, our CNN architecture comprised two convolutional layers, each employing 64 filters with a kernel size of 3 to capture intricate local patterns. These were followed by activation functions and two max-pooling layers for down-sampling. The extracted features were then fed into fully connected layers: first with 32 neurons, and finally an output layer employing a sigmoid activation function for binary classification (prospective/non-prospective). Dropout layers were optionally used for regularization. The model was trained for 50 epochs with a batch size of 32.

To optimize the accuracy of MPM and enhance the performance of our stacking ensemble, we strategically employed several machine learning algorithms, including this CNN, to leverage their diverse strengths in capturing different aspects of the complex geological data (Dube, Verster 2023)

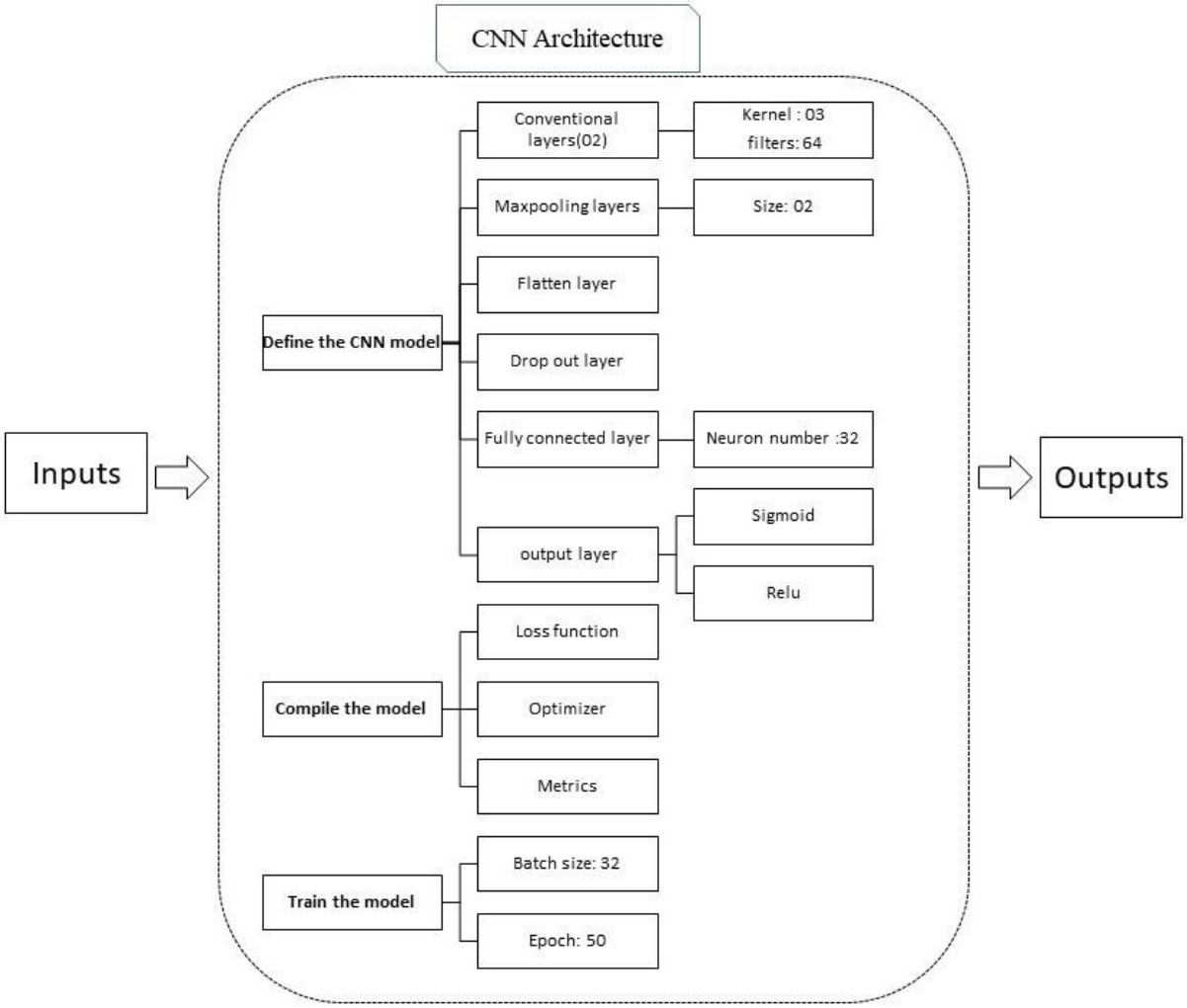

Figure 22: CNN Architecture

4.5. Ensemble method :

Ensemble learning is a powerful paradigm in machine learning that combines the predictions of multiple individual models, often referred to as "weak learners" or "base models," to yield a more robust and accurate overall prediction. The fundamental goal of ensemble methods is to reduce individual model errors and improve the generalization performance of the final predictive system (Dietterich 2000; Rocca 2021; Hajihosseinlou, Maghsoudi, Ghezelbash 2024). The effectiveness of ensembles in achieving high accuracy by synergistically leveraging the strengths of less accurate constituent models is well-established.

4.5.1. Types of ensemble methods :

4.5.1.1. Bagging (Bootstrap Aggregating): Imagine you have a dataset, and instead of training one powerful model on the entire thing, you create multiple smaller datasets by randomly sampling the original data with replacement. This means some data points might appear multiple times in a single smaller dataset, while others might be left out. Then, you train a separate "base" model (like a decision tree) on each of these smaller datasets. For the final prediction, you aggregate the results of all these models. For classification, this often involves taking a majority vote, and for regression, it's usually an average. RFs are a prime example of a bagging ensemble using decision trees.

4.5.1.2. Boosting: Unlike bagging, boosting focuses on sequentially training models. Each new model tries to correct the errors made by the previous ones. It achieves this by assigning more weight to the data points that were misclassified by earlier models. This forces subsequent models to focus on the "harder" examples. The final prediction is made by a weighted combination of the individual model predictions.

4.5.1.3. Stacking (Stacked Generalization): Stacking is a sophisticated meta-learning approach that aims to enhance predictive modeling by recognizing the unique strengths of different base models and capitalizing on the complementary properties of their underlying (Mojaddadi et al. 2017; Zhao et al. 2024). This method offers the potential for improved generalization, flexibility in model combination, and enhanced interpretability of the resulting meta-model. By intelligently combining diverse model predictions, stacking can effectively leverage the distinct advantages of each contributing model and potentially mitigate individual model weaknesses, including overfitting. However, it's important to acknowledge that successful implementation often requires careful tuning and sufficient computational resources.

4.5.1.4. Voting (or Averaging): This is a simpler ensemble technique where multiple independent models are trained on the same dataset. For classification, the final prediction is determined by the class that receives the most votes among the models. For regression, the final prediction is the average (or sometimes a weighted average) of the predictions made by the individual models. This method works well when you have a diverse set of well-performing models.

Among the various ensemble techniques, this study focuses on **stacking**. Stacking is a sophisticated meta-learning approach that aims to enhance predictive modeling by recognizing the unique strengths of different base models and capitalizing on the complementary properties of their underlying algorithms (Mojaddadi et al., 2017; Zhao et al., 2024b). This method offers the potential for improved generalization, flexibility in model combination, and enhanced interpretability of the resulting meta-model. By intelligently combining diverse model predictions, stacking can effectively leverage the distinct advantages of each contributing model and potentially mitigate individual model weaknesses, including overfitting. However, it's important to acknowledge that successful implementation often requires careful tuning and sufficient computational resources.

In this research, we selected a stacking ensemble strategy to integrate the predictive capabilities of three distinct machine learning approaches particularly suited for Mineral Prospectivity Mapping and whose characteristics (strengths and weaknesses, detailed in Table 08) offer valuable complementarity: Random Forest , Light Gradient Boosting Machine (Light GBM), and Convolutional Neural Networks (CNN). Our hypothesis is that by combining these diverse models through stacking, we can effectively harness their individual strengths and compensate for their limitations, ultimately leading to a more robust and accurate predictive model for identifying prospective areas of mineralization.

Table 8: Strenghts and weaknesses of machine learning models: RF, Light GBM, CNN

Method	Strengths	Weaknesses
RF	- Robust to overfitting. - Handles high-dimensional data well. - Provides feature importance.	- Slower inference compared to simpler models. - Less interpretable than a single decision tree.
Light GBM (Gradient Boosting Machine)	- High efficiency in training and prediction. - Handles large datasets efficiently. - Good predictive performance.	- May require careful parameter tuning. - Prone to overfitting with insufficient data
CNN (Convolutional Neural Network)	- Excellent at handling spatial data like images. - Automatic feature extraction. - State-of-the-art performance in computer vision tasks.	Data-hungry, requiring large labeled datasets. - Limited interpretability of complex architectures. - Computationally intensive for deep networks.

4.6. MPM workflow for data driven methods:

This study systematically identifies potential mineral-rich zones through a three-stage process. Initially, we meticulously prepare a comprehensive dataset of relevant geological factors. Subsequently, we employ machine learning algorithms to perform classification tasks, discerning patterns indicative of mineralization. Finally, the results are synthesized into a Mineral Prospectivity Map (MPM), visually representing the likelihood of mineral deposits across the study area.

The MPM functions by integrating prospecting data characteristics at each spatial location, effectively condensing this information into a single pixel. Each pixel's value is derived from the correlation data generated by the various machine learning models applied, considering a range of attributes associated with known mineral deposits. This integrated approach enhances our ability to predict the presence or absence of mineralization in previously unexplored regions.

Our machine learning methodology adheres to a standard two-phase process: a training phase where the models learn from labeled data and a subsequent validation phase to assess their predictive performance (Batista et al ., 2004). The dataset is partitioned into 75% for training the models and 25% for rigorously testing their generalization capabilities (Daviran et al. 2021).

The supervised data-driven methods employed rely on well-defined locations of both mineral deposits and non-deposit areas. To ensure robust model training, we maintain a balanced number of positive and negative samples. Positive samples accurately represent the spatial coordinates of already discovered mineral positive samples represent the spatial coordinates of known mineral deposits already discovered (Boutaleb 2001). Conversely, negative samples denote locations where mineralization is absent (Carranza, Laborte 2015c; Yousefi et al. 2021; Zuo et al. 2021).

Crucially, the geological characteristics of these non-deposit locations are distinctly different from those of deposit locations (Ghezelbash et al. 2023). These negative samples were strategically selected based on their demonstrably low probability of hosting mineralization (Farahbakhsh, Maughan, R. Dietmar Müller 2023b), with a particular focus on areas of Quaternary age where the potential for positive samples is exceptionally low. Existing geological maps (Algérie. Direction des mines et de la géologie, Office national de la géologie 1987; Fleury et al. 1969; Popov et al. 1965) corroborate the lack of significant mineralization in these extensive regions, stretching over 800 km from northeastern Algeria to the Maghreb Atlas in the west, with only a single known deposit.

Furthermore, proximity considerations guided our sampling strategy. Positive samples, representing known deposits, are generally spaced approximately 3 km apart. In contrast, negative samples are deliberately positioned at a minimum distance of 10 km from any positive sample. This spatial separation strategy reinforces the principle that the likelihood of

encountering the target mineralization decreases with increasing distance from known deposits (Fig. 16). This carefully designed data setup ensures that our models are trained on a diverse and representative range of data, allowing for effective validation of their predictive accuracy.

The selection of mappable exploration criteria was a meticulous process, prioritizing factors known to play a significant role in mineral accumulation and the formation of polymetallic deposits. Correlations are established by considering the spatial relationships between known deposits and key geological features, including major tectonic structures, significant geological formations, and specific lithological units, the overall structure of MPM workflow us illustrated in figure 23

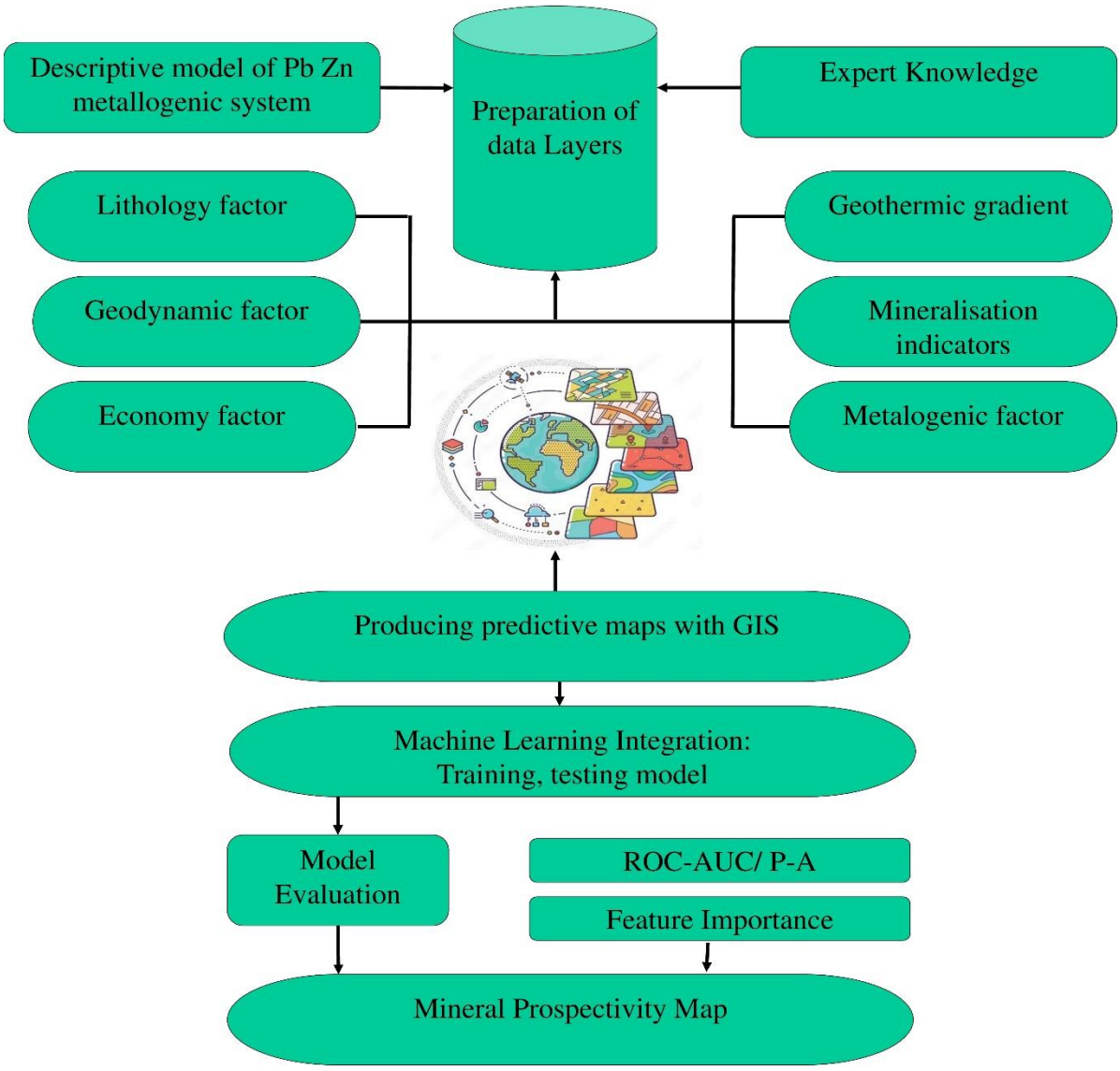

Figure 23: Work flowchart organizing and illustrating GIS & Machine learning combination.

4.7. Model's evaluation:

4.7.1. Correlation matrix:

In machine learning, model effectiveness is assessed through performance evaluation. Correlation matrices, visual and statistical tools, reveal the strength and direction of linear relationships between variables via coefficients (-1 to +1). Heatmaps typically visualize these pairwise correlations, highlighting interdependencies for feature selection and model development. They aid in understanding data patterns and guiding analytical choices (Steiger 1980).

4.7.2. Performance metrics

In order to evaluate the performance of the model on the Pb-Zn prospection maps, using various statistical metrics. By employing these statistical functions, we gain insights into the models' accuracy, robustness, and overall effectiveness in the classification task

The Classification metrics serve as quantitative measures to evaluate the performance of machine learning models designed to assign input data points to predefined categories (Carvalho, Pereira, Cardoso 2019). Among these metrics, accuracy quantifies the overall correctness of the model's predictions. It is determined by calculating the ratio of correctly classified instances to the total number of instances in the dataset.

$$Accuracy = \frac{TP + TN}{TP + TN + FP + FN}$$

The Precision focuses on the proportion of true positive predictions. It aims to avoid false positives out of all positive predictions made by the model. It helps assess the model's ability to avoid false positives.

$$Precision = \frac{TP}{TP+FP}$$

The sensitivity or Recall assesses the model's capacity to capture positive cases; it measures the proportion of true positive predictions out of all actual positive instances.

$$Sensitivity = \frac{TP}{TP+FN}$$

The Specificity measures the proportion of true negative predictions out of all actual negative instances. It assesses the model's ability to avoid false negatives.

$$Specificity = \frac{TN}{TN+FP}$$

The F1 score combines precision and recall into a single metric, providing a balanced assessment of a model's performance.

$$f1 - score = \frac{sensitivity}{sensitivity * precision}$$

4.7.3. feature importance:

The feature importance analysis was conducted to identify the key factors influencing the occurrence of Pb-Zn mineralization. A range of geological variables, including metallogenic and tectonic parameters, were considered to characterize the favorable conditions for ore formation. To evaluate the relative influence of each factor, we applied the feature importances attribute from the meta-model used in the stacking ensemble method.

Each normalized evidential map was assigned a weight based on its importance as determined by the machine learning model. These weights represent the relative contribution of each factor to the overall mineralization potential. The final mineral prospectivity map (MPM) was generated by summing the weighted maps, thus integrating all relevant geological evidence into a single predictive output. The predictive results from the five individual models were computed using Python and subsequently imported into ArcGIS for spatial visualization and

4.7.4. Frequency Ratio (FR) Plot:

The FR Plot shows how each mineral potential class relates to the actual deposit occurrences normalized by area. A higher FR (>1) means that the class is more favorable for mineralization than random chance.

Chapter 5: Results & Discussions

1. Knowledge driven methods:

1.1. AHP

1.1.1. Construction of the Pairewise matrix:

The first step in applying the AHP method is to construct a pairwise comparison matrix. This matrix is used to evaluate the relative importance of various criteria influencing mineral prospectivity, such as geological age, structural features, and economic indicators. Each criterion is compared to the others using a numerical scale ranging from 1 to 9 (Table 09). When a criterion is considered less important than another, reciprocal values (e.g., 1/3, 1/5) are assigned. This process helps organize expert judgments in a consistent manner and establishes a clear hierarchy among the influencing factors. Below are the matrix values, weight calculations, and consistency check results (Table 10).

Table 9: pairwise matrix

Criteria	Geologic Age	Metallogenic Factors	Economic Factor	Proximity to Fold	Proximity to Fault	Fault Density	Proximity to Thrust	Geothermic Gradient
Geologic Age	1	3	3	1	3	3	3	1
Metallogenic Factors	1/3	1	1	3	1/3	3	3	5
Economic Factor	1/5	1	1	3	3	7	5	7
Proximity to Fold	1/3	1/3	1/3	1	3	3	3	5
Proximity to Fault	1/5	3	1/3	1/3	1	3	3	3
Fault Density	1/3	1/3	1/7	1/3	1/3	1	3	3
Proximity to Thrust	1/5	1/3	1/5	1/3	1/3	1/3	1	3
Geothermic Gradient	1/3	1/5	1/7	1/5	1/5	1/3	1/3	1

Table 10: normalize pairwise matrix

Criteria	Geologic Age	Metallogenic Factors	Economic Factor	Proximity to Fold	Proximity to Fault	Fault Density	Proximity to Thrust	Geothermic Gradient
Geologic Age	0,341	0,326	0,488	0,109	0,268	0,145	0,141	0,036
Metallogenic Factors	0,114	0,109	0,163	0,326	0,030	0,145	0,141	0,179
Economic Factor	0,068	0,109	0,163	0,326	0,268	0,339	0,234	0,250
Proximity to Fold	0,114	0,036	0,054	0,109	0,268	0,145	0,141	0,179
Proximity to Fault	0,068	0,326	0,054	0,036	0,089	0,145	0,141	0,107
Fault Density	0,114	0,036	0,023	0,036	0,030	0,048	0,141	0,107
Proximity to Thrust	0,068	0,036	0,033	0,036	0,030	0,016	0,047	0,107
Geothermic Gradient	0,114	0,022	0,023	0,022	0,018	0,016	0,016	0,036

1.1.2. Model Evaluation of AHP

Below are the matrix values, weight calculations, and consistency check results.

Table 11: AHP Results

Criteria	W_i	P_i	λ_i	CI	CR
Geologic Age	0,23	2,21	9,54	0,137	0,097
Metallogenic Factors	0,15	1,39	9,20		
Economic Factor	0,22	2,10	9,59		
Proximity to Fold	0,13	1,20	9,19		
Proximity to Fault	0,12	1,18	9,73		
Fault Density	0,07	0,55	8,21		
Proximity to Thrust	0,05	0,39	8,42		
Geothermic Gradient	0,03	0,26	7,83		

Interpretation :

The consistency of the pairwise comparisons was evaluated, yielding a Consistency Index (CI) of 0.137 and a corresponding Consistency Ratio (CR) of 0.097. This CR value is comfortably below the acceptable threshold of 0.1, indicating a high level of consistency in the expert judgments and thus, the reliability of the derived weights. A CR above 0.1 would suggest potential inconsistencies in the pairwise comparisons that might compromise the validity of the AHP results.

The calculated weights reveal the relative importance of each criterion in controlling Pb-Zn mineralization in northeastern Algeria. Geologic Age (0.23) emerges as the most influential factor, highlighting the critical role of the region's geological history and specific formations in the occurrence of these deposits. The Economic Factor (0.22) closely follows, underscoring the significant impact of economic viability and accessibility on prospectivity assessment in the area. Metallogenic Factors (0.15) also play a substantial role, reflecting the importance of regional metallogenic events and related geological features.

In contrast, criteria such as Geothermic Gradient (0.03) and Proximity to Thrust (0.05) exhibit lower weights, suggesting a less direct influence on Pb-Zn mineralization within the specific geological context of northeastern Algeria, although they might still contribute to the overall favorability to a lesser extent. The remaining criteria, Proximity to Fold (0.13), Proximity to Fault (0.12), and Fault Density (0.07), hold intermediate levels of importance.

These derived weights will be integral in the subsequent Pb-Zn prospectivity modeling. By weighting the spatial data layers corresponding to each criterion according to their calculated importance, the model will prioritize areas with favorable geological ages, economic accessibility, and significant metallogenic indicators in delineating potential target zones in northeastern Algeria.

1.1.3. Model prospectivity mapping using AHP method:

The Analytic Hierarchy Process (AHP) is applied to assign weights to key exploration criteria through pairwise comparisons. These weights reflect the relative importance of each factor in identifying prospective zones. After verifying the consistency of the judgments, the weights were applied in ArcMap. Each standardized criterion map was multiplied by its corresponding weight using the *Raster Calculator*. The weighted layers were then summed to generate the final MPM (figure 24), highlighting areas with the highest potential for mineralization.

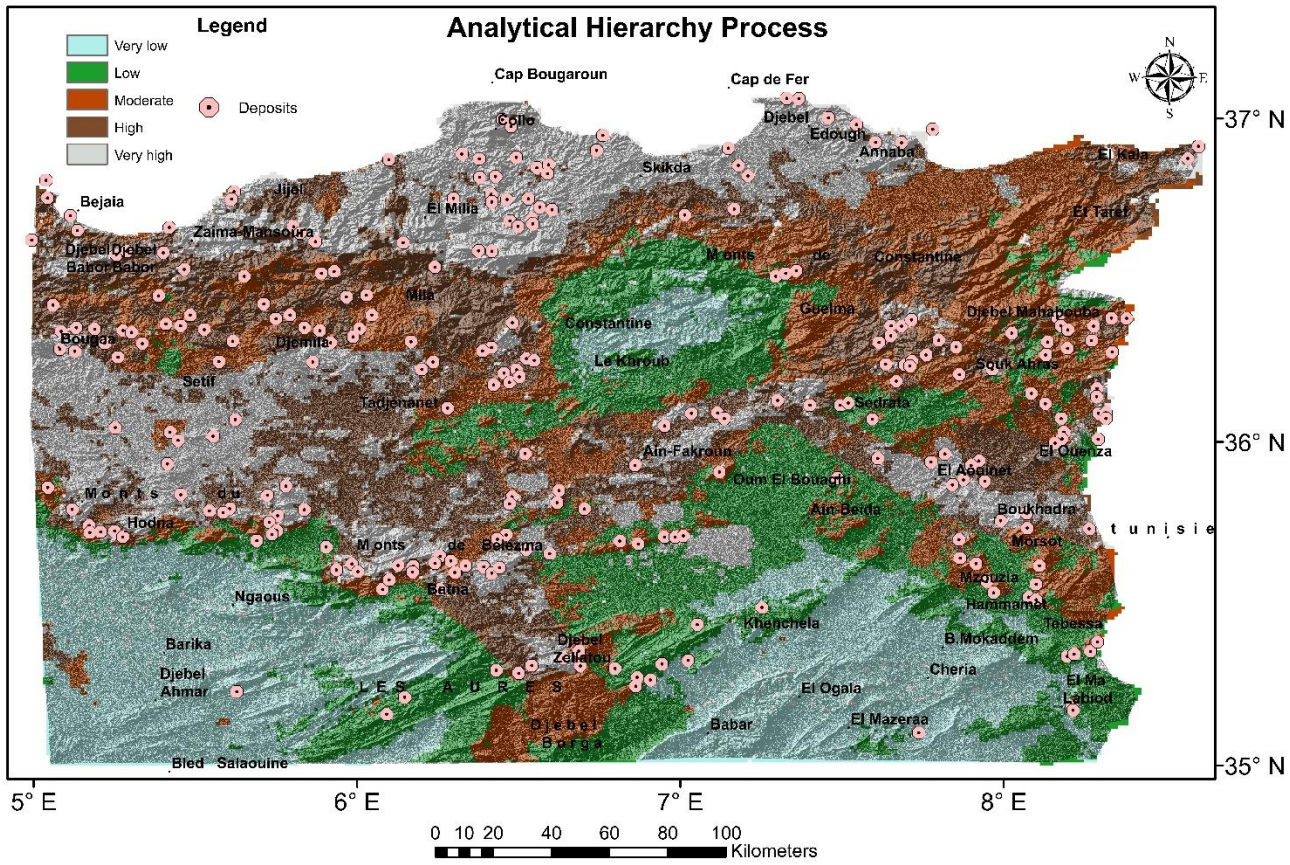

Figure 24: Predictive Pb-Zn deposits probability maps derived by AHP method

Discussion

The MPM for Pb-Zn deposits in northeastern Algeria, generated using an AHP model, integrates several key prospective factors

prospectivity zones are concentrated in the central portions of the mapped area from the borders of Bejaia to Edough region. Deposits of this region are linked to the magmatic activity and the presence of the most important deposit of Pb Zn in Oued Amizour, which can be explained with the significant role of economic factor in weight assessment from AHP method

There also seem to be some linear trends of higher prospectivity extending in a roughly central eastern part direction, particularly in the Mount of Hodna region.

Many of the red circles (known Pb-Zn deposits) do seem to fall within or close to the "Moderate," "High," and "Very High" prospectivity zones located in the evaporitic region in the eastern part near to Boukhadra and Ouenza deposit. This suggests a degree of success in our model's ability to identify areas associated with known mineralization

thereby reinforcing the model's reliability in highlighting the significant contribution of geological age to the ore formation process

Results & Discussions

The rule set emphasized the interaction between fault proximity and existence of folds and thrust formations. As a result, areas near faults with moderate to high geochemical values received higher weights, even if other factors like lithology were only moderately favorable

1.1.4. Model Validation of the AHP-Based Mineral Prospectivity Map

To assess the predictive performance of the AHP-based MPM, a combination of statistical metrics and spatial analysis techniques within a GIS environment was applied. Using spatial analyst tools, the distribution of known mineral deposits across the five mineral potential classes was evaluated. This included quantifying the number of deposits captured in each class and calculating performance metrics such as the Area Under the ROC Curve (AUC) to determine the model's ability to distinguish between mineralized and non-mineralized zones. The outcomes of this validation are summarized in the following tables.

Table 12: Distribution of Captured Deposits and Non-Deposits by Mineral Potential Class for AHP

Potential Class	Deposits Captured	Non-Deposits Captured	Surface Area (km²)
Class 1 (Very Low)	3	218	12 640
Class 2 (Low)	29	25	13 368
Class 3 (Moderate)	92	4	16 805
Class 4 (High)	82	0	14 556
Class 5 (Very High)	46	0	5 156

Table 13: Confusion Matrix for AHP Model Validation

Category	Definition	Value
True Positives (TP)	Deposits in high potential (Class 4–5)	128
False Negatives (FN)	Deposits in low potential (Class 1–3)	124
False Positives (FP)	Non-deposits in high potential (Class 4–5)	0
True Negatives (TN)	Non-deposits in low potential (Class 1–3)	247

Table 14: Fuzzy Logic Model Prediction Performance Metrics

Metric	Formula	Result
Accuracy	(TP + TN) / Total	75.15
Precision	TP / (TP + FP)	100
Recall	TP / (TP + FN)	50.79
F1 Score	2 × (Precision × Recall) / (Precision + Recall)	67.37

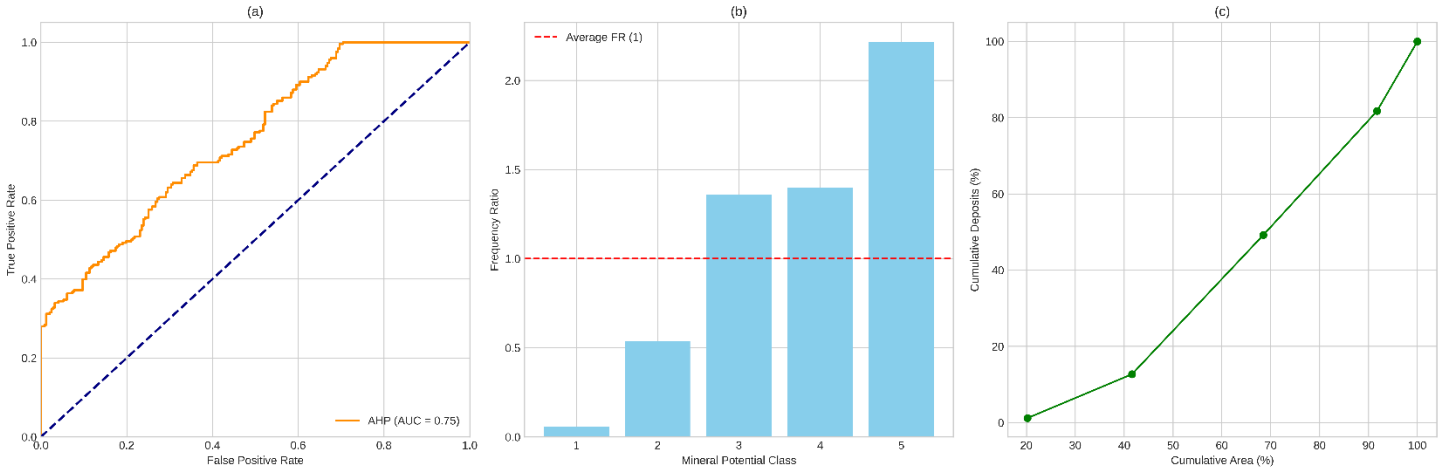

Figure 25: Validation of the AHP Logic-Based MPM Using: (a) ROC Curve, (b) Frequency Ratio, (c) Cumulative Area Analysis

Interpretation:

The validation of the AHP-based MPM reveals a satisfactory level of predictive performance, as indicated by the Receiver Operating Characteristic (ROC) curve with an Area Under the Curve (AUC) of 0.75. This AUC value suggests a good ability of the AHP model to discriminate between areas with and without known mineral deposits, demonstrating its capacity to effectively rank locations based on the weighted combination of hierarchical criteria deemed important for mineralization. The ROC analysis underscores the utility of the AHP framework in synthesizing expert knowledge and preferences for spatial mineral potential assessment.

Further evaluation using Frequency Ratio (FR) analysis across the derived mineral potential classes (1-5) demonstrates a clear trend of increasing deposit density with higher potential classes. Classes 3, 4, and 5 exhibit FR values greater than 1, confirming the model's success in delineating prospective zones where the weighted influence of prioritized geological and other relevant factors is highest. This enrichment of known deposits in the higher potential classes validates the hierarchical weighting scheme employed in the AHP and its effectiveness in translating expert judgment into spatially explicit prospectivity estimates.

The efficiency of the AHP-based MPM for guiding exploration is highlighted by the cumulative area versus cumulative deposits curve, which shows a significant proportion of known deposits being concentrated within a relatively smaller cumulative area classified as having higher potential. This indicates the model's capability to prioritize exploration targets and reduce the search space by effectively identifying the most promising regions based on the weighted integration of multi-criteria evidence. The overall validation results support the application of the AHP as a structured and transparent knowledge-driven approach for MPM.

1.2. Fuzzy Logic:

1.2.1. Model prospectivity mapping using Fuzzy Logic method :

The final prospectivity map, generated through fuzzy logic integration, represents the spatial variation in the degree of mineral potential across the study area. Each pixel value on the map ranges between 0 and 1, indicating the degree of membership to the class "favorable for mineralization. (figure 26)

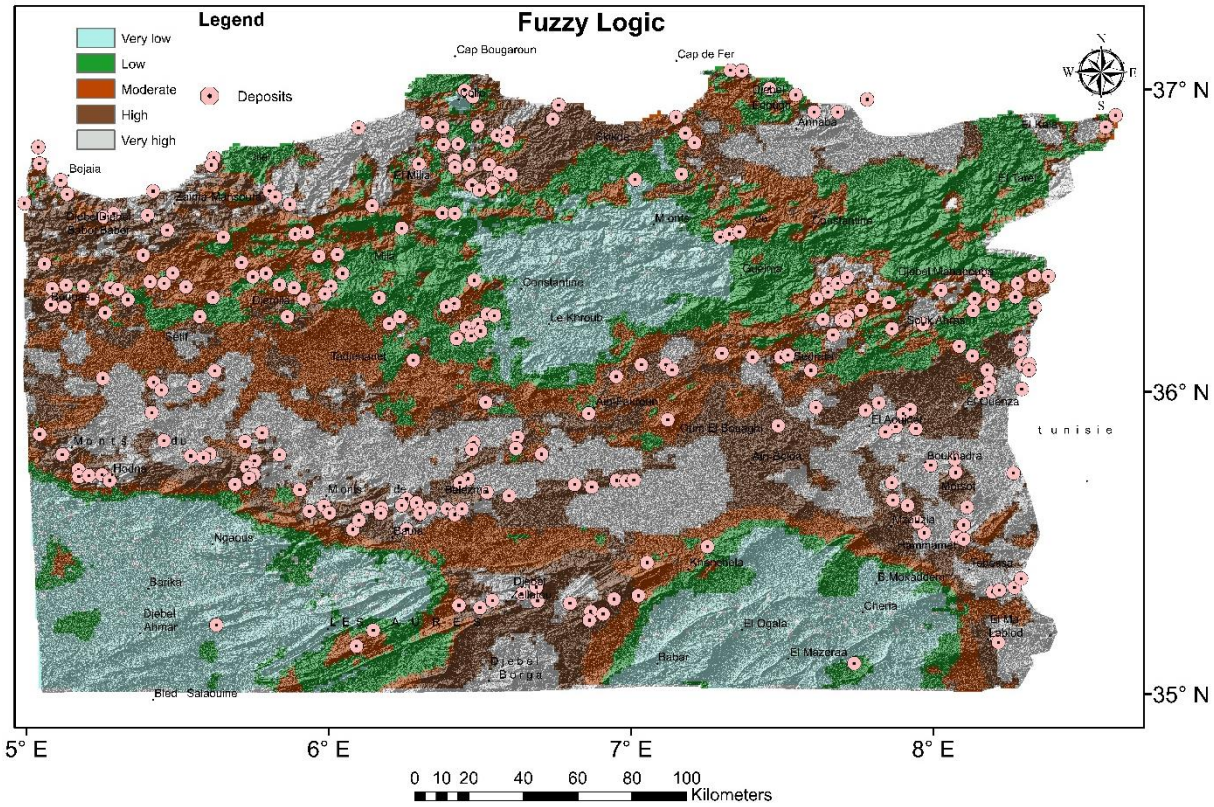

Figure 26: Predictive Pb-Zn deposits probability maps derived by Fuzzy Logic

The resulting mineral prospectivity map delineates five distinct classes, ranging from the highest to the lowest potential for Pb-Zn mineralization. Notably, high prospectivity zones are primarily concentrated along the northeastern fault corridor within the Hodna Sétifien district, exhibiting a strong spatial correlation with areas of intense hydrothermal alteration. This corridor also encompasses existing mining operations such as Chabet el Hamra, Kherzet Youcef, and Ain El Kahla, as well as several mineral occurrences including Kef Semmah and Ain Sedjra in the Guergour Mountains. The elevated prospectivity scores in this corridor are attributed to the synergistic presence of favorable carbonate lithologies, structural control exerted by regional faults, and the recognized association of stratabound-type mineralization, a common characteristic of the region's deposits. Furthermore, these mineralization are associated with carbonate rocks of Jurassic and Lower Cretaceous age, a lithology considered highly favorable for mineral accumulation,. Additionally, the littoral margin zones, extending from Oued Amizour through Oued El Kebir to Boussoufa, demonstrate relatively high to very

high potential, likely due to intensive Tertiary magmatic activity that could have generated hydrothermal fluids enriched in Pb-Zn. Conversely, the lowest potential regions are observed in the central part of the study area around Constantine and the southeastern region within the Saharan Atlas, a pattern that can be plausibly linked to a relative absence of significant tectonic activity in these areas.

1.2.2. Model Validation of the Fuzzy Logic-Based Mineral Prospectivity Map

The fuzzy logic-based MPM was validated through statistical and spatial analysis using GIS tools. Known deposits were compared across the five potential classes, and performance was assessed using metrics like the Area Under the Curve (AUC). The results confirm the model's ability to predict mineralized zones and are summarized in the following tables.

Table 15: Distribution of Captured Deposits and Non-Deposits by Mineral Potential Class FOR Fuzzy Logic

Potential Class	Deposits Captured	Non-Deposits Captured	Surface Area (m^2)
Class 1 (Very Low)	1	206	10772170000
Class 2 (Low)	29	38	13792270000
Class 3 (Moderate)	78	3	15332260000
Class 4 (High)	110	0	15366070000
Class 5 (Very High)	32	0	7262462000

Table 16: Confusion Matrix for Fuzzy Logic Model Validation

Category	Definition	Value
True Positives (TP)	Deposits in high potential (Class 4–5)	142
False Negatives (FN)	Deposits in low potential (Class 1–3)	108
False Positives (FP)	Non-deposits in high potential (Class 4–5)	0
True Negatives (TN)	Non-deposits in low potential (Class 1–3)	247

Table 17: Fuzzy Logic Model Prediction Performance Metrics

Metric	Formula	Result
Accuracy	(TP + TN) / Total	78.27%
Precision	TP / (TP + FP)	100%
Recall	TP / (TP + FN)	56.8 %
F1 Score	2 × (Precision × Recall) / (Precision + Recall)	72.4 %

Results & Discussions

The fuzzy logic model demonstrates a strong and reliable predictive capability for mineral prospectivity, achieving a high overall accuracy of 78.4%. Notably, it exhibits perfect precision (100%) in identifying high-potential zones (classes 4 and 5), meaning all highlighted areas accurately correspond to known mineral deposits without any false positives. However, the model's recall is moderate (57.7%), indicating that it correctly identified only 57.7% of the known mineral deposits, with a significant portion (42.3%, or 110 out of 260 deposits) falling into low to moderate potential zones (classes 1 to 3).

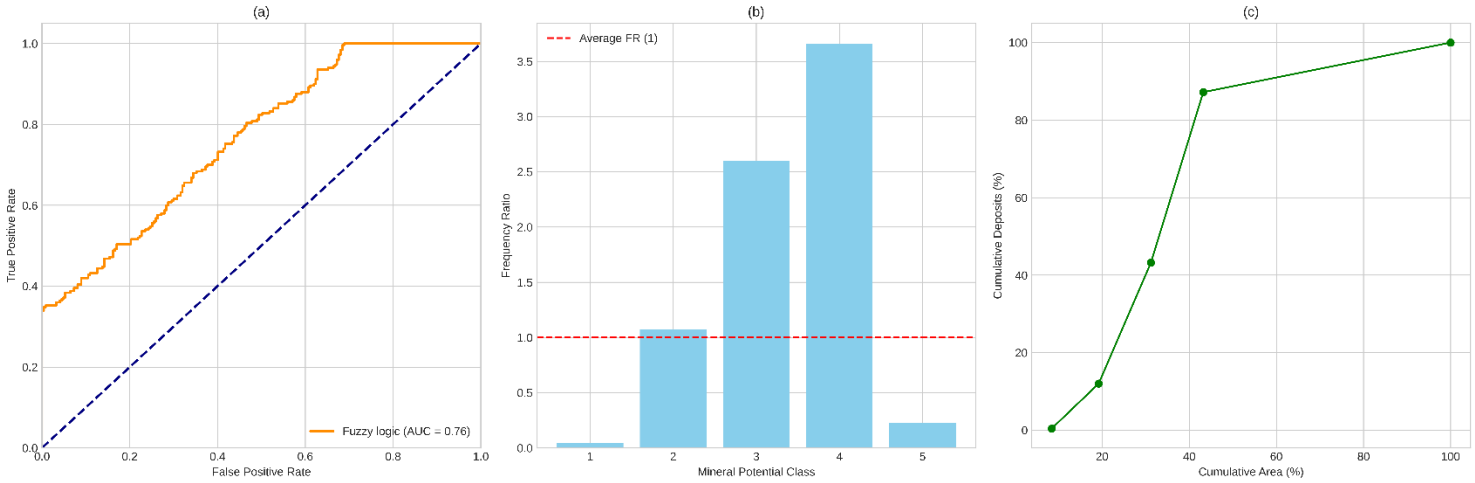

Figure 27: Validation of the Fuzzy Logic-Based Mineral Prospectivity Model Using: (a) ROC Curve, (b) Frequency Ratio, (c) Cumulative Area Analysis

The evaluation of the fuzzy logic-based MPM reveals a robust capacity for identifying potential mineralization zones, as evidenced by the ROC curve in figure 27 (a) exhibiting an Area Under the Curve (AUC) of 0.76. This value signifies a good discriminatory ability, indicating that the model effectively ranks areas with known deposits higher than those without across a range of potential thresholds inherent in the continuous output of the fuzzy logic process. The ROC analysis underscores the potential of fuzzy logic in handling the inherent uncertainty and vagueness associated with geological datasets for MPM.

Further validation through Frequency Ratio (FR) analysis shown in figure 27 (b) across the derived mineral potential classes (1-5) demonstrates a clear positive correlation between higher potential classes and the presence of known deposits. Classes 3 and 4 exhibit significantly elevated FR values, confirming the model's success in delineating prospective areas where the confluence of favorable fuzzy membership degrees for various predictive factors is highest. However, the lower FR observed in Class 5, despite representing the highest potential, suggests a need for further refinement in the fuzzy rule base or membership function definitions to ensure a consistent enrichment of deposits within the most prospective category.

The efficiency of the fuzzy logic MPM in prioritizing exploration efforts is highlighted in figure 27 (c) by the cumulative area versus cumulative deposits curve. The steep initial incline indicates that a relatively small proportion of the study area classified as having high mineral

potential captures a substantial percentage of the known deposits. This demonstrates the model's utility in reducing the search space and focusing resources on the most promising regions identified through the aggregation of weighted fuzzy evidence layers. The overall suite of validation metrics supports the application of fuzzy logic as a valuable tool in MPM, offering a flexible framework for integrating diverse and imprecise geological information.

2. Data driven methods :

2.1. Correlation matrix

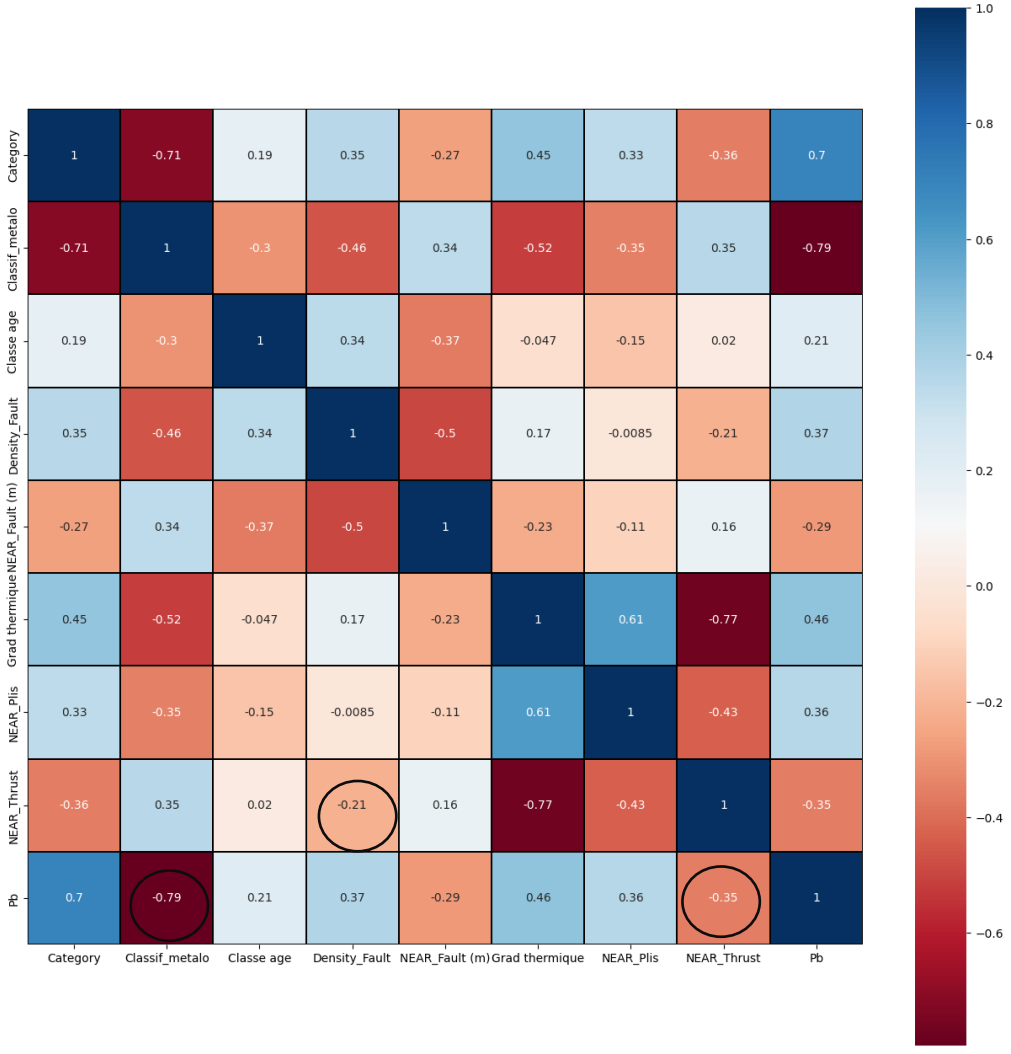

Figure 28: Correlation matrix

Fig.28 illustrates the correlation matrix; negative values between some features and the target; it signifies an inverse relationship between the two indicating that changes in one variable are associated with opposing changes in the other

2.2. Confusion Matrix:

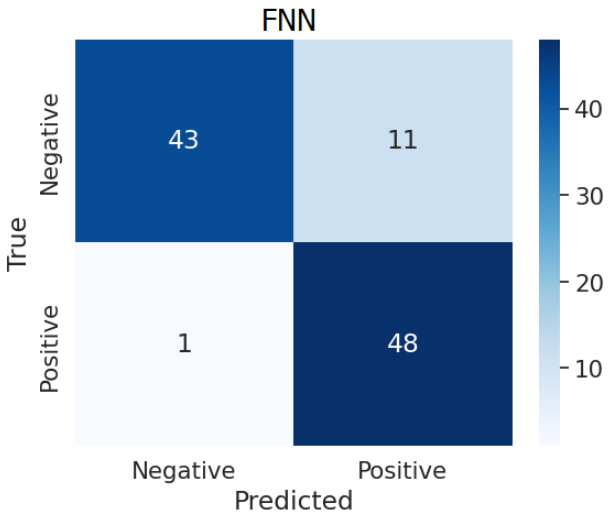

Figure 29: Confusion matrices of the FNN model

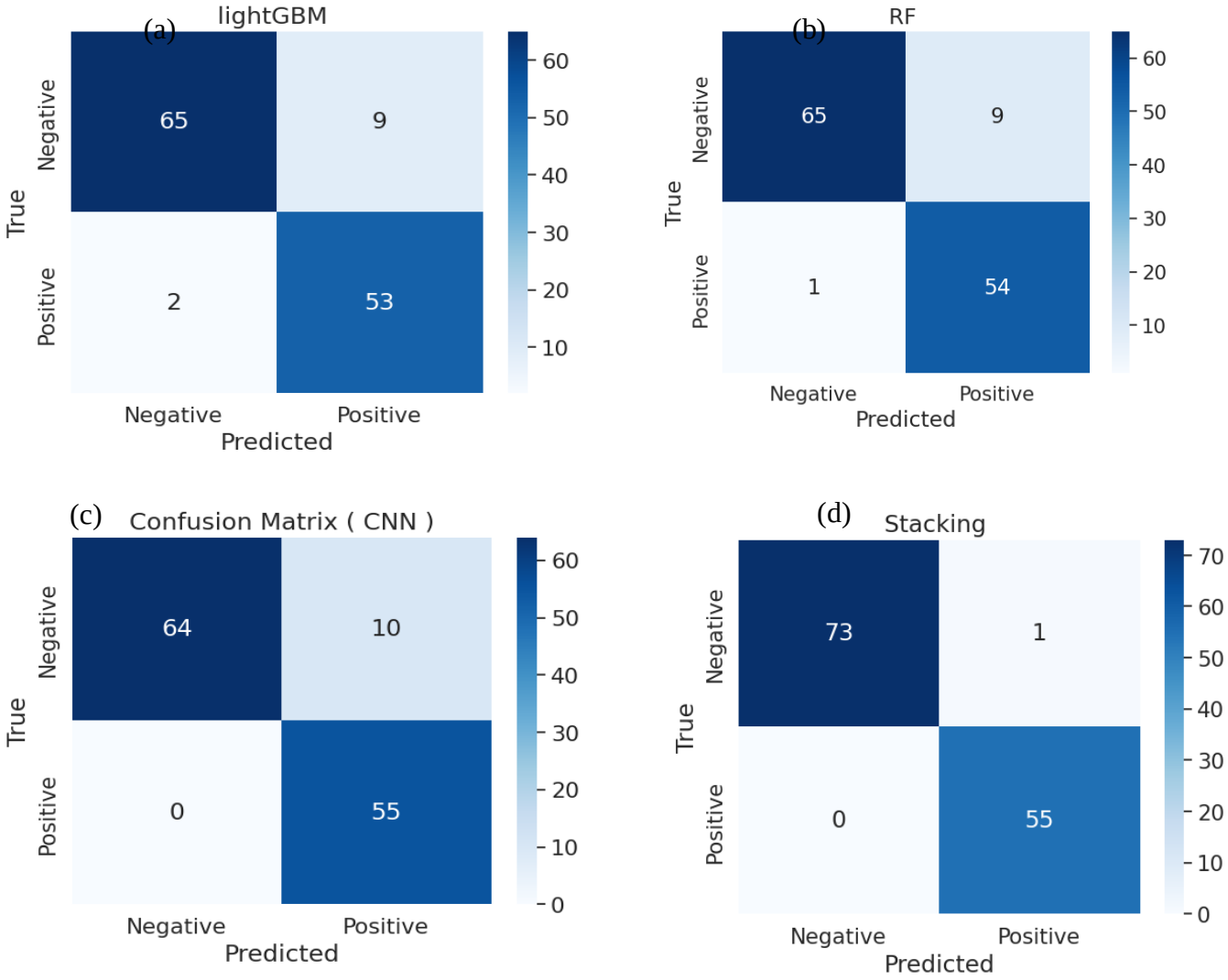

Figure 30: Confusion matrix: (a) Light GBM, (b) RF, (c) CNN and (d) stacking model

2.3. Performance metrics of ML models

The Table 18 presents the performance metrics of various machine learning models including FNN, RF, Light GBM, CNN, and stacking in terms of accuracy, sensitivity, specificity, precision, and F1 score.

Table 18: Performance Evaluation of ML algorithms

Model/Evaluation	Accuracy	Sensitivity	Specificity	Precision	F1 score
FNN	88,35%	97,96%	88,35%	81,36%	88,89%
RF	92.25%	98.18%	87.84%	85.71%	91.53%
Light GBM	90.70%	94.55%	87.84%	85.25%	89.66%
CNN	92.25%	100.00%	86.49%	84.62%	91.67%
Stacking	97.67%	100.00%	95.95%	94.83%	97.35%

The evaluation of our machine learning models reveals that the Feedforward Neural Network (FNN), when individually optimized, achieved a respectable accuracy of 88.35%, demonstrating its capability to learn patterns indicative of Pb-Zn mineralization. It exhibited a high sensitivity of 97.96%, indicating a strong ability to identify areas with deposits. However, compared to the stacked ensemble model, the FNN showed lower performance across all other metrics: its specificity (87.84%) and precision (81.36%) were notably lower, suggesting a higher rate of false negatives and false positives, respectively. Consequently, its F1-score (88.89%), a balanced measure of precision and sensitivity, also fell short of the stacking model's superior 97.35%. This comparison highlights the advantage of the ensemble approach; by combining the diverse learning capabilities of multiple well-performing models like RF, Light GBM, and CNN, the stacking method significantly enhances the overall predictive accuracy and robustness compared to relying on a single, albeit optimized, FNN for complex MPM. The ensemble's ability to leverage the strengths of each base model ultimately leads to a more reliable and balanced prediction of prospective areas.

2.4. ROC-AUC of ML models

To rigorously assess the generalization and robustness of our machine learning models in identifying key mineral controls and preventing overfitting or convergence issues, we evaluated their performance using Receiver Operating Characteristic (ROC) curves and the corresponding Area Under the Curve (AUC). The AUC provides a quantitative measure of a model's ability

to distinguish between positive (deposit) and negative (non-deposit) instances. A higher AUC value, approaching the ideal of 1, indicates superior discriminatory power, as the ROC curve trends towards the top-left corner.

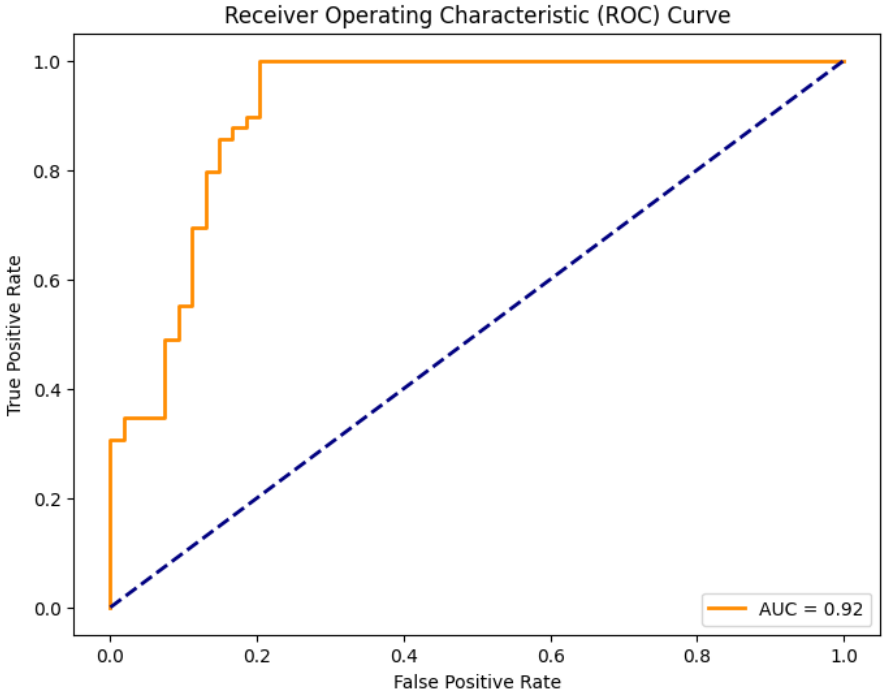

Figure 31: ROC curves for FNN model

The FNN model was trained using these parameters, and its performance was evaluated using the ROC curve the ROC curve. (Fig. 31). An AUC value greater than 0.8 is considered acceptable (Nahm, 2022).

The model showed an excellent predicting performance with an AUC of 92 % , it indicates its ability to correctly identify the prospective areas,

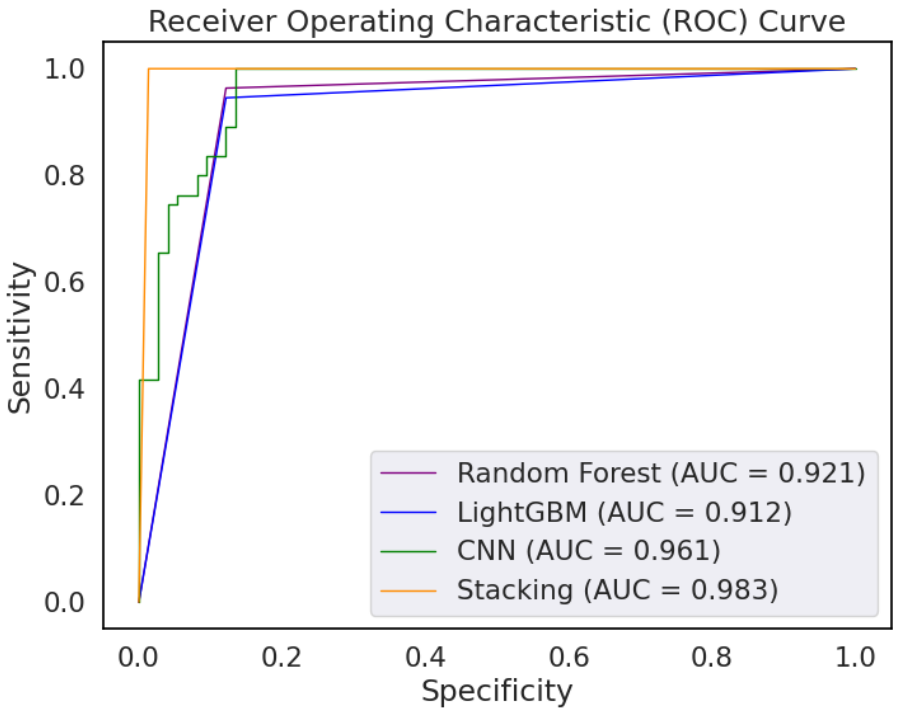

Figure 32: ROC curves for RF, Light GBM, CNN and stacking model.

Figure 32 displays the ROC curves for the four models under their optimized parameter settings. The stacking ensemble demonstrably outperformed all individual models, achieving an impressive AUC exceeding 98%, with its ROC curve positioned closest to the optimal top-left corner. Following the stacking model, the CNN also exhibited excellent predictive capability with an AUC of 96.1%, indicating a strong ability to differentiate between known and potential deposit locations. In comparison, Random Forest and Light GBM achieved AUC values of 92.1% and 91.2%, respectively, suggesting slightly lower discriminatory power than the CNN and the stacking ensemble. The closer a model's AUC is to 1, the better its ability to consistently rank positive instances higher than negative instances, as reflected by its ROC curve's proximity to the top-left corner. The high AUC of the stacking model and CNN underscores their effectiveness in accurately predicting Pb-Zn mineral prospectivity in our study area.

2.5. Feature importance:

The analysis of feature importance provides critical insights into the factors driving Pb-Zn mineralization occurrence. Our study incorporated a range of geological features, including metallogenic and tectonic controls, which define the favorable conditions for ore formation. Figure 33 and 34 illustrates the relative importance of these features as determined by the four machine learning models employed.

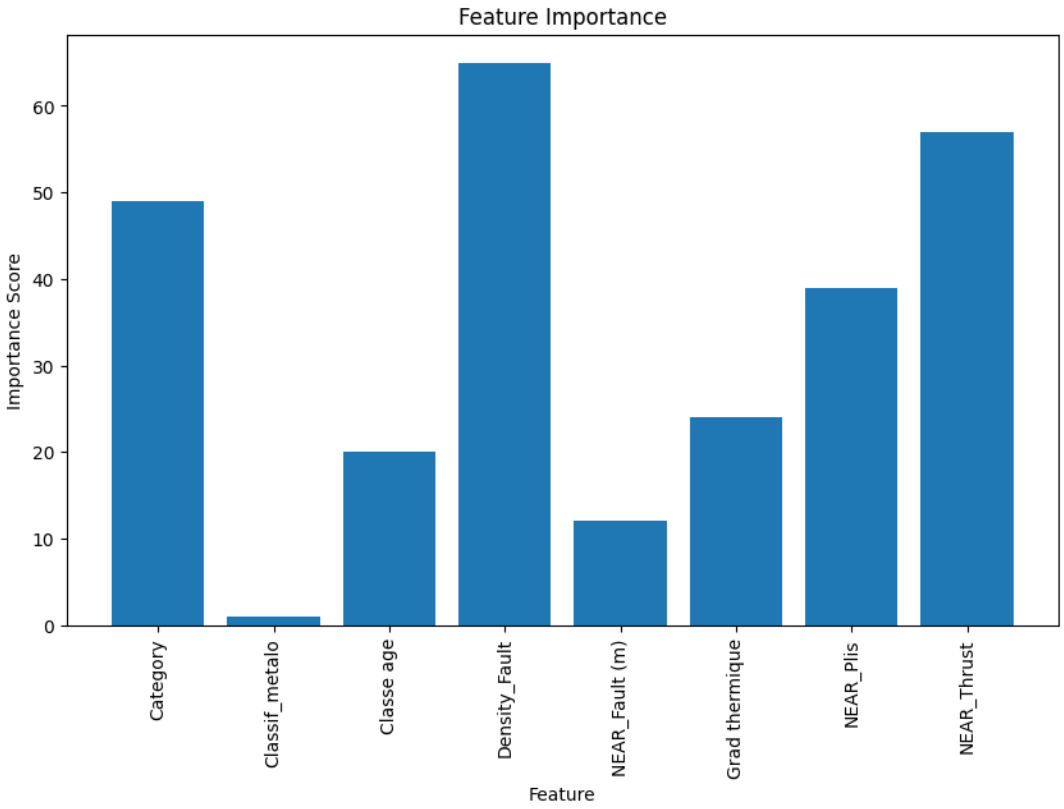

Figure 33: The importance of geological feature for exploration targeting criteria used for generating predictive models from FNN algorithm

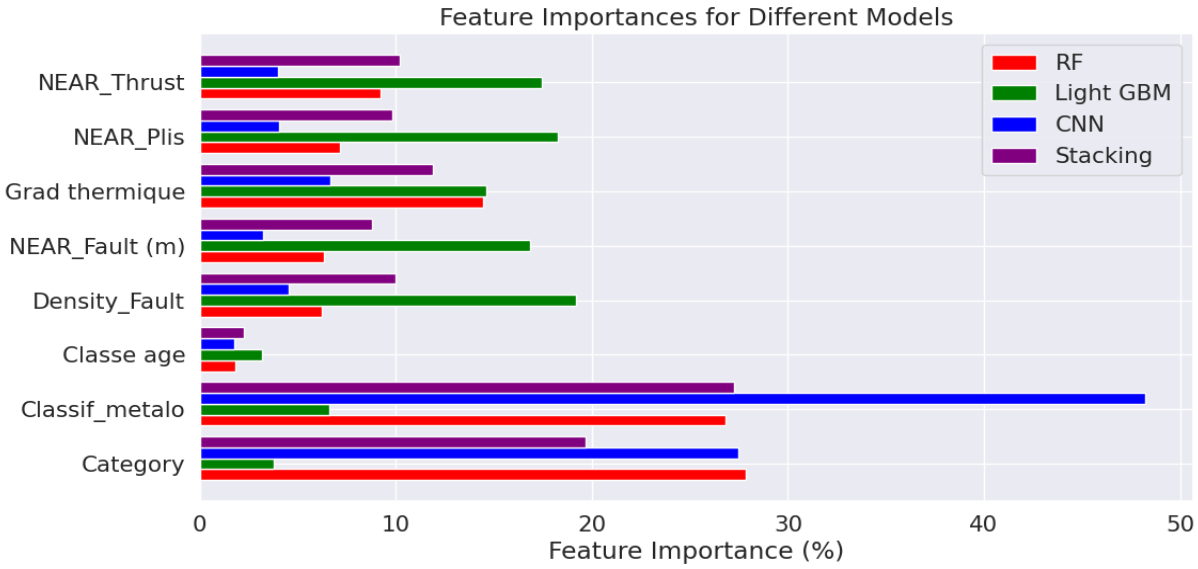

Figure 34: The importance of geological feature for exploration targeting criteria used for generating predictive models: RF, Light GBM, CNN, and stacking method.

Across the Convolutional Neural Network (CNN) and the stacked ensemble model, the metallogenic factor (Classif_metalo) emerges as the most influential predictor, highlighting its significant role in mineral existance. The deposit category (Category) consistently ranks as the second most important feature in these models. Examining the influence of this category

suggests a strong spatial correlation, where larger, economically significant deposits (higher categories) notably increase the probability of discovering new mineralization in their approximate areas.

In contrast, the Light GBM model emphasizes the importance of tectonic features. Specifically, fault density, proximity to faults, proximity to folds, and proximity to thrust sheets are identified as the major contributing factors to mineral potential, exhibiting relatively similar levels of influence. This underscores the role of these structural elements in creating pathways and traps that facilitate the circulation and accumulation of hydrothermal fluids rich in Pb-Zn mineralization.

The Random Forest model aligns with the CNN and stacking results by highlighting the significance of the deposit category and metallogenic factors. This suggests that areas proximal to known, substantial Pb-Zn deposits and those characterized by favorable regional metallogenic settings are strong indicators of further mineralization potential.

In summary, while the models exhibit some variations in the specific ranking of features, the metallogenic factor and deposit category consistently emerge as highly influential across the CNN and stacked ensemble, emphasizing the importance of regional geological context and the spatial clustering of significant deposits. Light GBM, on the other hand, underscores the crucial role of tectonic structures in controlling hydrothermal fluid flow and mineralization. RF reinforces the significance of existing deposits and metallogenic settings. These insights into feature importance provide valuable guidance for targeted mineral exploration efforts in northeastern Algeria.

2.6. Mineral Potential maps derived from ML algorithms :

the resulting mineral prospectivity maps generated by each of the machine learning algorithms employed in this study, effectively highlighting areas with high potential for Pb-Zn deposits in northeastern Algeria. These maps visually synthesize the complex relationships learned by each model from the integrated geological, geodynamic, and metallogenic datasets

Figures, 35, 36, 37, 38, 39 showcase the prospectivity maps derived from the **Feedforward Neural Network (FNN)**, the **Random Forest (RF)**, the **Light Gradient Boosting Machine (Light GBM)**, the **Convolutional Neural Network (CNN)**, and the final **Stacking Ensemble** model. By visualizing the spatial distribution of predicted prospectivity scores, these maps provide a direct and interpretable output, identifying zones deemed most favorable for Pb-Zn mineralization based on the unique learning patterns and feature importance assessments of each individual algorithm and their combined predictive power in the ensemble approach.

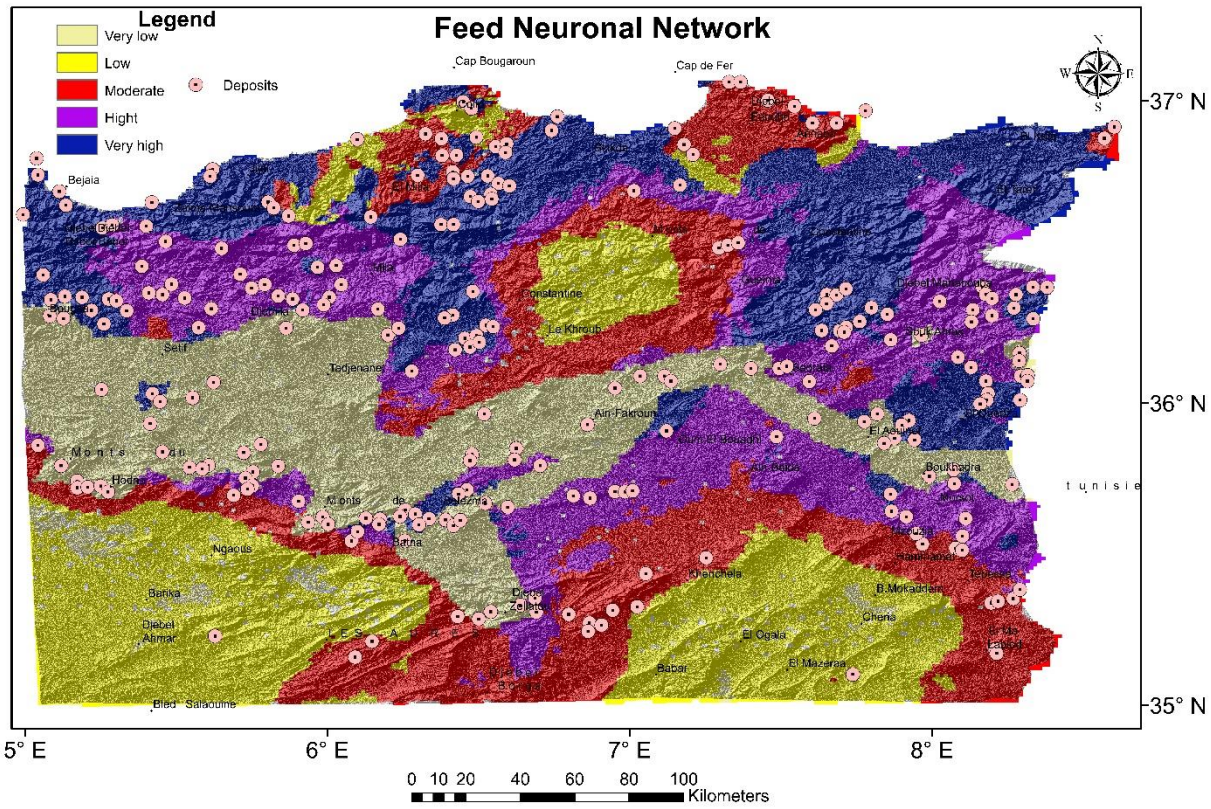

Figure 35: Predictive Pb-Zn deposits probability maps derived by FNN.

The MPM derived from FNN model in figure 35 demonstrated a high potential areas of polymetallic mineralization located majorly in the kabylian basement characterized by a sever technic activity that resulted the thrusts and faults along the area , serving as pathways for hydrothermal fluids circulation. Embracing their pivotal role in creating troupes for polymetallic accumulation

It is also noticed that there is a dense presence of mineralization in setifian domain and the “neritic constantinois”, these deposits are stratabound" mineralization, which are partially stratiform at the deposit scale, and fracture fillings. (Boutaleb et al., 1999) . and occurs inside dolomitic formations, Dolomitization plays a crucial role in the formation of Mississippi Valley-Type (MVT) deposits

The regions of low probability of mineralization are located in the saharan Atlas.

The unfavorable areas for Pb-Zn mineralization occurrence are dominated by continental facies, characterized by coarse-grained detrital rocks and the presence of evaporites, they are located generally in the saharan Atlas. Conversely, areas with marine or transitional facies, often featuring finer-grained sediments and a more geochemically diverse environment, are more prospective.

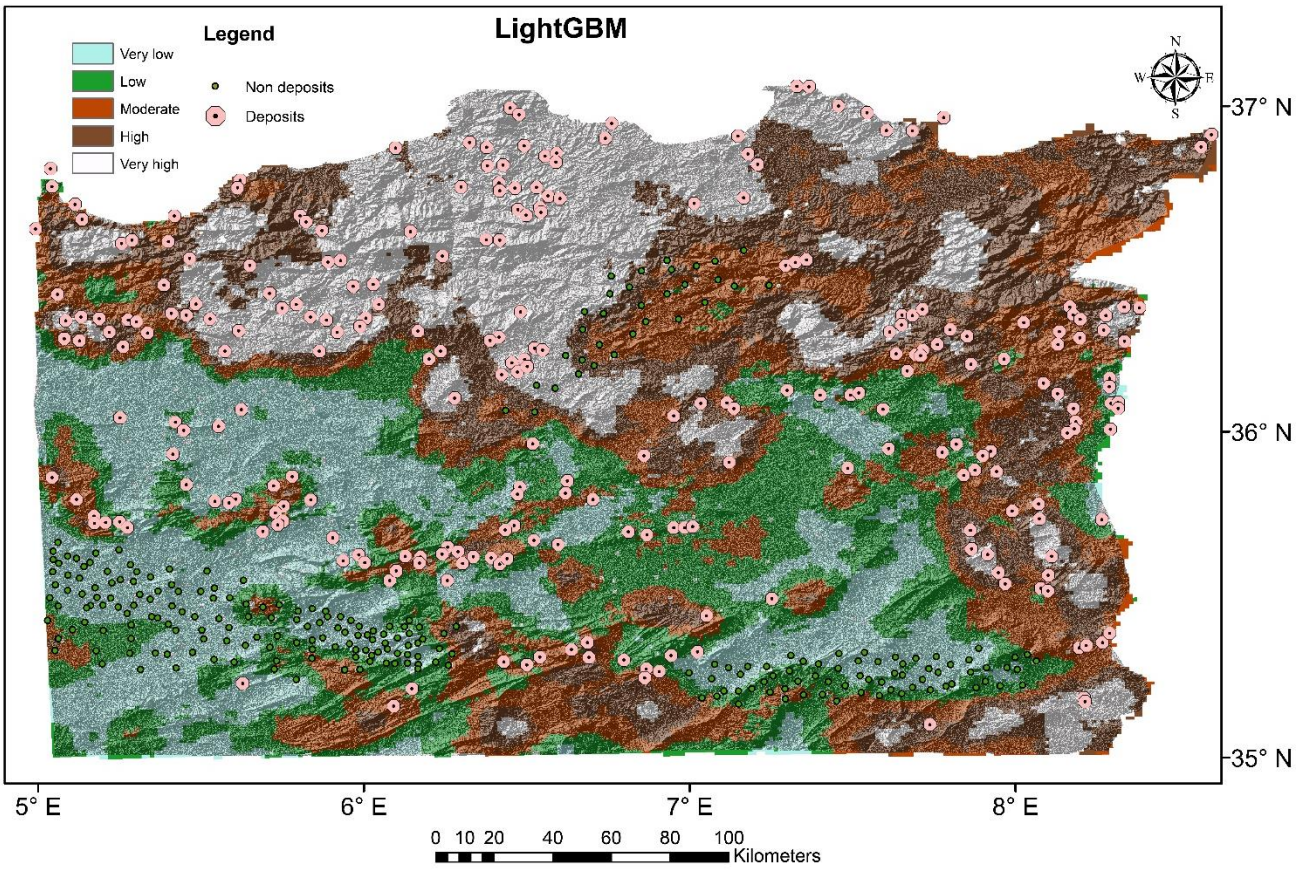

Figure 36: Predictive Pb-Zn deposits probability maps derived by Light GBM..

Light GBM: The Mineral Prospectivity Map (MPM) generated by Light GBM (Fig. 36) highlights the north-central region and its immediate surroundings as having a high probability of Pb-Zn occurrences. This elevated potential aligns with areas that have experienced significant tectonic activity, notably including the normal fault system of the Algerian border basin of Lesser Kabylia (Collo region) (Arab et al. 2016; Seffari et al. 2023). Specifically, the Skikda area, encompassing Beni Toufout, Cap Bougaroune, and Filfila (Kolli 1997a; Ouabadi 1994) shows a strong prospectivity potential. These zones are largely characterized by Calc-alkaline granitic rocks, such as the Cap Bougaroun Granite and the Beni Toufout Granites, which are considered favorable host rocks for polymetallic mineralization. Furthermore, the Edough Massif also presents high mineral potential in areas near Ain Barbar, Mellaha, and Sefsaf. This mineralization is attributed to the interaction between magmatic-hydrothermal hypersaline fluids originating from concealed rare-metal granites and various metamorphic fluids (Marignac et al. 2016) . In the northern part of the internal domain, mineral occurrences are associated with hydrothermal processes linked to extensional tectonics during the Miocene-Quaternary period, particularly along the faulted margins of subsidence basins near basement highs (Ysbaa et al. 2021). The interplay of geodynamic movements and the contacts between subsiding basins and paleo-horst boundaries, giving rise to major tectonic features like thrusts, warrants focused future exploration in these regions. Conversely, the Saharan Atlas region is identified by Light GBM as having a low probability of Pb-Zn mineralization.

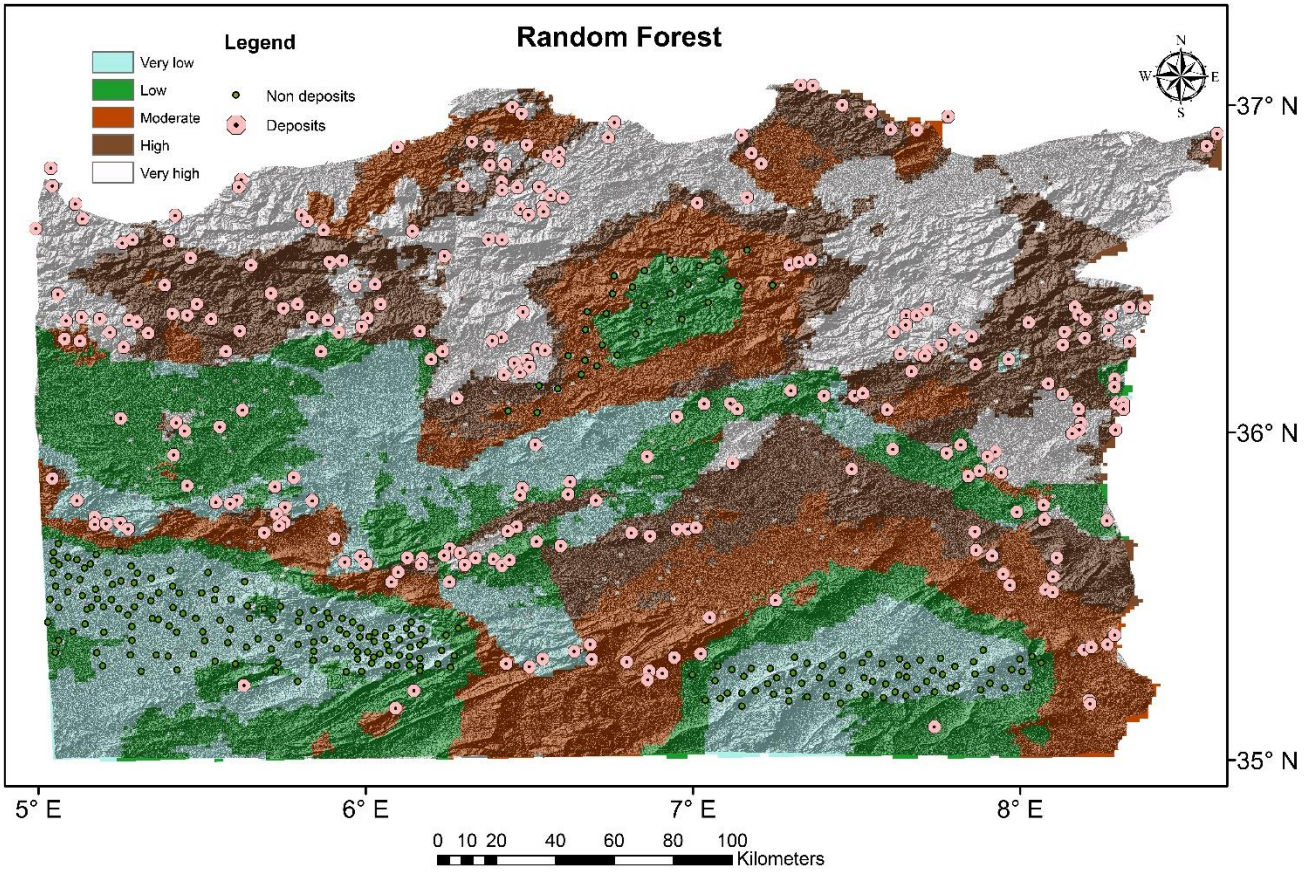

Figure 37: Predictive Pb-Zn deposits probability maps derived by RF.

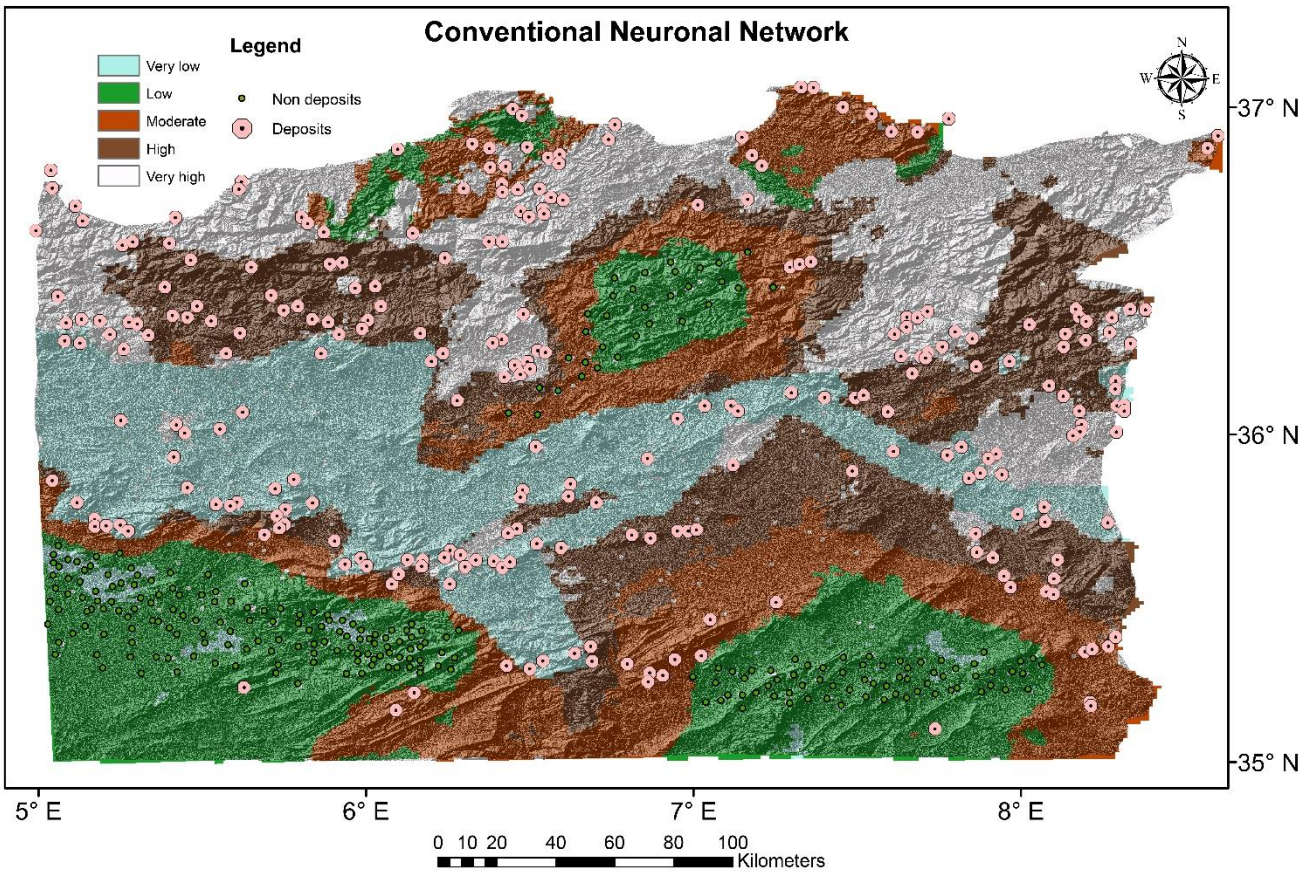

Figure 38: Predictive Pb-Zn deposits probability maps derived by CNN.

RF and CNN : The Mineral Prospectivity Maps (MPMs) produced by both the RF (Fig. 37) and Convolutional Neural Network (CNN) (Fig. 38) models display notable similarities, with high potential zones concentrated along the littoral margins of the study area. These prospective regions are in close proximity to the significant zinc-lead deposits of Oued Amizour, El Aouana, and Oued El Kebir. These deposits are associated with Neogene calc-alkaline volcanic activity, and these sites, characterized by both volcanic and plutonic features, have experienced hydrothermal activity conducive to the formation of Volcanogenic Massive Sulfide (VMS) deposits (Lekoui, 2018; Boutaleb et al., 2023) Furthermore, the area extending from Cap Bougaroune to Filfila in the north also exhibits high potential, largely attributed to the presence of rhyolite and granitic rocks. In the far east, Kef Oum Teboul also shows enhanced prospectivity. In the south, the mineralization zones of Boukhdema, Kef Semmah, and Djebel Felten are located within the Neritic and Setifian domains. Here, the mineralization is stratabound, occurring within carbonate formations that provide highly favorable metallogenic conditions for ore development.

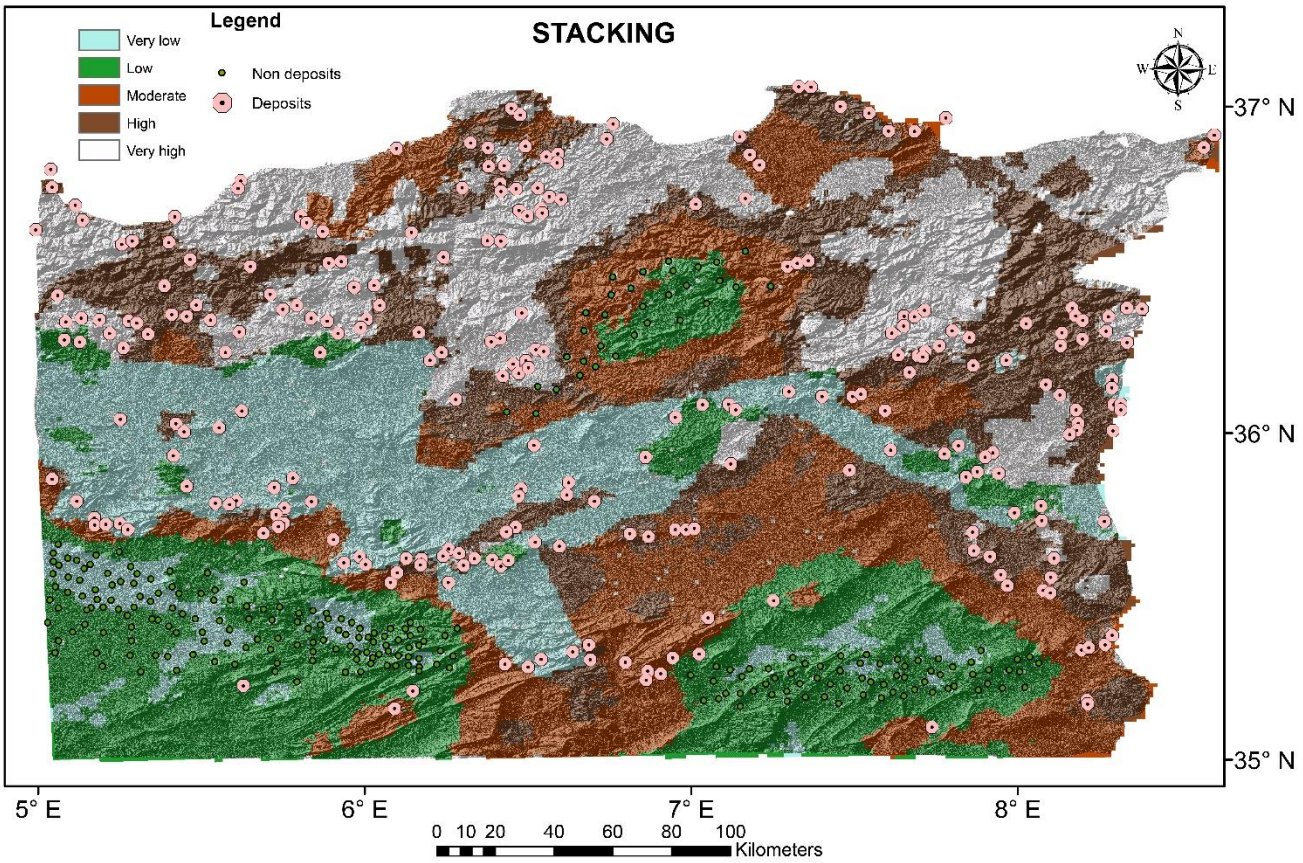

Figure 39: Predictive Pb-Zn deposits probability maps derived by stacking ensemble model.

Stacking: The Mineral Prospectivity Map (MPM) generated by the stacking ensemble algorithm (Fig. 39) reveals two key regions with significant potential for Pb-Zn mineralization: the Algerian coast and the Northeastern Tell. Along the Algerian coast, extending from Béjaia to Annaba and encompassing areas like Oued Amizour, El Aouana, and the Collo region, past volcanic activity has created a favorable environment for mineral deposit formation, demonstrating a clear spatial and likely genetic link to Neogene magmatism. The second prominent zone of high potential is situated within the external domain, specifically in the southern Tellian units of Constantine and Boudoukha (Lakhdar et al., 2022)), south of Sétif, and further eastward into the diapiric district. Here, the geological conditions at the contact zone between the allochthonous foreland and the Atlas foreland structural units are exceptionally conducive to mineralization, frequently associated with Mississippi Valley Type (MVT) deposits. These deposits, sharing characteristics with fault-related mineralization in sedimentary basins and exhibiting an epigenetic origin, suggest a high probability for polymetallic occurrences across the Setifian region and Hodna, the Belezma region and Aurès, as well as within the diapiric district.

2.7. Validation of the Data-Driven Mineral Prospectivity Model (MPM):

To validate the reliability of the final mineral prospectivity model developed using data-driven methods, particularly the stacking ensemble approach, three mineralized sites not used in the initial training dataset were examined. All three occur within zones classified as high-potential, reinforcing the predictive performance and spatial accuracy of the model (see Figure 40).

- **Bir Béni Salah** hosts Hg-Pb-Zn mineralization of presumed hydrothermal origin, exhibiting metasomatic, vein-type structures characteristic of mercurial-polymetallic systems (Bourahla et al., 2000)
- **Achaiche**, situated in Petite Kabylie, displays Pb-Zn-Cu mineralization related to post-orogenic magmatism (Ouabadi 1994; Satouh 2007). The deposit is structurally controlled by mineralized veins and fractures and occurs in volcanic and intrusive settings including granites, rhyolites, and andesites (Tchouiko, Kroviakov 1974)
- **Zitouna** is characterized by polymetallic mineralizations (Pb-Zn-Cu) hosted in sedimentary rocks like sandstones and clays. The ore distribution is controlled by fracturing and stratigraphic discontinuities, with mineralization occurring as veins and disseminations.

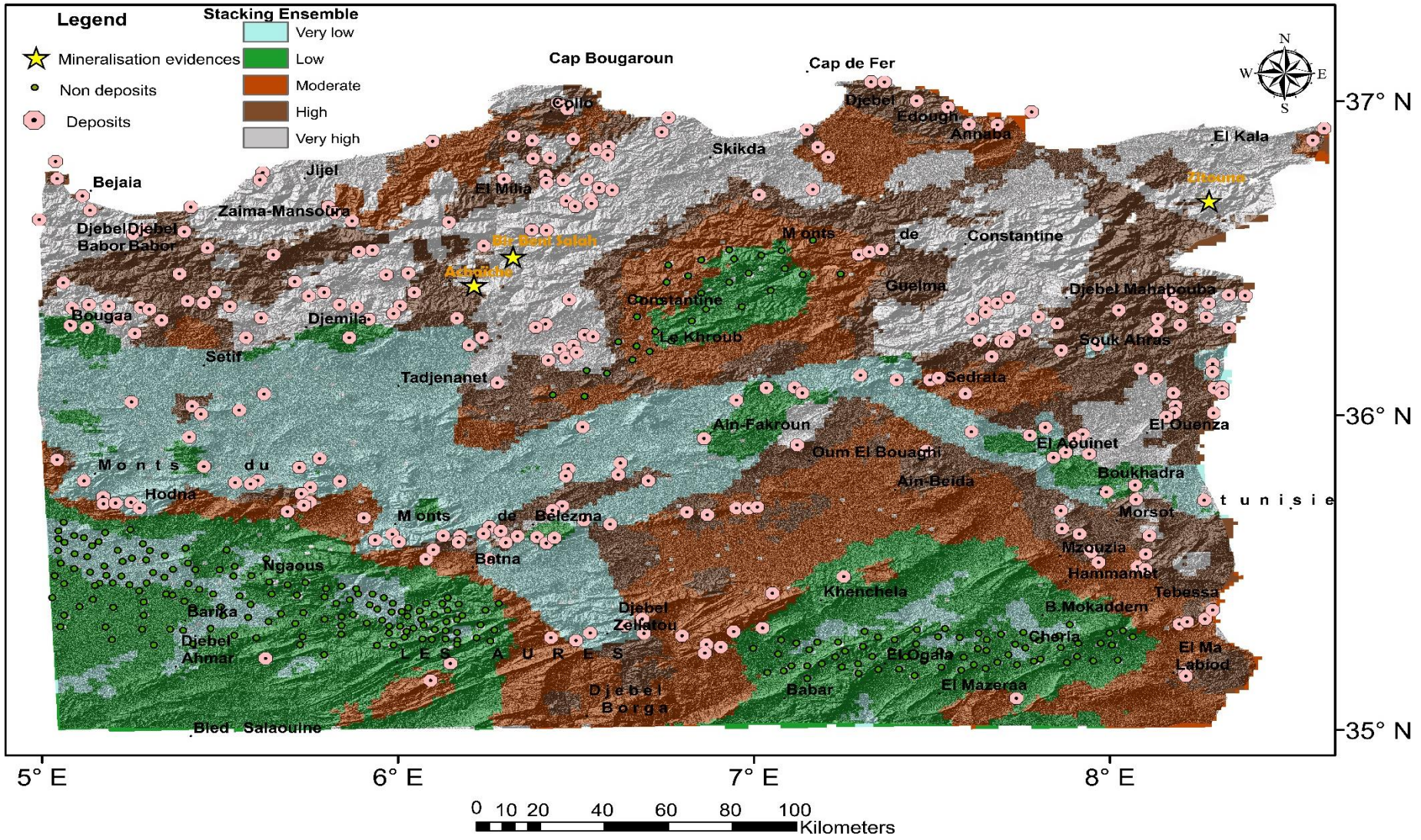

Figure 40: New mineralization evidences implemented in the Predictive Pb-Zn deposits probability maps derived by stacking ensemble model

3. Comparaison between knowledge driven and data driven methods in MPM

Both knowledge-driven and data-driven approaches, through their respective models and algorithms, produced mineral prospectivity maps (MPMs) highlighting the distribution of potential mineralized zones within the study area. To evaluate the effectiveness and differences between these methods, we conducted a quantitative assessment based on performance metrics.

As presented in Table 19, we provide a detailed comparison that includes key metrics such as accuracy, sensitivity (true positive rate), the surface area covered by high-potential zones (Classes 4 and 5), and a qualitative description of their spatial distribution.

Table 19: Comparison of Evaluation Metrics and Spatial Distribution Across MPM Models

Model/Evaluation	Accuracy (%)	Sensitivity (%)	Surface (km^2)		Description	
			Very low	Very high	Very low zones	Very high zones
AHP	75.15	50.79	5156	12640	Central part, Southeast, Southwest	Skikda, Mount of Hodna, Ouenza
Fuzzy	78.27%	56.8	7262	10772	Central part, Southeast, Southwest	Littoral region, Setif, Mount of Hodna
FNN	88,35%	97	10250	18500	Central part, Southeast to Southwest	Littoral parts, Extreme East (diapiric zone)
RF	92.25%	98	8500	17500	Southeast, Southwest	Extreme East & West Littoral, Central zones
Light GBM	90.70%	94	6000	12500	Southeast, Southwest	Central North, Eddough region
CNN	92.25%	100	10250	18500	Central part, Southeast to Southwest	Littoral parts, Extreme East (diapiric zone)
Stacking	97.67%	100	7250	15000	Central part (East to West)	Extreme Northeast & Northwest, Some Littoral regions

The knowledge-driven methods (AHP and Fuzzy Logic) demonstrate moderate performance, with accuracy values ranging from **75.15% to 78.27%** and sensitivity between **50.79% and**

56.8%. These methods are largely dependent on expert judgment and predefined rules, which can introduce subjectivity and limit adaptability to complex patterns.

In contrast, data-driven methods such as FNN, RF, Light GBM, CNN, and Stacking show significantly higher accuracy (**88.35% to 97.67%**) and sensitivity (**94.55% to 100%**), reflecting their ability to learn from large datasets and uncover hidden relationships. These models also tend to better capture high-potential zones, as shown by the larger surfaces assigned to the "Very High" class.

In summary, while knowledge-driven methods provide interpretability and are useful in data-scarce contexts, data-driven approaches outperform them in predictive accuracy and deposit detection efficiency, making them more suitable for complex mineral prospectivity modeling when sufficient data is available.

General Conclusion

1. Introduction

This thesis presents a comprehensive investigation into the application of advanced spatial analysis and machine learning techniques for mineral exploration targeting , specifically focusing on undiscovered Pb-Zn deposits in northeastern Algeria. The primary objective was to transform the conceptual geological models governing Pb-Zn accumulation into mathematical quantifiable, spatially explicit functions. These functions, dependent on materialized geological input factors, were designed to generate predictive models capable of identifying potential areas susceptible to hosting concealed mineralization within the study area.

Numerous studies worldwide have demonstrated the strong correlation between geological features and the spatial distribution of mineralization. These studies, often at a local scale, have shown the effectiveness of integrating geospatial data to delineate ore deposits with high accuracy. Inspired by this approach, and leveraging the abundance of Pb-Zn deposits within a favorable metallogenic context, provided a rich dataset to construct robust numerical models for revealing unprospected deposits. This undertaking involved four major methodological steps: meticulous preparation of predictive layers within a GIS environment, detailed spatial analysis of regional lineaments, and the integration of two distinct methodological paradigms for mineral prospectivity mapping.

To achieve the objectives of this thesis, the research was structured into four main stages:

The first paradigm encompassed knowledge-driven methods, namely the Analytic Hierarchy Process (AHP) and Fuzzy Logic, which represent classical approaches to MPM.. The second paradigm explored data-driven machine learning algorithms, including optimized Feed-forward Neural Networks (FNNs) – highly effective for binary classification tasks – and a stacking ensemble approach that synergistically combined multiple base models suitable for MPM.

The fundamental difference between these methodological approaches lies in how they treat input data and make predictions. Knowledge-driven methods rely on expert judgment to assign weights to input factors, and model validation is achieved by comparing the predictive outputs with known deposit locations. These methods help to assess how well the model can reproduce areas of known mineralization.

Unlike knowledge-driven techniques, data-driven models are intrinsically trained on real-world data of known deposits, allowing algorithms to autonomously learn complex relationships and assign implicit weights to features based on their statistical influence on ore occurrence.

By incorporating both approaches, this study was able to compare and cross-validate the outputs, leading to a more robust assessment of the region’s mineral potential. The integration of classical and advanced techniques has allowed for a more comprehensive and data-informed

model, improving the accuracy and reliability of Pb-Zn prospectivity mapping in northeastern Algeria.

Ultimately, this research contributes to the advancement of mineral exploration methodologies in Algeria and provides a practical framework for future studies aiming to identify and evaluate undiscovered mineral resources using both traditional and modern geospatial techniques.

2. Metallogenic Controls on Pb-Zn Mineralization in Northeastern Algeria

The comprehensive interpretation of integrated geological and geophysical data, combined with insights from relevant scientific literature on ore formation processes in northeastern Algeria, has illuminated key metallogenic controls on Pb-Zn mineralization within the study area. The spatial analysis and the geological model developed for this research, based on a regional-scale analysis of metallogenic elements, lithological associations, and structural features, provided significant results regarding the delineation of potential mineralized zones.

A primary finding highlights the profound influence of geodynamic movements on the distribution and occurrence of Pb-Zn mineralization. Major structural elements, including faults, thrusts, and folds, acted as crucial conduits for hydrothermal fluid circulation, facilitating the accumulation of Pb-Zn deposits. This structural control is clearly manifested in the distinct alignment of mineralization indices along prominent tectonic lineaments. Specifically, across northern parts, the majority of mineralization occurrences are strongly correlated with significant NW-SE and E-W trending tectono-lineaments. Within the Eastern Saharan Atlas and the Hodna/Setifian regions, Pb-Zn mineralization commonly clusters in proximity to or along major NE-SW and NW-SE trending accidents, as well as adjacent to large-scale tectonic structures such as anticlines and diapiric intrusions.

Furthermore, the study confirms the critical role of magmatic activity, particularly in the coastal sectors. The presence of the region's largest Pb-Zn deposits”Oued Amizour” is strongly linked to Tertiary magmatism, suggesting a significant genetic association. This strong spatial and temporal relationship indicates a high possibility for the discovery of additional deposits in areas adjacent to or associated with the magmatic structures.

3. Classical methods VS Artificial methods for MPM

The comparative analysis of knowledge-driven and data-driven methodologies applied to MPM yielded critical insights into their respective strengths and limitations for identifying undiscovered Pb-Zn deposits. The results clearly demonstrated that data-driven machine learning algorithms generally outperformed their knowledge-driven counterparts in terms of overall predictive accuracy and discriminatory power. Specifically, while knowledge-driven models (AHP and Fuzzy Logic) achieved overall accuracies of approximately 75-78% and AUC values ranging from 0.75-0.76, the various machine learning algorithms (FNN, LightGBM, RF, CNN and the Stacking ensemble) exhibited superior performance, often

reaching AUCs between 0.90 and 0.98. This enhanced performance of data-driven models is attributable to their capacity to autonomously discern and leverage intricate, often non-linear, relationships within the extensive geodatabase, effectively capturing patterns that may not be explicitly codified in expert knowledge.

Despite the superior accuracy of data-driven models, a nuanced understanding of their performance is essential. Both Fuzzy Logic and AHP models demonstrated perfect precision (100%) in classifying high-potential zones, meaning every area they delineated as highly prospective genuinely contained a known deposit. This highlights the inherent reliability and interpretability of knowledge-driven approaches, as their classifications directly reflect established geological principles and expert judgment. However, this high precision came at the cost of lower recall rates (e.g., Fuzzy Logic at 56.8% and AHP at 50.79%), indicating that these models missed a notable proportion of known deposits that fell outside their strictly defined high-potential criteria. Conversely, while achieving higher recall and overall accuracy, some data-driven models may offer less direct interpretability regarding the specific geological rationale behind their predictions.

The findings underscore a fundamental trade-off: knowledge-driven methods excel in transparency and the reliability of their positive predictions based on explicit geological understanding, whereas data-driven methods offer superior statistical accuracy and the ability to learn complex patterns from large datasets. This research highlights the significant potential of advanced machine learning techniques to enhance MPM, particularly when sufficient and high-quality data are available. Ultimately, the integration and comparative assessment of both paradigms were instrumental in providing a holistic understanding of prospectivity in northeastern Algeria, offering a foundation for robust exploration targeting strategies that could potentially leverage the strengths of each approach in future hybrid models.

4. Limitations :

Limitations in MPM models stem from several key factors, highlighting that no single "best" model exists for all exploration scenarios. The optimal choice depends on:

- Model Optimization and Overfitting Risk: Both data-driven models (like FNN, CNN, LightGBM, RF, and Stacking) and knowledge-driven approaches (AHP, Fuzzy Logic) require meticulous tuning to prevent overfitting. Without careful calibration, models may perform well on training data but poorly on new, unseen data, limiting their real-world applicability.

- Data Availability and Quality: A fundamental constraint is the availability and quality of predictor variables, including geochemical, geophysical, and remote sensing data. Gaps or inconsistencies in these datasets can significantly impact model accuracy and generalizability, potentially hindering the identification of subtle mineralization features.

General Conclusion

- Limited Generalizability with Restricted Datasets: Models trained on a limited set of geological features or specific environments will have constrained generalizability to diverse geological settings. Expanding datasets to incorporate a wider range of predictor variables and geological contexts is crucial for improving a model's ability to identify potential mineralized zones in different areas.

5. Future Directions for Mitigation

Recognizing these limitations is crucial for advancing the application of Artificial Intelligence in mineral exploration. Future research should proactively address these by:

- **Incorporating Additional Data Sources:** Expanding datasets to include more diverse and comprehensive geological, geochemical, and geophysical information.
- **Exploring More Advanced Algorithms:** Investigating cutting-edge machine learning and **deep learning architectures** that might be better equipped to handle the complexities of geological data.
- **Conducting Localized Studies:** Focusing on areas with higher data availability to refine models and improve the accuracy and reliability of prospectivity predictions in specific, well-characterized regions.

By acknowledging and actively working to overcome these limitations, we can continually enhance the utility and reliability of machine learning in guiding mineral exploration efforts.

Bibliography

ABBASSENE, Fatiha, 2016. Contraintes chronologiques et pétro-géochimiques du magmatisme sur l'évolution pré-et post-collisionnelle de la marge algérienne : secteur de la Petite Kabylie [en ligne]. phdthesis. Université de Bretagne occidentale - Brest ; Université des Sciences et de la Technologie Houari-Boumediène (Algérie). [Consulté le 25 février 2025]. Disponible à l'adresse : https://theses.hal.science/tel-01345948

ABD-ALHAI, Mahmoud Mohamed, ARAFFA, Sultan Awad Sultan, MEKKAWI, Mahmoud Mohamed et ELGALLADI, Ahmed Abdel-Moniem, 2023. A reconnaissance study for tracing and ordering new mineralisation zones using integrated remote sensing, GIS, and aeromagnetic techniques, west Allaqi-Heiani-Suture,Egypt. NRIAG Journal of Astronomy and Geophysics. 31 décembre 2023. Vol. 12, n° 1, pp. 19-44. DOI 10.1080/20909977.2022.2156068.

ABEDI, Maysam, NOROUZI, Gholam-Hossain et BAHROUDI, Abbas, 2012. Support vector machine for multi-classification of mineral prospectivity areas. Computers & Geosciences [en ligne]. 8 janvier 2012. Vol. 46. [Consulté le 30 novembre 2024]. DOI 10.1016/j.cageo.2011.12.014. Disponible à l'adresse : https://discovery.researcher.life/article/support-vector-machine-for-multi-classification-of-mineral-prospectivity-areas/636c7ddc87fb3381bb9caff51102af0a?eos_user_id=4967607&expiry_in_minutes=5&usersource=paperpal&utm_source=paperpal&utm_medium=website&utm_campaign=organic

AFALFIZ, 1992. Etude des carottes de sondages miniers éxécutés sur l'indice polymétallique de Tiri (Chahna Jijel, Algérie). In : Séminaire national des Sciences de la Terre [en ligne]. 1992. [Consulté le 20 février 2024]. Disponible à l'adresse : https://pascal-francis.inist.fr/vibad/index.php?action=getRecordDetail&idt=6495867

AFALFIZ, A., 1990. Etude comparative paragénétique et géochimique des indices minéralisés à Fe, Pb, Zn, Cu, Ba de la partie occidentale du massif cristallophyllien de Petite Kabylie, Algérie. PhD Thesis. Thèse de magister. 202p. Alger.

AFALFIZ, A., GUY, B. et SEMROUD, B., 1998. Etude métallogénique des indices minéralisés à Fe, Pb, Zn, Cu, Ba, Ag dans les métacarbonates du socle métamorphique de la région de Taher, Petite Kabylie, Algérie. Mémoires du Service géologique de l'Algérie. 1998. N° 9, pp. 57-76.

AFZAL, Peyman, FARHADI, Sasan, BOVEIRI KONARI, Mina, SHAMSEDDIN MEIGOONI, Mojtaba et DANESHVAR SAEIN, Lili, 2022. Geochemical Anomaly Detection in the Irankuh District Using Hybrid Machine Learning Technique and Fractal Modeling. Geopersia [en ligne]. mars 2022. N° Online First. [Consulté le 4 décembre 2024]. DOI 10.22059/geope.2022.336072.648644. Disponible à l'adresse : https://doi.org/10.22059/geope.2022.336072.648644

AGTERBERG, F. P., BONHAM-CARTER, G. F. et WRIGHT, D. F., 1990. Statistical Pattern Integration for Mineral Exploration*. In : GAÁL, GABOR et MERRIAM, DANIEL F. (éd.), Computer Applications in Resource Estimation [en ligne]. Amsterdam : Pergamon. pp. 1-21. Computers and Geology. [Consulté le 7 février 2025]. ISBN 978-0-08-037245-7. Disponible à l'adresse : https://www.sciencedirect.com/science/article/pii/B9780080372457500068

AISSA, CHEILLETZ, A., GASQUET, D. et MARIGNAC, Ch, 1995. Alpine metamorphic core complexes and metallogenesis: the Edough case (NE Algeria). In : Mineral deposits: from their

origin to their environmental impacts. In: Proceedings of 3rd Biennial SGA Meeting, Prague. AA Balkema, Rotterdam. 1995. pp. 23-26.

AISSA, D., 1982. LES GISEMENTS ET INDICES METALLIFERES DU MASSIF DE L'EDOUGH. [en ligne]. 1982. [Consulté le 19 décembre 2023]. Disponible à l'adresse : http://pascal-francis.inist.fr/vibad/index.php?action=getRecordDetail&idt=PASCALGEODEBRGM8320408963

AISSA, Djamal Eddine, 1997. Les minéralisations tertiaires de l'Edough (NE Algérie) : métallogénie d'un « métamorphic core complex » miocène [en ligne]. phdthesis. Institut National Polytechnique de Lorraine. [Consulté le 22 février 2025]. Disponible à l'adresse : https://hal.univ-lorraine.fr/tel-01776115

AISSA, Djamal Eddine, 1998. Géologie et métallogénie sommaire du massif de l'Edough (NE Algérie). Mémoire Service géologique d'Algérie. 1998. Vol. 9, pp. 7-55.

ALBAWI, Saad, MOHAMMED, Tareq Abed et AL-ZAWI, Saad, 2017. Understanding of a convolutional neural network. In : 2017 International Conference on Engineering and Technology (ICET) [en ligne]. Antalya : IEEE. août 2017. pp. 1-6. [Consulté le 5 octobre 2023]. ISBN 978-1-5386-1949-0. Disponible à l'adresse : https://ieeexplore.ieee.org/document/8308186/

ALBRECHT, Conrad M, FISHER, Chris, FREITAG, Marcus, HAMANN, Hendrik F, PANKANTI, Sharathchandra, PEZZUTTI, Florencia et ROSSI, Francesca, 2019. Learning and Recognizing Archeological Features from LiDAR Data. In : 2019 IEEE International Conference on Big Data (Big Data) [en ligne]. décembre 2019. pp. 5630-5636. [Consulté le 1 mars 2025]. Disponible à l'adresse : https://ieeexplore.ieee.org/abstract/document/9005548

ALGÉRIE. DIRECTION DES MINES ET DE LA GÉOLOGIE, OFFICE NATIONAL DE LA GÉOLOGIE et Ministère de l'industrie lourde, Office national de la géologie, 1987. Carte des gîtes minéraux de l'Algérie -CONSTANTINE NORD- au 1:500 000. [carte]. Alger, Algérie : Office national de la géologie.

ALI HOSSEINI, Seyed et ABEDI, Maysam, 2015. Data Envelopment Analysis: A knowledge-driven method for mineral prospectivity mapping. Computers & Geosciences. septembre 2015. Vol. 82, pp. 111-119. DOI 10.1016/j.cageo.2015.06.006.

ANDRÉE, Bo Pieter Johannes, CHAMORRO, Andres, SPENCER, Phoebe, KOOMEN, Eric et DOGO, Harun, 2019. Revisiting the relation between economic growth and the environment; a global assessment of deforestation, pollution and carbon emission. Renewable and Sustainable Energy Reviews. 1 octobre 2019. Vol. 114, pp. 109221. DOI 10.1016/j.rser.2019.06.028.

APPIAH-TWUM, Michael, XU, Wenbo et SUNKARI, Emmanuel Daanoba, 2024. Mapping Lithology with Hybrid Attention Mechanism–Long Short-Term Memory: A Hybrid Neural Network Approach Using Remote Sensing and Geophysical Data. Remote Sensing. janvier 2024. Vol. 16, n° 23, pp. 4613. DOI 10.3390/rs16234613.

ARAB, Mohamed, RABINEAU, Marina, DÉVERCHÈRE, Jacques, BRACENE, Rabah, BELHAI, Djelloul, ROURE, François, MAROK, Abbas, BOUYAHIAOUI, Boualem, GRANJEON, Didier, ANDRIESSEN, Paul et SAGE, Françoise, 2016. Tectonostratigraphic evolution of the eastern Algerian margin and basin from seismic data and onshore-offshore correlation. Marine and Petroleum Geology. 1 novembre 2016. Vol. 77, pp. 1355-1375. DOI 10.1016/j.marpetgeo.2016.08.021.

ARANHA, Malcolm et PORWAL, Alok, 2022. EGU22-124 : Unsupervised machine learning driven Prospectivity analysis of REEs in NE India [en ligne]. Copernicus Meetings. [Consulté le 1 mars 2025]. Disponible à l'adresse : https://meetingorganizer.copernicus.org/EGU22/EGU22-124.html

BARATOUX, Lenka, LEXA, Ondrej, COSGROVE, John W. et SCHULMANN, Karel, 2005. The quantitative link between fold geometry, mineral fabric and mechanical anisotropy: as exemplified by the deformation of amphibolites across a regional metamorphic gradient. Journal of Structural Geology. 1 avril 2005. Vol. 27, n° 4, pp. 707-730. DOI 10.1016/j.jsg.2005.01.001.

BATISTA, Gustavo E. A. P. A., PRATI, Ronaldo C. et MONARD, Maria Carolina, 2004. A study of the behavior of several methods for balancing machine learning training data. ACM SIGKDD Explorations Newsletter. 1 juin 2004. Vol. 6, n° 1, pp. 20-29. DOI 10.1145/1007730.1007735.

BEHERA, Satyabrata et PANIGRAHI, Mruganka K., 2022. Gold prospectivity mapping and exploration targeting in Hutti-Maski schist belt, India: Synergistic application of Weights-of-Evidence (WOE), Fuzzy Logic (FL) and hybrid (WOE-FL) models. Journal of Geochemical Exploration. 1 avril 2022. Vol. 235, pp. 106963. DOI 10.1016/j.gexplo.2022.106963.

BEHNIA, Pouran, HARRIS, Jeff, LIU, Haiming, JØRGENSEN, Taus R. C., NAGHIZADEH, Mostafa et ROOTS, Eric A., 2023. Random forest classification for volcanogenic massive sulfide mineralization in the Rouyn-Noranda Area, Quebec. Ore Geology Reviews. 1 octobre 2023. Vol. 161, pp. 105612. DOI 10.1016/j.oregeorev.2023.105612.

BELANTEUR, O., 2001. Le magmatisme miocène de l'Algérois: chronologie de mise en place, pétrologie et implications géodynamiques. These de doctorat, USTHB, Alger. 2001.

BELLION, Yves, 1972. Etude géologique et hydrogéologique de la terminaison occidentale des Monts de Bélezma (Algérie) [en ligne]. PhD Thesis. Thèse de Doctorat de 3ème Cycle, Paris VI. [Consulté le 8 novembre 2023]. Disponible à l'adresse : https://pascal-francis.inist.fr/vibad/index.php?action=getRecordDetail&idt=12923884

BELLON, Hervé, 1976. Séries magmatiques néogènes et quaternaires du pourtour de la Méditerranée occidentale, comparées dans leur cadre géochronométrique. Implications géodynamiques [en ligne]. thesis. Université Paris-Sud Orsay. [Consulté le 14 décembre 2024]. Disponible à l'adresse : https://hal.science/tel-02429739

BENALI, Hanafi, 2007. Les minéralisation associées aux roches magmatiques tertiaires du Nord de l'Algérie: typologie, pétrologie, cadre géodynamique, et implication métallogéniques. PhD Thesis.

BENCHAREF, Mohammed Hichem, BOUBAYA, Djamel, ABOUD, Essam et AYFER, Simge, 2022. Role of an advanced gravity data analysis in improving the geologic understanding of the northern Tebessa region, Northeastern Algeria. Journal of African Earth Sciences. 1 décembre 2022. Vol. 196, pp. 104693. DOI 10.1016/j.jafrearsci.2022.104693.

BIGDELI, Amirreza, MAGHSOUDI, Abbas et GHEZELBASH, Reza, 2022. Application of self-organizing map (SOM) and K-means clustering algorithms for portraying geochemical anomaly patterns in Moalleman district, NE Iran. Journal of Geochemical Exploration. 1 février 2022. Vol. 233, pp. 106923. DOI 10.1016/j.gexplo.2021.106923.

BIGDELI, Amirreza, MAGHSOUDI, Abbas et GHEZELBASH, Reza, 2024. A comparative study of the XGBoost ensemble learning and multilayer perceptron in mineral prospectivity modeling: a case study of the Torud-Chahshirin belt, NE Iran. Earth Science Informatics. 1 février 2024. Vol. 17, n° 1, pp. 483-499. DOI 10.1007/s12145-023-01184-4.

BLAYAC, Joseph, 1912. Esquisse géologique du Bassin de la Seybouse et de quelque régions voisines. Adolphe Jourdan.

BLES, J. L., 1969. Contribution à l'étude des déformations cassantes de la feuille de Morsott (SE Constantinois–Algérie). Les microfracturations et leurs relations avec les failles et les plis. Publications du Service Géologique de l'Algérie,(Série N 11). Bulletin. 1969. N° 39, pp. 7-17.

BLEVIN, Phillip L., CHAPPELL, Bruce W. et ALLEN, Charlotte M., 1996. Intrusive metallogenic provinces in eastern Australia based on granite source and composition. [en ligne]. 1996. [Consulté le 23 avril 2025]. Disponible à l'adresse : https://pubs.geoscienceworld.org/gsa/books/edited-volume/472/chapter/3799926

BOLFA, Joseph, 1948. Contribution à l'étude des sites métallifères de la kabyle de Collo et de la région de Bône. [en ligne]. 1948. [Consulté le 16 décembre 2024]. Disponible à l'adresse : http://kent.cdha.fr:8080/Record.htm?idlist=1&record=19200632124910288149

BONHAM-CARTER, Graeme, 1994. Geographic Information Systems for Geoscientists: Modelling with GIS. Elsevier. ISBN 978-0-08-042420-0.

BOSCH, Delphine, HAMMOR, Dalila, MECHATI, Mehdi, FERNANDEZ, Laure, BRUGUIER, Olivier, CABY, Renaud et VERDOUX, Patrick, 2014. Geochemical study (major, trace elements and Pb–Sr–Nd isotopes) of mantle material obducted onto the North African margin (Edough Massif, North Eastern Algeria): Tethys fragments or lost remnants of the Liguro–Provençal basin? Tectonophysics. 2014. Vol. 626, pp. 53-68.

BOSSIÈRE, Gérard, 1980. Un complexe métamorphique polycyclique et sa blastomylonitisation [en ligne]. PhD Thesis. Paris. [Consulté le 20 février 2024]. Disponible à l'adresse : https://www.ccdz.cerist.dz/admin/notice.php?id=135247

BOUGUERRA, Hamza, TACHI, Salah Eddine, BOUCHEHED, Hamza, GILJA, Gordon, ALOUI, Nadir, HASNAOUI, Yacine, ALICHE, Abdelmalek, BENMAMAR, Saâdia et NAVARRO-PEDREÑO, Jose, 2023. Integration of High-Accuracy Geospatial Data and Machine Learning Approaches for Soil Erosion Susceptibility Mapping in the Mediterranean Region: A Case Study of the Macta Basin, Algeria. Sustainability. janvier 2023. Vol. 15, n° 13, pp. 10388. DOI 10.3390/su151310388.

BOUILLIN, 1977. Géologie alpine de la petite kabylie dans les régions de collo et d'el milia (algérie) [en ligne]. Toulouse. [Consulté le 5 novembre 2023]. Disponible à l'adresse : https://www.ccdz.cerist.dz/admin/notice.php?id=134999

BOUILLIN, DURAND-DELGA, M. et OLIVIER, Ph, 1986. Betic-Rifian and Tyrrhenian arcs: distinctive features, genesis and development stages. In : Developments in geotectonics [en ligne]. Elsevier. pp. 281-304. [Consulté le 19 février 2024]. Disponible à l'adresse : https://www.sciencedirect.com/science/article/pii/B9780444426888500175

BOUILLIN, J.-P., BOSSIÈRE, G., BOURROUILH, R., COUTELLE, A., DURAND-DELGA, M. et GÉLARD, J.-P., 1984. Mise au point sur l'âge des socles métamorphiques kabyles (Algérie). Comptes-rendus des séances de l'Académie des sciences. Série 2, Mécanique-physique, chimie, sciences de l'univers, sciences de la terre. 1984. Vol. 298, n° 15, pp. 655-660.

BOURAHLA, Mohamed et AFALFIZ, Kamel, 2000. Contribution à l'étude géologique et gîtologique de l'indice polymétallique de Bir Béni Salah (Collo, Skikda, Algérie).

BOUTALEB, Abdelhak, 2001. Les minéralisations à Pb-Zn du domaine Sétifien-Hodna: Gitologie, pétrographie des dolomies, microthermométrie et implications métallogéniques. Alger: USTHB. French. 2001.

BOUTALEB, Abdelhak, AFALFIZ, A., AÏSSA, D. E., KOLLI, O., MARIGNAC, C. H. et TOUAHRI, B., 2000. Métallogénie et évolution géodynamique de la chaîne tellienne en Algérie. Bull Serv, Géol, Algérie. 2000. Vol. 11, n° 1, pp. 3-27.

BOUTALEB, Abdelhak, AISSA, Djamal-Eddine et KOLLI, Omar, 2023. SYNTHÈSE SUR LES GISEMENTS DE Pb-Zn DE LA CHAÎNE TELLIENNE DE L'ALGÉRIE. In : . pp. pp.191-200. ISBN 978-9931-9936-1-2.

BOUTALEB, Abdelhak, AISSA, Djamal-Eddine et OMAR, Kolli, 2023. SYNTHÈSE SUR LES GISEMENTS DE Pb-Zn DE LA CHAÎNE TELLIENNE DE L'ALGÉRIE. In : . pp. pp.191-200. ISBN 978-9931-9936-1-2.

BOUTALEB, Abdelhak et AÏSSA, Djamel Eddine, 1999. Les gîtes plombo-zincifères du Hodna : minéralisations corn parables au type «Vallée du Mississipi>> (Nord-Est Algérien). . 1999.

BREIMAN, Leo, 2001. Random Forests. Machine Learning. 1 octobre 2001. Vol. 45, n° 1, pp. 5-32. DOI 10.1023/A:1010933404324.

BROCHU, Eric, CORA, Vlad M. et DE FREITAS, Nando, 2010. A Tutorial on Bayesian Optimization of Expensive Cost Functions, with Application to Active User Modeling and Hierarchical Reinforcement Learning [en ligne]. 12 décembre 2010. arXiv. arXiv:1012.2599. [Consulté le 28 avril 2024]. Disponible à l'adresse : http://arxiv.org/abs/1012.2599

BROWN, W. M., GEDEON, T. D., GROVES, D. I. et BARNES, R. G., 2000. Artificial neural networks: A new method for mineral prospectivity mapping. Australian Journal of Earth Sciences. 1 août 2000. Vol. 47, n° 4, pp. 757-770. DOI 10.1046/j.1440-0952.2000.00807.x.

BRUGUIER, Olivier, BOSCH, Delphine, CABY, Renaud, VITALE-BROVARONE, Alberto, FERNANDEZ, Laure, HAMMOR, Dalila, LAOUAR, Rabah, OUABADI, Aziouz, ABDALLAH, Nachida et MECHATI, Mehdi, 2017. Age of UHP metamorphism in the Western Mediterranean: Insight from rutile and minute zircon inclusions in a diamond-bearing garnet megacryst (Edough Massif, NE Algeria). Earth and Planetary Science Letters. 15 septembre 2017. Vol. 474, pp. 215-225. DOI 10.1016/j.epsl.2017.06.043.

BUREAU, D., 1973. CONDITIONS DE SEDIMENTATION DU VALANGINIEN INFERIEUR AU NORD DE L'AURES. [en ligne]. 1973. [Consulté le 8 novembre 2023]. Disponible à l'adresse : https://pascal-francis.inist.fr/vibad/index.php?action=getRecordDetail&idt=PASCALGEODEBRGM7520082151

CARDOSO-FERNANDES, Joana, TEODORO, Ana C., LIMA, Alexandre et RODA-ROBLES, Encarnación, 2020. Semi-Automatization of Support Vector Machines to Map Lithium (Li) Bearing Pegmatites. Remote Sensing. janvier 2020. Vol. 12, n° 14, pp. 2319. DOI 10.3390/rs12142319.

CARRANZA, Emmanuel John, 2008. Geochemical Anomaly and Mineral Prospectivity Mapping in GIS. Elsevier. ISBN 978-0-08-093031-2.

CARRANZA, Emmanuel John M., 2009. Objective selection of suitable unit cell size in data-driven modeling of mineral prospectivity. Computers & Geosciences. 1 octobre 2009. Vol. 35, n° 10, pp. 2032-2046. DOI 10.1016/j.cageo.2009.02.008.

CARRANZA, Emmanuel John M. et HALE, Martin, 2001a. Logistic Regression for Geologically Constrained Mapping of Gold Potential, Baguio District, Philippines. Exploration and Mining Geology. 1 juillet 2001. Vol. 10, n° 3, pp. 165-175. DOI 10.2113/0100165.

CARRANZA, Emmanuel John M. et HALE, Martin, 2001b. Geologically Constrained Fuzzy Mapping of Gold Mineralization Potential, Baguio District, Philippines. Natural Resources Research. 1 juin 2001. Vol. 10, n° 2, pp. 125-136. DOI 10.1023/A:1011500826411.

CARRANZA, Emmanuel John M. et LABORTE, Alice G., 2015a. Data-driven predictive mapping of gold prospectivity, Baguio district, Philippines: Application of Random Forests algorithm. Ore Geology Reviews. 1 décembre 2015. Vol. 71, pp. 777-787. DOI 10.1016/j.oregeorev.2014.08.010.

CARRANZA, Emmanuel John M. et LABORTE, Alice G., 2015b. Random forest predictive modeling of mineral prospectivity with small number of prospects and data with missing values in Abra (Philippines). Computers & Geosciences. 1 janvier 2015. Vol. 74, pp. 60-70. DOI 10.1016/j.cageo.2014.10.004.

CARRANZA, Emmanuel John M. et LABORTE, Alice G., 2015c. Random forest predictive modeling of mineral prospectivity with small number of prospects and data with missing values in Abra (Philippines). Computers & Geosciences. janvier 2015. Vol. 74, pp. 60-70. DOI 10.1016/j.cageo.2014.10.004.

CARVALHO, Diogo V., PEREIRA, Eduardo M. et CARDOSO, Jaime S., 2019. Machine Learning Interpretability: A Survey on Methods and Metrics. Electronics. août 2019. Vol. 8, n° 8, pp. 832. DOI 10.3390/electronics8080832.

CHEN, Cuihua, DAI, Hongzhang, LIU, Yue et HE, Binbin, 2011. Mineral prospectivity mapping integrating multi-source geology spatial data sets and logistic regression modelling. In : Proceedings 2011 IEEE International Conference on Spatial Data Mining and Geographical Knowledge Services [en ligne]. juin 2011. pp. 214-217. [Consulté le 8 janvier 2025]. Disponible à l'adresse : https://ieeexplore.ieee.org/abstract/document/5969034

CHEN, Guoxiong et CHENG, Qiuming, 2016. Singularity analysis based on wavelet transform of fractal measures for identifying geochemical anomaly in mineral exploration. Computers & Geosciences. 1 février 2016. Vol. 87, pp. 56-66. DOI 10.1016/j.cageo.2015.11.007.

CHEN, Lirong, GUAN, Qingfeng, FENG, Bin, YUE, Hanqiu, WANG, Junyi et ZHANG, Fan, 2019. A Multi-Convolutional Autoencoder Approach to Multivariate Geochemical Anomaly Recognition. Minerals. mai 2019. Vol. 9, n° 5, pp. 270. DOI 10.3390/min9050270.

CHEN, Yongliang et WU, Wei, 2017. Application of one-class support vector machine to quickly identify multivariate anomalies from geochemical exploration data. Geochemistry: Exploration, Environment, Analysis. août 2017. Vol. 17, n° 3, pp. 231-238. DOI 10.1144/geochem2016-024.

CHEN, Yongliang et WU, Wei, 2018. Isolation Forest as an Alternative Data-Driven Mineral Prospectivity Mapping Method with a Higher Data-Processing Efficiency. Natural Resources Research. 2018. Vol. 28, pp. 31-46. DOI 10.1007/s11053-018-9375-6.

CHEN, Zhiyi, XIONG, Yihui, YIN, Bojun, SUN, Siquan et ZUO, Renguang, 2023. Recognizing geochemical patterns related to mineralization using a self-organizing map. Applied Geochemistry. 1 avril 2023. Vol. 151, pp. 105621. DOI 10.1016/j.apgeochem.2023.105621.

CHENG, Qiuming, 1999. Multifractality and spatial statistics. Computers & Geosciences. 15 novembre 1999. Vol. 25, n° 9, pp. 949-961. DOI 10.1016/S0098-3004(99)00060-6.

CHENG, Qiuming, 2007. Mapping singularities with stream sediment geochemical data for prediction of undiscovered mineral deposits in Gejiu, Yunnan Province, China. Ore Geology Reviews. 2007. Vol. 32, n° 1-2, pp. 314-324.

CHENG, Qiuming et AGTERBERG, F. P., 1999. Fuzzy Weights of Evidence Method and Its Application in Mineral Potential Mapping. Natural Resources Research. 1 mars 1999. Vol. 8, n° 1, pp. 27-35. DOI 10.1023/A:1021677510649.

CHENG, Qiuming et ZHAO, Pengda, 2011. Singularity theories and methods for characterizing mineralization processes and mapping geo-anomalies for mineral deposit prediction. Geoscience Frontiers. 1 janvier 2011. Vol. 2, n° 1, pp. 67-79. DOI 10.1016/j.gsf.2010.12.003.

CHUNG, C. F. et AGTERBERG, F. P., 1980. Regression models for estimating mineral resources from geological map data. Journal of the International Association for Mathematical Geology. 1 octobre 1980. Vol. 12, n° 5, pp. 473-488. DOI 10.1007/BF01028881.

COMAS, Menchu, PLATT, J.P., SOTO, Juan et WATTS, A., 1999. The origin and Tectonic History of the Alboran Basin: Insights from Leg 161 Results. In : Integrated Ocean Drilling Program: Preliminary Reports. pp. 555-580.

DAVID, Louis, 1956. Etude géologique des monts de la haute Medjerda [en ligne]. Paris. [Consulté le 23 février 2025]. Disponible à l'adresse : https://www.ccdz.cerist.dz/admin/notice.php?id=135228

DAVIRAN, Mehrdad, MAGHSOUDI, Abbas, GHEZELBASH, Reza et PRADHAN, Biswajeet, 2021. A new strategy for spatial predictive mapping of mineral prospectivity: Automated hyperparameter tuning of random forest approach. Computers & Geosciences. 1 mars 2021. Vol. 148, pp. 104688. DOI 10.1016/j.cageo.2021.104688.

DELFAUD, J, 1974. LES GRANDS TRAITS DE LA PALEOGEOGRAPHIE DE L'ALGERIE SEPTENTRIONALE DURANT LE JURASSIQUE SUPERIEUR ET LE CRETACE INFERIEUR. LES GRANDS TRAITS DE LA PALEOGEOGRAPHIE DE L'ALGERIE SEPTENTRIONALE DURANT LE JURASSIQUE SUPERIEUR ET LE CRETACE INFERIEUR. 1974.

DENG, Kewang, ZHAO, Huijie, LI, Na et WEI, Wei, 2021. Identification of minerals in hyperspectral imagery based on the attenuation spectral absorption index vector using a multilayer perceptron. Remote Sensing Letters. 4 mai 2021. Vol. 12, n° 5, pp. 449-458. DOI 10.1080/2150704X.2021.1903612.

DHILLON, Anamika et VERMA, Gyanendra K., 2020. Convolutional neural network: a review of models, methodologies and applications to object detection. Progress in Artificial Intelligence. 1 juin 2020. Vol. 9, n° 2, pp. 85-112. DOI 10.1007/s13748-019-00203-0.

DIETTERICH, Thomas G., 2000. Ensemble Methods in Machine Learning. In : Multiple Classifier Systems [en ligne]. Berlin, Heidelberg : Springer Berlin Heidelberg. pp. 1-15. Lecture Notes in Computer Science. [Consulté le 26 avril 2025]. ISBN 978-3-540-67704-8. Disponible à l'adresse : http://link.springer.com/10.1007/3-540-45014-9_1

DOMZIG, Anne, 2007. Déformation active et récente, et structuration tectonosédimentaire de la marge sous-marine algérienne. . 2007.

DU, Xishihui, ZHOU, Kefa, CUI, Yao, WANG, Jinlin et ZHOU, Shuguang, 2021. Mapping Mineral Prospectivity Using a Hybrid Genetic Algorithm–Support Vector Machine (GA–SVM) Model. ISPRS International Journal of Geo-Information. novembre 2021. Vol. 10, n° 11, pp. 766. DOI 10.3390/ijgi10110766.

DUBE, Lindani et VERSTER, Tanja, 2023. Enhancing classification performance in imbalanced datasets: A comparative analysis of machine learning models. Data Science in Finance and Economics. 2023. Vol. 3, n° 4, pp. 354-379. DOI 10.3934/DSFE.2023021.

DURAND DELGA, 1969. Mise au point sur la structure du Nord-Est de la Berbérie [en ligne]. Bulletin du Service de la carte géologique d'Algérie. Disponible à l'adresse : https://www.abebooks.fr/Mise-au-point-structure-Nord-Est-Berb%C3%A9rie/221799754/bd

DURAND DELGA, 1980. Le Cadre structural de la Mediterranee occidentale. Géologie des chaînes alpines issues de la TéthysGeology of the Alpine chains born of the Tethys. 1980. pp. 67-85.

EL AZZOUZI, M., MAURY, R.C., René R, FOURCADE, S., COULON, C., BELLON, H., OUABADI, A., SEMROUD, B., MEGARTSI, H., COTTEN, Joseph, BELANTEUR, O., LOUNI-HACINI, A., COUTELLE, A., PIQUE, A., CAPDEVILA, R., HERNANDEZ, J. et REHAULT, J.P., 2003. Evolution spatiale et temporelle du magmatisme néogène de la marge septentrionale du Maghreb : manifestation d'un détachement lithosphérique. Notes et Mémoires du Service Géologique Maroc. 2003. Vol. 447, pp. 107-116.

ELBEGUE, Abderrahmane Aref, ALLEK, Karim et ZEGHOUANE, Hocine, 2022. Geological mapping using extreme gradient boosting and the deep neural networks: application to silet area, central Hoggar, Algeria. Acta Geophysica. 1 août 2022. Vol. 70, n° 4, pp. 1581-1599. DOI 10.1007/s11600-022-00814-7.

ENGLE, Mark A., NYE, Charles W., NEUPANE, Ghanashyam, QUILLINAN, Scott A., MCLAUGHLIN, Jonathan Fred, MCLING, Travis et MARTÍN-FERNÁNDEZ, Josep A., 2022. Predicting Rare Earth Element Potential in Produced and Geothermal Waters of the United States via Emergent Self-Organizing Maps. Energies. janvier 2022. Vol. 15, n° 13, pp. 4555. DOI 10.3390/en15134555.

EVANS, Mark A. et FISCHER, Mark P., 2012. On the distribution of fluids in folds: A review of controlling factors and processes. Journal of Structural Geology. 1 novembre 2012. Vol. 44, pp. 2-24. DOI 10.1016/j.jsg.2012.08.003.

FACCENNA, Claudio, PIROMALLO, Claudia, CRESPO-BLANC, Ana, JOLIVET, Laurent et ROSSETTI, Federico, 2004. Lateral slab deformation and the origin of the western Mediterranean arcs. Tectonics [en ligne]. 2004. Vol. 23, n° 1. [Consulté le 19 février 2024]. DOI 10.1029/2002TC001488. Disponible à l'adresse : https://onlinelibrary.wiley.com/doi/abs/10.1029/2002TC001488

FAN, Mingjing, XIAO, Keyan, SUN, Li, ZHANG, Shuai et XU, Yang, 2022. Automated Hyperparameter Optimization of Gradient Boosting Decision Tree Approach for Gold Mineral Prospectivity Mapping in the Xiong'ershan Area. Minerals. décembre 2022. Vol. 12, n° 12, pp. 1621. DOI 10.3390/min12121621.

FARAHBAKHSH, Ehsan, MAUGHAN, Jack et MÜLLER, R. Dietmar, 2023a. Prospectivity modelling of critical mineral deposits using a generative adversarial network with oversampling and positive-unlabelled bagging. Ore Geology Reviews. 1 novembre 2023. Vol. 162, pp. 105665. DOI 10.1016/j.oregeorev.2023.105665.

FARAHBAKHSH, Ehsan, MAUGHAN, Jack et MÜLLER, R Dietmar, 2023. Critical mineral prospectivity mapping on the Gawler craton using a new machine learning framework. . 2023.

FARAHBAKHSH, Ehsan, MAUGHAN, Jack et MÜLLER, R. Dietmar, 2023b. Prospectivity modelling of critical mineral deposits using a generative adversarial network with oversampling and positive-unlabelled bagging. Ore Geology Reviews. novembre 2023. Vol. 162, pp. 105665. DOI 10.1016/j.oregeorev.2023.105665.

FARHADI, Sasan, TATULLO, Samuele, BOVEIRI KONARI, Mina et AFZAL, Peyman, 2024. Evaluating StackingC and ensemble models for enhanced lithological classification in geological mapping. Journal of Geochemical Exploration. 1 mai 2024. Vol. 260, pp. 107441. DOI 10.1016/j.gexplo.2024.107441.

FEIZI, Faranak, KARBALAEI-RAMEZANALI, Amirabbas et TUSI, Hosein, 2017. Mineral Potential Mapping Via TOPSIS with Hybrid AHP–Shannon Entropy Weighting of Evidence: A Case Study for Porphyry-Cu, Farmahin Area, Markazi Province, Iran. Natural Resources Research. 1 octobre 2017. Vol. 26, n° 4, pp. 553-570. DOI 10.1007/s11053-017-9338-3.

FERNANDEZ, Laure, BOSCH, Delphine, BRUGUIER, Olivier, HAMMOR, Dalila, CABY, Renaud, ARNAUD, Nicolas, MONIÉ, Patrick, ABDALLAH, Nachida, VERDOUX, Patrick, OUABADI, Aziouz et LAOUAR, Rabah, 2020. Vestiges of a fore-arc oceanic crust in the Western Mediterranean: Geochemical constraints from North-East Algeria. Lithos. 1 octobre 2020. Vol. 370-371, pp. 105649. DOI 10.1016/j.lithos.2020.105649.

FERNANDEZ, Laure, BOSCH, Delphine, BRUGUIER, Olivier, HAMMOR, Dalila, CABY, Renaud, MONIÉ, Patrick, ARNAUD, Nicolas, TOUBAL, Abder, GALLAND, Béatrice et DOUCHET, Chantal, 2016. Permo-Carboniferous and early Miocene geological evolution of the internal zones of the Maghrebides – New insights on the western Mediterranean evolution. Journal of Geodynamics. 1 mai 2016. Vol. 96, pp. 146-173. DOI 10.1016/j.jog.2015.10.001.

FLEURY, Jean-Jacques, MOKADDEM, Miloud, POPOV, A., ERLING, J. C. et OFFICE NATIONAL DE LA RECHERCHE GÉOLOGIQUE ET MINIÈRE, 1969. Carte des gîtes minéraux de l'Algérie -ORAN NORD- au 1:500 000 [en ligne]. [carte]. Alger, Algérie : Service géologique. Disponible à l'adresse : Library Catalog - www.sudoc.abes.fr

FORSON, Eric Dominic, KWAYISI, Daniel, KAZAPOE, Raymond Webrah, NTORI, Clement, ADJEI, Solomon Kwasi, MAHAMUDA, Abu, SULEMAN, Shaibu, AMEYOE, Paul et AMEDZRO, Kennedy Yaw, 2024. Application of a hybrid BWM-TOPSIS approach for mineral potential mapping. Heliyon [en ligne]. 15 juin 2024. Vol. 10, n° 11. [Consulté le 28 janvier 2025]. DOI 10.1016/j.heliyon.2024.e31743. Disponible à l'adresse : https://www.cell.com/heliyon/abstract/S2405-8440(24)07774-0

FRAZIER, Peter I., 2018. A Tutorial on Bayesian Optimization [en ligne]. 8 juillet 2018. arXiv. arXiv:1807.02811. [Consulté le 28 avril 2024]. Disponible à l'adresse : http://arxiv.org/abs/1807.02811

FRIEDMAN, Jerome H., 2001. Greedy Function Approximation: A Gradient Boosting Machine. The Annals of Statistics. 2001. Vol. 29, n° 5, pp. 1189-1232.

FRIZON DE LAMOTTE, D., MICHARD, A. et SADDIQI, O., 2006. Some recent developments on the Maghreb geodynamics. 2006. ELSEVIER FRANCE-EDITIONS SCIENTIFIQUES MEDICALES ELSEVIER 65 RUE CAMILLE ….

FRY, N., 1979. Random point distributions and strain measurement in rocks. Tectonophysics. 10 novembre 1979. Vol. 60, n° 1, pp. 89-105. DOI 10.1016/0040-1951(79)90135-5.

FU, Changliang, CHEN, Kaixu, YANG, Qinghua, CHEN, Jianping, WANG, Jianxiong, LIU, Junlai, XIANG, Yunchuan, LI, Yanhua et RAJESH, H. M., 2021. Mapping gold mineral

prospectivity based on weights of evidence method in southeast Asmara, Eritrea. Journal of African Earth Sciences. 1 avril 2021. Vol. 176, pp. 104143. DOI 10.1016/j.jafrearsci.2021.104143.

GAO, Meng, WANG, Gongwen, CARRANZA, Emmanuel John M., QI, Siyan, ZHANG, Wen, PANG, Zhenshan, LI, Xiuzhang et XIAO, Fengli, 2024. 3D Au Targeting using Machine Learning with Different Sample Combination and Return-Risk Analysis in the Sanshandao-Cangshang District, Shandong Province, China. Natural Resources Research. 1 février 2024. Vol. 33, n° 1, pp. 51-74. DOI 10.1007/s11053-023-10279-0.

GATTIGLIA, Gabriele, 2025. Managing Artificial Intelligence in Archeology. An overview. Journal of Cultural Heritage. 1 janvier 2025. Vol. 71, pp. 225-233. DOI 10.1016/j.culher.2024.11.020.

GÉLARD, Jean-Pierre, 1979. Geologie du nord-est de la grande Kabylie: un segment des zones internes de l'orogene littoral maghrebin. Institut des sciences de la terre.

GEOFFROY, J. G. De et WIGNALL, T. K., 2012. Statistical Models for Optimizing Mineral Exploration. Springer Science & Business Media. ISBN 978-1-4613-1861-3.

GERY, B, H, FEINBERG, C, LORENZ et J, MAGNE, 1981. DEFINITION D'UNE SERIE-TYPE DE L'"OLIGO-MIOCENE KABYLE" ANTENAPPES DANS LE DJEBEL AISSA-MIMOUN (GRANDE KABYLIE, ALGERIE). DEFINITION D'UNE SERIE-TYPE DE L'"OLIGO-MIOCENE KABYLE" ANTENAPPES DANS LE DJEBEL AISSA-MIMOUN (GRANDE KABYLIE, ALGERIE). 1981.

GHEZELBASH, Reza, MAGHSOUDI, Abbas, SHAMEKHI, Mehdi, PRADHAN, Biswajeet et DAVIRAN, Mehrdad, 2023. Genetic algorithm to optimize the SVM and K-means algorithms for mapping of mineral prospectivity. Neural Computing and Applications. 1 janvier 2023. Vol. 35, n° 1, pp. 719-733. DOI 10.1007/s00521-022-07766-5.

GIRI, Ram Nivas, JANGHEL, Rekh Ram, GOVIL, Himanshu et MISHRA, Gaurav, 2024. A stacked ensemble learning-based framework for mineral mapping using AVIRIS-NG hyperspectral image. Journal of Earth System Science. 30 mai 2024. Vol. 133, n° 2, pp. 107. DOI 10.1007/s12040-024-02317-z.

GLACON, J, 1952. Les Monts du Hodna (partie orientale) [en ligne]. [s.n.]. [Consulté le 23 février 2025]. Monographies régionales. Disponible à l'adresse : https://cir.nii.ac.jp/crid/1130282268704782464

GRAÏNE, Khadidja et MARIGNAC, Christian, 2001. DÉPÔTS PYRITEUX ET MINÉRALISATIONS Zn- Pb-(Cu) DU MASSIF VOLCANO-PLUTONIQUE D' AMIZOUR (BEJAÏA, ALGÉRIE). TYPOLOGIE ET GENÈSE DES MINÉRALISATIONS. ·. . 2001. Vol. 12.

GRAVELLE, M., 1959. Etudes géologiques et prospection minière dans le massif éruptif d'Oued Amizour (Algérie). Pub. Serv. Cart. Géol. Alg. 1959. pp. 149-216.

GRUNSKY, E. C. et CARITAT, P. de, 2019. State-of-the-art analysis of geochemical data for mineral exploration. Geochemistry: Exploration, Environment, Analysis. 12 juillet 2019. Vol. 20, n° 2, pp. 217-232. DOI 10.1144/geochem2019-031.

GUIRAUD, René, 1973. Evolution post-triasique de l'avant-pays de la chaîne alpine en Algérie [en ligne]. PhD Thesis. Toulouse. [Consulté le 8 novembre 2023]. Disponible à l'adresse : https://www.ccdz.cerist.dz/admin/notice.php?id=135080

HADDOUCHE, Omar, ABDELHAK, Boutaleb, MADJID, Chamam, SAADIA, Ysbaa, HANAFI, Hammouche et DJAMEL, Boubaya, 2016. Pb-Zn (Ba) deposits of the oriental Saharan Atlas (north-east of Algeria): distribution, control and implications for mining exploration. Arabian Journal of Geosciences. mai 2016. Vol. 9, n° 5, pp. 422. DOI 10.1007/s12517-016-2406-x.

HADDOUCHE, Omar, BOUTALEB, Abdelhak et BENHAMOUD, Imène, 2015. Contexte structural des minéralisations liées à la bordure nord des Monts des Aurès (NE de l'Algérie) et des régions voisines: exemple des gisements à BA-Pb (Zn-Cu) d'Ichmoul et d'Ain Mimoun. Bulletin du Service Géologique de l'Algérie. 2015. Vol. 25, n° 1, pp. 3-19.

HAJIHOSSEINLOU, Mahsa, MAGHSOUDI, Abbas et GHEZELBASH, Reza, 2023. A Novel Scheme for Mapping of MVT-Type Pb–Zn Prospectivity: LightGBM, a Highly Efficient Gradient Boosting Decision Tree Machine Learning Algorithm. Natural Resources Research [en ligne]. 12 août 2023. [Consulté le 10 septembre 2023]. DOI 10.1007/s11053-023-10249-6. Disponible à l'adresse : https://doi.org/10.1007/s11053-023-10249-6

HAJIHOSSEINLOU, Mahsa, MAGHSOUDI, Abbas et GHEZELBASH, Reza, 2024. Stacking: A novel data-driven ensemble machine learning strategy for prediction and mapping of Pb-Zn prospectivity in Varcheh district, west Iran. Expert Systems with Applications. 1 mars 2024. Vol. 237, pp. 121668. DOI 10.1016/j.eswa.2023.121668.

HAO, Libo, ZHAO, Xinyun, ZHAO, Yuyan, LU, Jilong et SUN, Liji, 2014. Determination of the geochemical background and anomalies in areas with variable lithologies. Journal of Geochemical Exploration. 1 avril 2014. Vol. 139, pp. 177-182. DOI 10.1016/j.gexplo.2013.11.007.

HARRIS, DeVerle et PAN, Guocheng, 1999. Mineral Favorability Mapping: A Comparison of Artificial Neural Networks, Logistic Regression, and Discriminant Analysis. Natural Resources Research. 1 juin 1999. Vol. 8, n° 2, pp. 93-109. DOI 10.1023/A:1021886501912.

HASNAOUI, Yacine, TACHI, Salah Eddine, BOUGUERRA, Hamza, BENMAMAR, Saâdia, GILJA, Gordon, SZCZEPANEK, Robert, NAVARRO-PEDREÑO, Jose et YASEEN, Zaher Mundher, 2024. Enhanced machine learning models development for flash flood mapping using geospatial data. Euro-Mediterranean Journal for Environmental Integration. 1 septembre 2024. Vol. 9, n° 3, pp. 1087-1107. DOI 10.1007/s41207-024-00553-9.

HE, Binbin, 2012. Mineral Prospectivity Mapping Method Integrating Multi-Sources Geology Spatial Data Sets and Case-Based Reasoning. Journal of Geographic Information System. 1 janvier 2012. Vol. 4, pp. 77-85. DOI 10.4236/jgis.2012.42011.

HERKAT, M., 1999. La sédimentologie du haut niveau marin du Crétacé supérieur de l'Atlas saharien oriental et de l'Aurès: Stratigraphie séquentielle, analyse quantitative des biocénoses, évolution paléogéographique et contexte géodynamique. PhD Thesis. Thèse. Doct., FSTGAT (USTHB), Alger. Algérie.

HOLYLAND, P. W. et OJALA, V. J., 1997. Computer-aided structural targeting in mineral exploration: Two- and three-dimensional stress mapping. Australian Journal of Earth Sciences. 1 août 1997. Vol. 44, n° 4, pp. 421-432. DOI 10.1080/08120099708728323.

JOLIVET, Laurent et FACCENNA, Claudio, 2000. Mediterranean extension and the Africa-Eurasia collision. Tectonics. décembre 2000. Vol. 19, n° 6, pp. 1095-1106. DOI 10.1029/2000TC900018.

JOOSHAKI, Mohammad, NAD, Alona et MICHAUX, Simon, 2021. A Systematic Review on the Application of Machine Learning in Exploiting Mineralogical Data in Mining and Mineral Industry. Minerals. août 2021. Vol. 11, n° 8, pp. 816. DOI 10.3390/min11080816.

JORDÃO, Helga, AZEVEDO, Leonardo, SOUSA, António Jorge et SOARES, Amílcar, 2022. Generative Adversarial Network Applied to Ore Type Modeling in Complex Geological Environments. Mathematical Geosciences. 1 octobre 2022. Vol. 54, n° 7, pp. 1165-1182. DOI 10.1007/s11004-022-10008-y.

KAZI-TANI, Nacereddine, 1986. Evolution géodynamique de la bordure nord-africaine [en ligne]. Bordeaux. [Consulté le 25 février 2025]. Disponible à l'adresse : https://www.ccdz.cerist.dz/admin/notice.php?id=135227

KE, Guolin, MENG, Qi, FINLEY, Thomas, WANG, Taifeng, CHEN, Wei, MA, Weidong, YE, Qiwei et LIU, Tie-Yan, 2017. LightGBM: A highly efficient gradient boosting decision tree. In : Advances in Neural Information Processing Systems [en ligne]. 2017. pp. 3147-3155. [Consulté le 10 septembre 2023]. Disponible à l'adresse : https://cerist.summon.serialssolutions.com/2.0.0/link/0/eLvHCXMwtV1NS8NAEF2UehA8KFZaP_fiqVSSTUy6oodW_ABrUayCp5AmmxLQWGwK-u-d2c1uYrUHD15C2YZs0jednZ3Me0OIw46s9pxPED4spKFlhVy4jgi9UeLyyHdjwUPrWIwSKVvgDZ7dpwFmtnX3o3LsX4GHMYAeibR_AN9cFAbgM5gAHMEI4PjTDH5djbrqLb-se0UpDimuYTiLmikghbkr6uWFFfVx737Vu1UEdtQ2fvnEGpBU8ihb43dZMZa3IFafygLquOjZgxXsovTmMv0-wwZBBmGhvMx9akwozYoEeqVqSeb61ZnDME1E8WhFnsL2K3kK5VphLwLbXiXUrn2vPLHiPx1b6W8Wa7FjKw3f7zrZc-uXqSr0GMQr3IdJUTb9NU6j_Exk7ceHZVJDpTVscNG76VdesjrMV22P9b2hYGz0NplNK0HGcJ3US_olvTNQbpAlkW2SUw3FCe1SBQQ1QFANBNVAUA0ERSDq5ODyYnh-3VbTBhOlMRKYZ2FbZC1EskOWS1Jk3CAUmegsiSNX8JELISy3ecxiD4JFL-x0hNMkh3OXY8GUBVbQQfEfCPK4awX5R94kjUXTbi_-aoeslvjukloCfxWxR1YiqS2-L3_jL_k1RH4

KESLER, Stephen E., MARTINI, Anna M., APPOLD, Martin S., WALTER, Lynn M., HUSTON, Ted J. et FURMAN, Francis C., 1996. Na-Cl-Br systematics of fluid inclusions from Mississippi Valley-type deposits, Appalachian Basin: Constraints on solute origin and migration paths. Geochimica et Cosmochimica Acta. 1 janvier 1996. Vol. 60, n° 2, pp. 225-233. DOI 10.1016/0016-7037(95)00390-8.

KIEKEN, Maurice, 1962. Esquisse tectonique de l'Algérie (Algérie du Nord): exposé sur les connaissances actuelles de la structure de l'Algérie et présentation d'une carte tectonique [en ligne]. Service del la carte géologique de l'Algérie. [Consulté le 19 février 2024]. 31. Disponible à l'adresse : https://pascal-francis.inist.fr/vibad/index.php?action=getRecordDetail&idt=6921184

KÖHLER, Martin, HANELLI, Delira, SCHAEFER, Stefan, BARTH, Andreas, KNOBLOCH, Andreas, HIELSCHER, Peggy, CARDOSO-FERNANDES, Joana, LIMA, Alexandre et TEODORO, Ana C., 2021. Lithium Potential Mapping Using Artificial Neural Networks: A Case Study from Central Portugal. Minerals. octobre 2021. Vol. 11, n° 10, pp. 1046. DOI 10.3390/min11101046.

KOLLI, Omar, 1997a. Géologie et citologie des minéralisations ABO-Pb-Zn (Cu-Fe) du socle cristallin de grande kabylie" évolution métallogénique au cours du cycle alpin". PhD Thesis.

KOLLI, Omar, 1997b. Géologie et citologie des minéralisations ABO-Pb-Zn (Cu-Fe) du socle cristallin de grande kabylie « évolution métallogénique au cours du cycle alpin » [en ligne]. Thesis. [Consulté le 25 janvier 2025]. Disponible à l'adresse : http://repository.usthb.dz//xmlui/handle/123456789/4808

KOLLI, Omar, 1997c. Géologie et citologie des minéralisations ABO-Pb-Zn (Cu-Fe) du socle cristallin de grande kabylie" évolution métallogénique au cours du cycle alpin" [en ligne]. PhD Thesis. [Consulté le 25 janvier 2025]. Disponible à l'adresse : https://dspace.usthb.dz/bitstream/handle/123456789/4808/r%C3%A9sum%C3%A9.pdf?sequence=1&isAllowed=y

KONG, Linghao, FENG, Wenkai, YI, Xiaoyu, XUE, Zhenghai et BAI, Luyao, 2025. Enhanced landslide susceptibility mapping in data-scarce regions via unsupervised few-shot learning. Gondwana Research. 1 février 2025. Vol. 138, pp. 31-46. DOI 10.1016/j.gr.2024.10.011.

KUMAR, Ashish et DIMITRAKOPOULOS, Roussos, 2022. Updating geostatistically simulated models of mineral deposits in real-time with incoming new information using actor-critic reinforcement learning. Computers & Geosciences. 1 janvier 2022. Vol. 158, pp. 104962. DOI 10.1016/j.cageo.2021.104962.

KUMARI, Priyanka, SOOR, Sampriti, SHETTY, Amba et KOOLAGUDI, Shashidhar G., 2023. A Fully-Automated Framework for Mineral Identification on Martian Surface Using Supervised Learning Models. IEEE Access. 2023. Vol. 11, pp. 13121-13137. DOI 10.1109/ACCESS.2023.3243061.

LAFITTE, Robert, 1939. Structure et relief de l'Aurès (Algérie). Bulletin de l'Association de géographes français. 1939. Vol. 16, n° 119, pp. 34-40.

LAKHDAR, Bouabsa, HANNA, Kihal et FRÉDÉRIC, Hatert, 2022. Mineralogy and Paragenesis Associations of Polymetallic Deposits (Pb-Zn-Cu-Ag) of Boudoukha and Sidi Kambar—NE Algeria. In : Recent Research on Geomorphology, Sedimentology, Marine Geosciences and Geochemistry [en ligne]. Springer, Cham. 2022. pp. 355-357. [Consulté le 30 octobre 2023]. Disponible à l'adresse : https://link.springer.com/chapter/10.1007/978-3-030-72547-1_76

LAOUAR, Rabah, LEKOUI, Abdelmalek, BOUIMA, Tayeb, SALMI-LAOUAR, Sihem, BOUHLEL, Salah, ABDALLAH, Nachida, BOYCE, Adrian J. et FALLICK, Anthony E., 2018. Petrology, geochemistry and stable isotope studies of the Miocene igneous rocks and related sulphide mineralisation of Oued Amizour (NE Algeria). Ore Geology Reviews. 1 octobre 2018. Vol. 101, pp. 312-329. DOI 10.1016/j.oregeorev.2018.07.026.

LAUZON, Dany et GLOAGUEN, Erwan, 2024. Quantifying uncertainty and improving prospectivity mapping in mineral belts using transfer learning and Random Forest: A case study of copper mineralization in the Superior Craton Province, Quebec, Canada. Ore Geology Reviews. 1 mars 2024. Vol. 166, pp. 105918. DOI 10.1016/j.oregeorev.2024.105918.

LEACH, David. L., BRADLEY, Dwight C., HUSTON, David, PISAREVSKY, Sergei A., TAYLOR, Ryan D. et GARDOLL, Steven J., 2010. Sediment-Hosted Lead-Zinc Deposits in Earth History. Economic Geology. 1 mai 2010. Vol. 105, n° 3, pp. 593-625. DOI 10.2113/gsecongeo.105.3.593.

LEACH, David L., BRADLEY, Dwight, LEWCHUK, Michael T., SYMONS, David T., DE MARSILY, Ghislain et BRANNON, Joyce, 2001. Mississippi Valley-type lead–zinc deposits through geological time: implications from recent age-dating research. Mineralium Deposita. 1 décembre 2001. Vol. 36, n° 8, pp. 711-740. DOI 10.1007/s001260100208.

LEACH, David L., SANGSTER, Donald F., KELLEY, Karen D., LARGE, Ross R., GARVEN, Grant, ALLEN, Cameron R., GUTZMER, Jens et WALTERS, Steve, 2005. Sediment-hosted lead-zinc deposits: A global perspective. [en ligne]. 2005. [Consulté le 8 novembre 2023]. Disponible à l'adresse : https://pubs.geoscienceworld.org/segweb/books/book/1940/chapter-standard/107715875/Sediment-Hosted-Lead-Zinc-DepositsA-Global

LEKOUI, ABDELMALEK, 2019. LES MINERALISATIONS LIEES AU MAGMATISME TERTIAIRE DE LA REGION D'OUED AMIZOUR : GEOCHIMIE, GITOLOGIE ET ETUDE DES ISOTOPES STABLES. USTHB.

LEKOUI, ABDELMALEK, LAOUAR, RABAH, AISSA, DJAMEL-EDDINE, BAGHDAD, ABDELMALEK, BOYCE, ADRIAN J., FALLICK, ANTHONY E. et SEFFARI, ABDERRAOUF, 2018. STABLE S-, O-AND C-ISOTOPE STUDY OF THE BELELEITA SKARNS AND RELATED W-AS-SN-BI-(AU) MINERALIZATION, EDOUGH, NE ALGERIA. Mineral and energy resources. 2018. pp. 73.

LEPRÊTRE, Rémi, LAMOTTE, Dominique Frizon de, COMBIER, Violaine, GIMENO-VIVES, Oriol, MOHN, Geoffroy et ESCHARD, Rémi, 2018. The Tell-Rif orogenic system (Morocco, Algeria, Tunisia) and the structural heritage of the southern Tethys margin. BSGF - Earth Sciences Bulletin. 2018. Vol. 189, n° 2, pp. 10. DOI 10.1051/bsgf/2018009.

LI, Cheng, XIAO, Keyan, SUN, Li, TANG, Rui, DONG, Xuchao, QIAO, Baocheng et XU, Dahong, 2024. CNN-Transformers for mineral prospectivity mapping in the Maodeng–Baiyinchagan area, Southern Great Xing'an Range. Ore Geology Reviews. 1 avril 2024. Vol. 167, pp. 106007. DOI 10.1016/j.oregeorev.2024.106007.

LI, He, LI, Xiaohui, YUAN, Feng, JOWITT, Simon M., ZHANG, Mingming, ZHOU, Jie, ZHOU, Taofa, LI, Xiangling, GE, Can et WU, Bangcai, 2020. Convolutional neural network and transfer learning based mineral prospectivity modeling for geochemical exploration of Au

mineralization within the Guandian–Zhangbaling area, Anhui Province, China. Applied Geochemistry. 1 novembre 2020. Vol. 122, pp. 104747. DOI 10.1016/j.apgeochem.2020.104747.

LI, Hengxiao, SUN, Youzhuang et QIAO, Sibo, 2025. Enhanced lithology identification with few-shot well-logging data using a Confidence-Enhanced Semi-Supervised Meta-Learning Approach. Measurement. 15 avril 2025. Vol. 247, pp. 116762. DOI 10.1016/j.measurement.2025.116762.

LI, Quanke, CHEN, Guoxiong et WANG, Detao, 2024. Mineral Prospectivity Mapping Using Semi-supervised Machine Learning. Mathematical Geosciences [en ligne]. 25 octobre 2024. [Consulté le 3 février 2025]. DOI 10.1007/s11004-024-10161-6. Disponible à l'adresse : https://doi.org/10.1007/s11004-024-10161-6

LI, Shi, CHEN, Jianping et XIANG, Jie, 2020. Applications of deep convolutional neural networks in prospecting prediction based on two-dimensional geological big data. Neural Computing and Applications. 1 avril 2020. Vol. 32, n° 7, pp. 2037-2053. DOI 10.1007/s00521-019-04341-3.

LI, Shi, LIU, Chang et CHEN, Jianping, 2023. Mineral Prospecting Prediction via Transfer Learning Based on Geological Big Data: A Case Study of Huayuan, Hunan, China. Minerals. avril 2023. Vol. 13, n° 4, pp. 504. DOI 10.3390/min13040504.

LI, Tong, ZUO, Renguang, XIONG, Yihui et PENG, Yong, 2021. Random-Drop Data Augmentation of Deep Convolutional Neural Network for Mineral Prospectivity Mapping. Natural Resources Research. 1 février 2021. Vol. 30, n° 1, pp. 27-38. DOI 10.1007/s11053-020-09742-z.

LI, Tongfei, XIA, Qinglin, OUYANG, Yongpeng, ZENG, Runling, LIU, Qiankun et LI, Taotao, 2024. Prospectivity and Uncertainty Analysis of Tungsten Polymetallogenic Mineral Resources in the Nanling Metallogenic Belt, South China: A Comparative Study of AdaBoost, GBDT, and XgBoost Algorithms. Natural Resources Research [en ligne]. 10 avril 2024. [Consulté le 12 mai 2024]. DOI 10.1007/s11053-024-10321-9. Disponible à l'adresse : https://doi.org/10.1007/s11053-024-10321-9

LI, Xiaohui, YUAN, Feng, ZHANG, Mingming, JOWITT, Simon M., ORD, Alison, ZHOU, Taofa et DAI, Wenqiang, 2019. 3D computational simulation-based mineral prospectivity modeling for exploration for concealed Fe–Cu skarn-type mineralization within the Yueshan orefield, Anqing district, Anhui Province, China. Ore Geology Reviews. 1 février 2019. Vol. 105, pp. 1-17. DOI 10.1016/j.oregeorev.2018.12.003.

LIN, Nan, FU, Jiawei, JIANG, Ranzhe, LI, Genjun et YANG, Qian, 2023. Lithological Classification by Hyperspectral Images Based on a Two-Layer XGBoost Model, Combined with a Greedy Algorithm. Remote Sensing. janvier 2023. Vol. 15, n° 15, pp. 3764. DOI 10.3390/rs15153764.

LIN, Qiuyi et ZUO, Renguang, 2024. Domain Adversarial Neural Network for Mapping Mineral Prospectivity. Mathematical Geosciences [en ligne]. 22 novembre 2024. [Consulté le 2 février 2025]. DOI 10.1007/s11004-024-10164-3. Disponible à l'adresse : https://doi.org/10.1007/s11004-024-10164-3

LIU, Chan Chiang, SOUSA JR., Manoel de Araújo et GOPINATH, Tumkur Rajarao, 2000. Regional Structural Analysis by Remote Sensing for Mineral Exploration, Paraiba State, Northeast Brazil. Geocarto International. 1 mars 2000. Vol. 15, n° 1, pp. 70-77. DOI 10.1080/10106040008542142.

LONGLEY, Paul, 2005. Geographic Information Systems and Science. John Wiley & Sons. ISBN 978-0-470-87000-6.

LU, Bingqing, MENG, Xue, DONG, Shanshan, ZHANG, Zekun, LIU, Chao, JIANG, Jiakui, HERRMANN, Hartmut et LI, Xiang, 2023. High-resolution mapping of regional VOCs using the enhanced space-time extreme gradient boosting machine (XGBoost) in Shanghai. Science of The Total Environment. 20 décembre 2023. Vol. 905, pp. 167054. DOI 10.1016/j.scitotenv.2023.167054.

MA, Yao, ZHAO, Jiangnan, SUI, Yu, LIAO, Shili et ZHANG, Zongyao, 2020. Application of Knowledge-Driven Methods for Mineral Prospectivity Mapping of Polymetallic Sulfide Deposits in the Southwest Indian Ridge between 46° and 52°E. Minerals. novembre 2020. Vol. 10, n° 11, pp. 970. DOI 10.3390/min10110970.

MAHDJOUB, Yamina, 1994. Pre-Alpine and Alpine metamorphism and kinematics in the Petite Kbylie massifs (eastern Algeria). Bull Serv Géol Algérie. 1994. Vol. 5, pp. 151-165.

MAHDJOUB, Yamina, CHOUKROUNE, Pierre et KIENAST, Jean-Robert, 1997. Kinematics of a complex Alpine segment; superimposed tectonic and metamorphic events in the Petite Kabylie Massif (northern Algeria). Bulletin de la Société Géologique de France. 1 septembre 1997. Vol. 168, n° 5, pp. 649-661.

MALEKI, Mehdi, NIROOMAND, Shojaeddin, RAJABPOUR, Shahrokh, BEIRANVAND POUR, Amin et EBRAHIMPOUR, Salahadin, 2022. Targeting local orogenic gold mineralisation zones using data-driven evidential belief functions: the Godarsorkh area, Central Iran. All Earth. 31 décembre 2022. Vol. 34, n° 1, pp. 259-278. DOI 10.1080/27669645.2022.2129132.

MARIGNAC, Ch et DJAMEL-EDDINE, Aissa, 2017. Etude des indices et gisements métallifères du massif de l'Edough. [en ligne]. 1 janvier 2017. [Consulté le 25 février 2025]. Disponible à l'adresse : http://depot.umc.edu.dz/handle/123456789/7372

MARIGNAC, Chr. et ZIMMERMANN, J.-L., 1983. Ages K-Ar de l'Événement Hydrothermal et des Intrusions Associées dans le District Minéralisé Miocène d'Aïn-Barbar (Est Constantinois, Algérie). Mineralium Deposita. 1 octobre 1983. Vol. 18, n° 3, pp. 457-467. DOI 10.1007/BF00204490.

MARIGNAC, Christian, AISSA, Djamal-Eddine, CHEILLETZ, A, GASQUET, Dominique et CHEILLETZ, Á, 2016. Edough-Cap de Fer Polymetallic District, Northeast Algeria: II. Metallogenic Evolution of a Late Miocene Metamorphic Core Complex in the Alpine Maghrebide Belt. In : . ISBN 978-3-319-31731-1.

MAURY, René, FOURCADE, Serge, COULON, Christian, EL AZZOUZI, M'hammed, BELLON, Hervé, COUTELLE, Alain, OUABADI, Aziouz, SEMROUD, Belkacem, MEGARTSI, M'hamed, COTTEN, Joseph, BELANTEUR, Ouardia, LOUNI-HACINI,

Amina, PIQUÉ, Alain, CAPDEVILA, Ramon, HERNANDEZ, Jean et RÉHAULT, Jean-Pierre, 2000. Post-collisional Neogene magmatism of the Mediterranean Maghreb margin: a consequence of slab breakoff. Comptes Rendus de l'Académie des Sciences - Series IIA - Earth and Planetary Science. 15 août 2000. Vol. 331, n° 3, pp. 159-173. DOI 10.1016/S1251-8050(00)01406-3.

MCMILLAN, Michael, HABER, Eldad, PETERS, Bas et FOHRING, Jennifer, 2021. Mineral prospectivity mapping using a VNet convolutional neural network. The Leading Edge. 1 février 2021. Vol. 40, n° 2, pp. 99-105. DOI 10.1190/tle40020099.1.

MIAO, Qunfeng, WANG, Pan, ZHAO, Hengqian, LI, Zhibin, QI, Yunfei, MAO, Jihua, LI, Meiyu et TANG, Guanglong, 2024. Mineral Prospectivity Prediction Based on Self-Supervised Contrastive Learning and Geochemical Data: A Case Study of the Gold Deposit in the Malanyu District, Hebei Province, China. Natural Resources Research. 1 août 2024. Vol. 33, n° 4, pp. 1377-1391. DOI 10.1007/s11053-024-10335-3.

MICHARD, André, NEGRO, François, SADDIQI, Omar, BOUYBAOUENE, Mohamed L., CHALOUAN, Ahmed, MONTIGNY, Raymond et GOFFÉ, Bruno, 2006. Pressure–temperature–time constraints on the Maghrebide mountain building: evidence from the Rif–Betic transect (Morocco, Spain), Algerian correlations, and geodynamic implications. Comptes Rendus Geoscience. 1 janvier 2006. Vol. 338, n° 1, pp. 92-114. DOI 10.1016/j.crte.2005.11.011.

MIRZABOZORG, Seyyed Ataollah Agha Seyyed, ABEDI, Maysam et YOUSEFI, Mahyar, 2024. Enhancing training performance of convolutional neural network algorithm through an autoencoder-based unsupervised labeling framework for mineral exploration targeting. Geochemistry. 1 novembre 2024. Vol. 84, n° 4, pp. 126197. DOI 10.1016/j.chemer.2024.126197.

MOHAMMADPOUR, Mahyadin, BAHROUDI, Abbas et ABEDI, Maysam, 2021. Three dimensional mineral prospectivity modeling by evidential belief functions, a case study from Kahang porphyry Cu deposit. Journal of African Earth Sciences. 1 février 2021. Vol. 174, pp. 104098. DOI 10.1016/j.jafrearsci.2020.104098.

MOJADDADI, Hossein, PRADHAN, Biswajeet, NAMPAK, Haleh, AHMAD, Noordin et GHAZALI, Abdul Halim bin, 2017. Ensemble machine-learning-based geospatial approach for flood risk assessment using multi-sensor remote-sensing data and GIS. Geomatics, Natural Hazards and Risk. 15 décembre 2017. Vol. 8, n° 2, pp. 1080-1102. DOI 10.1080/19475705.2017.1294113.

MUSTAFA, Ayyaz, TARIQ, Zeeshan, MAHMOUD, Mohamed, RADWAN, Ahmed E., ABDULRAHEEM, Abdulazeez et ABOUELRESH, Mohamed Omar, 2022. Data-driven machine learning approach to predict mineralogy of organic-rich shales: An example from Qusaiba Shale, Rub' al Khali Basin, Saudi Arabia. Marine and Petroleum Geology. 1 mars 2022. Vol. 137, pp. 105495. DOI 10.1016/j.marpetgeo.2021.105495.

NAJAFI, Ali, KARIMPOUR, Mohammad Hassan et GHADERI, Majid, 2014. Application of fuzzy AHP method to IOCG prospectivity mapping: A case study in Taherabad prospecting area, eastern Iran. International Journal of Applied Earth Observation and Geoinformation. 1 décembre 2014. Vol. 33, pp. 142-154. DOI 10.1016/j.jag.2014.05.003.

NOURI, Reza, AFZAL, Peyman, ARIAN, Mehran, JAFARI, Mohammadreza et FEIZI, Faranak, 2013. RECONNAISSANCE OF COPPER AND GOLD MINERALIZATION USING ANALYTICAL HIERARCHY PROCESS (AHP) IN THE RUDBAR 1:100,000 MAP SHEET, NORTHWEST IRAN. . 2013.

NWAZELIBE, Vincent E., UNIGWE, Chinanu O. et EGBUERI, Johnbosco C., 2023. Integration and comparison of algorithmic weight of evidence and logistic regression in landslide susceptibility mapping of the Orumba North erosion-prone region, Nigeria. Modeling Earth Systems and Environment. 1 mars 2023. Vol. 9, n° 1, pp. 967-986. DOI 10.1007/s40808-022-01549-6.

OGUNGBEMI, Oluwaseun Samuel, OYEBODE, Kazeem, BADMUS, Ganiyu Olabode et OGUNYEMI, Adebayo Tajudeen, 2022. Modeling of structural features from aeromagnetic maps using an improved deep learning technique. Earth Science Informatics. 1 décembre 2022. Vol. 15, n° 4, pp. 2665-2671. DOI 10.1007/s12145-022-00870-z.

OLIVEIRA, Lucas Abreu Blanes de, FREITAS, Gabriel do Nascimento, PESCE, Pedro Barros Cotta et CARNEIRO, Cleyton de Carvalho, 2023. Hybrid mineral model integrating probabilistic and machine learning approaches for the Brazilian pre-salt carbonate reservoirs. Geophysical Prospecting. 22 septembre 2023. Vol. 71, n° 8, pp. 1570-1598. DOI 10.1111/1365-2478.13378.

OONK, Stijn et SPIJKER, Job, 2015. A supervised machine-learning approach towards geochemical predictive modelling in archaeology. Journal of Archaeological Science. 1 juillet 2015. Vol. 59, pp. 80-88. DOI 10.1016/j.jas.2015.04.002.

OTELE, Charlie Gael Atangana, ONABID, Mathias Akong, ASSEMBE, Patrick Stephane et NKENLIFACK, Marcellin, 2021. Updated Lithological Map in the Forest Zone of the Centre, South and East Regions of Cameroon Using Multilayer Perceptron Neural Network and Landsat Images. Journal of Geoscience and Environment Protection. 4 juin 2021. Vol. 9, n° 6, pp. 120-134. DOI 10.4236/gep.2021.96007.

OUABADI, Aziouz, 1994. Petrologie, geochimie et origine des granitoides peralumineux a cordierite (cap bougaroun, beni-touffout et filfila) algerie nord-orientale [en ligne]. These de doctorat. Rennes 1. [Consulté le 2 novembre 2023]. Disponible à l'adresse : https://www.theses.fr/1994REN10182

PENG, Qingming, WANG, Zhongzheng, WANG, Gongwen, ZHANG, Wengao, CHEN, Zhengle et LIU, Xiaoning, 2023. 3D Mineral Prospectivity Mapping from 3D Geological Models Using Return–Risk Analysis and Machine Learning on Imbalance Data. Minerals. novembre 2023. Vol. 13, n° 11, pp. 1384. DOI 10.3390/min13111384.

PERTHUISOT, VINCENT et ROUVIER, HENRI, 1992. Les diapirs du Maghreb central et oriental: des appareils variés, résultats d'une évolution structurale et pétrogénétique complexe. Bulletin de la Société géologique de France. 1992. Vol. 163, n° 6, pp. 751-760.

PEUCAT, J. J., MAHDJOUB, Y. et DRARENI, A., 1996. UPb and RbSr geochronological evidence for late Hercynian tectonic and Alpine overthrusting in Kabylian metamorphic basement massifs (northeastern Algeria). Tectonophysics. 15 juin 1996. Vol. 258, n° 1, pp. 195-213. DOI 10.1016/0040-1951(95)00197-2.

POHL, Walter L., 2022. Metallogenic models as the key to successful exploration — a review and trends. Mineral Economics. 1 décembre 2022. Vol. 35, n° 3, pp. 373-408. DOI 10.1007/s13563-022-00325-3.

POPOV, A., DEBRAND-PASSARD, Serge, BASSETO, D., MAYA, C., BERNUDE, Y. et OFFICE NATIONAL DE LA RECHERCHE GÉOLOGIQUE ET MINIÈRE, 1965. Carte des gîtes minéraux de l'Algérie -ALGER- au 1:500 000. [carte]. Alger, Algérie : Service géologique.

PORWAL, Alok, CARRANZA, E J M et HALE, M, 2003. Artificial Neural Networks for Mineral-Potential Mapping: A Case Study from Aravalli Province, Western India. Natural Resources Research. 2003.

PORWAL, Alok, CARRANZA, Emmanuel John et HALE, M., 2003. Knowledge-Driven and Data-Driven Fuzzy Models for Predictive Mineral Potential Mapping. Natural Resources Research. 1 mars 2003. Vol. 12, n° 1, pp. 1-25. DOI 10.1023/A:1022693220894.

RAHIMI, Elham, SHEKARIAN, Younes, FARAHANI, Salman Mastri, ASGARI, G H Reza et NAKINI, Ali, 2020. New Approach in Application of the AHP–Fuzzy TOPSIS Method in Mineral Potential Mapping of the Natural Bitumen (Gilsonite): A Case Study from the Gilan-e-Gharb Block, the Kermanshah, West of Iran. American Journal of Engineering and Applied Sciences. 2020. Vol. 13, n° 1, pp. 96-110. DOI 10.3844/ajeassp.2020.96.110.

RAHIMI, Nima, KARGARANBAFGHI, Fariba, SHAHID, Mojtaba Rahimi et AFKHAMI, Shima, 2024. Using fuzzy Logic Method and Analytic Hierarchy Process to Mineral Potential Mapping in Janja Exploration Area (South of Nehbandan, Iran). . 2024.

RAOULT, 1969. Relations entre la Dorsale kabyle et les flyschs sur la transversale du Djebel Rhedir: phases tangentielles éocènes, paléogéographie (nord du Constantinois. Algérie). Bulletin de la Société géologique de France. 1969. Vol. 7, n° XI, pp. 523-543.

RAOULT, Jean-François, 1974. Géologie du centre de la chaîne numidique (nord du Constantinois, Algérie). Société géologique de France.

RIGOL-SANCHEZ, J. P., CHICA-OLMO, M. et ABARCA-HERNANDEZ, F., 2003. Artificial neural networks as a tool for mineral potential mapping with GIS. International Journal of Remote Sensing. 1 janvier 2003. Vol. 24, n° 5, pp. 1151-1156. DOI 10.1080/0143116021000031791.

ROCCA, Joseph, 2021. Ensemble methods: bagging, boosting and stacking. Medium [en ligne]. 21 mars 2021. [Consulté le 5 octobre 2023]. Disponible à l'adresse : https://towardsdatascience.com/ensemble-methods-bagging-boosting-and-stacking-c9214a10a205

RODRIGUEZ-GALIANO, GHIMIRE, B., ROGAN, J., CHICA-OLMO, M. et RIGOL-SANCHEZ, J. P., 2012. An assessment of the effectiveness of a random forest classifier for land-cover classification. ISPRS Journal of Photogrammetry and Remote Sensing. 1 janvier 2012. Vol. 67, pp. 93-104. DOI 10.1016/j.isprsjprs.2011.11.002.

ROMAGNY, Adrien, JOLIVET, Laurent, MENANT, Armel, BESSIÈRE, Eloïse, MAILLARD, Agnès, CANVA, Albane, GORINI, Christian et AUGIER, Romain, 2020. Detailed tectonic reconstructions of the Western Mediterranean region for the last 35 Ma, insights on driving mechanisms. Bulletin de la Société Géologique de France. 14 décembre 2020. Vol. 191, n° 1, pp. 37. DOI 10.1051/bsgf/2020040.

ROSENBAUM, Gideon et LISTER, Gordon S., 2004. Neogene and Quaternary rollback evolution of the Tyrrhenian Sea, the Apennines, and the Sicilian Maghrebides. Tectonics [en ligne]. 2004. Vol. 23, n° 1. [Consulté le 4 novembre 2024]. DOI 10.1029/2003TC001518. Disponible à l'adresse : https://onlinelibrary.wiley.com/doi/abs/10.1029/2003TC001518

ROUVIER, H., 1990. Les concentrations polymétalliques liées aux diapirs évaporitiques des confins algéro-tunisiens. Rapport interne EREM, Boumerdes-Algérie, 71p. 1990.

RUBO, Rafael Andrello, DE CARVALHO CARNEIRO, Cleyton, MICHELON, Mateus Fontana et GIORIA, Rafael dos Santos, 2019. Digital petrography: Mineralogy and porosity identification using machine learning algorithms in petrographic thin section images. Journal of Petroleum Science and Engineering. 1 décembre 2019. Vol. 183, pp. 106382. DOI 10.1016/j.petrol.2019.106382.

SAADALLAH, Abdelkader, 1992. Le cristallin de la Grande Kabylie (Algérie): sa place dans la chaîne des Maghrébides. PhD Thesis.

SAATY, Thomas L, 1977. A scaling method for priorities in hierarchical structures. Journal of Mathematical Psychology. 1 juin 1977. Vol. 15, n° 3, pp. 234-281. DOI 10.1016/0022-2496(77)90033-5.

SADAIAPPAN, Balamurugan, BALAKRISHNAN, Preethiya, C.R., Vishal, VIJAYAN, Neethu T., SUBRAMANIAN, Mahendran et GAUNS, Mangesh U., 2023. Applications of Machine Learning in Chemical and Biological Oceanography. ACS Omega. 9 mai 2023. Vol. 8, n° 18, pp. 15831-15853. DOI 10.1021/acsomega.2c06441.

SADEGHI, Martiya, BASTANI, Mehrdad, LUTH, Stefan, MALEHMIR, Alireza, BÄCKSTRÖM, Emma et MARSDEN, Paul, 2019. GIS-based mineral system approach for prospectivity mapping of iron-oxide apatite-bearing mineralisation in Bergslagen, Sweden. . 2019. Vol. 3.

SAHOUR, Hossein, GHOLAMI, Vahid, VAZIFEDAN, Mehdi et SAEEDI, Sirwe, 2021. Machine learning applications for water-induced soil erosion modeling and mapping. Soil and Tillage Research. 1 juillet 2021. Vol. 211, pp. 105032. DOI 10.1016/j.still.2021.105032.

SAMI, Lounis, 2011. Caractérisation géochimique des minéralisations à Pb-Zn, F, Ba, Cu, Fe et Hg des confins Algéro-Tunisiens [en ligne]. Alger. [Consulté le 2 novembre 2023]. Disponible à l'adresse : https://www.ccdz.cerist.dz/admin/notice.php?id=000000000000000040069000000

SANGALLI, Arturo A. L., 1996. Lattices of fuzzy objects. International Journal of Mathematics and Mathematical Sciences. 1996. Vol. 19, n° 4, pp. 970953. DOI 10.1155/S0161171296001056.

SARANATHAN, Arun M. et PARENTE, Mario, 2021. Adversarial feature learning for improved mineral mapping of CRISM data. Icarus. 1 février 2021. Vol. 355, pp. 114107. DOI 10.1016/j.icarus.2020.114107.

SAREMI, Mobin, BAGHERI, Milad, AGHA SEYYED MIRZABOZORG, Seyyed Ataollah, HASSAN, Najmaldin Ezaldin, HOSEINZADE, Zohre, MAGHSOUDI, Abbas, REZANIA, Shahabaldin, RANJBAR, Hojjatollah, ZOHEIR, Basem et BEIRANVAND POUR, Amin, 2024. Evaluation of Deep Isolation Forest (DIF) Algorithm for Mineral Prospectivity Mapping of Polymetallic Deposits. Minerals. octobre 2024. Vol. 14, n° 10, pp. 1015. DOI 10.3390/min14101015.

SATOUH, Adel, 2007. Pètrogèochimie et minèralisaitons des roches magmatiques de la règion de collo (NE-algèrien) [en ligne]. Annaba. [Consulté le 14 décembre 2024]. Disponible à l'adresse : https://www.ccdz.cerist.dz/admin/notice.php?id=000000000000000515190000000

SAVORNIN, Justin, 1920. Etude géologique de la région du Hodna et du plateau sétifien. Ancienne maison bastide-Jourdan, Jules carbonel, imprimeiur-libraire de l ….

SCHAAF, Alexander et BOND, Clare E., 2019. Quantification of uncertainty in 3-D seismic interpretation: implications for deterministic and stochastic geomodeling and machine learning. Solid Earth. 5 juillet 2019. Vol. 10, n° 4, pp. 1049-1061. DOI 10.5194/se-10-1049-2019.

SEFFARI, Abderraouf, ABDALLAH, Nachida, BRUGUIER, Olivier, BOSCH, Delphine, AFALFIZ, Abdehafid, YELLES-CHAOUCHE, AbdelKrim, LEKOUI, Abdelmalek et OUABADI, Aziouz, 2023. Opening of the Algerian Basin: Petrological, geochemical and geochronological constraints from the Yaddene Complex (Lesser Kabylia, Northeastern Algeria). Journal of African Earth Sciences. janvier 2023. Vol. 197, pp. 104783. DOI 10.1016/j.jafrearsci.2022.104783.

SEMROUD, Belkacem, 1993. Caractères pétrologiques des laves miocènes de la région de Béjaïa-Amizour (Algérie). Bulletin du Service Géologique de l'Algérie. 1993. Vol. 4, n° 1, pp. 55-64.

SENANAYAKE, Indishe P., KIEM, Anthony S., HANCOCK, Gregory R., METELKA, Václav, FOLKES, Chris B., BLEVIN, Phillip L. et BUDD, Anthony R., 2023. A Spatial Data-Driven Approach for Mineral Prospectivity Mapping. Remote Sensing. janvier 2023. Vol. 15, n° 16, pp. 4074. DOI 10.3390/rs15164074.

SHABANI, Ali, ZIAII, Mansour, MONFARED, Mehrdad Solimani, SHIRAZY, Adel et SHIRAZI, Aref, 2022. Multi-Dimensional Data Fusion for Mineral Prospectivity Mapping (MPM) Using Fuzzy-AHP Decision-Making Method, Kodegan-Basiran Region, East Iran. Minerals. décembre 2022. Vol. 12, n° 12, pp. 1629. DOI 10.3390/min12121629.

SHAHRIARI, Bobak, SWERSKY, Kevin, WANG, Ziyu, ADAMS, Ryan P. et DE FREITAS, Nando, 2016. Taking the Human Out of the Loop: A Review of Bayesian Optimization. Proceedings of the IEEE. janvier 2016. Vol. 104, n° 1, pp. 148-175. DOI 10.1109/JPROC.2015.2494218.

SHI, Zixian, ZUO, Renguang et ZHOU, Bao, 2023. Deep Reinforcement Learning for Mineral Prospectivity Mapping. Mathematical Geosciences. 1 août 2023. Vol. 55, n° 6, pp. 773-797. DOI 10.1007/s11004-023-10059-9.

SHIN, Hoo-Chang, ROTH, Holger R., GAO, Mingchen, LU, Le, XU, Ziyue, NOGUES, Isabella, YAO, Jianhua, MOLLURA, Daniel et SUMMERS, Ronald M., 2016. Deep Convolutional Neural Networks for Computer-Aided Detection: CNN Architectures, Dataset Characteristics and Transfer Learning. IEEE Transactions on Medical Imaging. mai 2016. Vol. 35, n° 5, pp. 1285-1298. DOI 10.1109/TMI.2016.2528162.

SI, Si, ZHANG, Huan, KEERTHI, S. Sathiya, MAHAJAN, Dhruv, DHILLON, Inderjit S. et HSIEH, Cho-Jui, 2017. Gradient boosted decision trees for high dimensional sparse output. In : International conference on machine learning [en ligne]. PMLR. 2017. pp. 3182-3190. [Consulté le 6 novembre 2023]. Disponible à l'adresse : http://proceedings.mlr.press/v70/si17a.html

SINGH, Rahul Kumar, RAY, D. et SARKAR, B. C., 2018. Recurrent neural network approach to mineral deposit modelling. In : 2018 4th International Conference on Recent Advances in Information Technology (RAIT) [en ligne]. mars 2018. pp. 1-5. [Consulté le 2 février 2025]. Disponible à l'adresse : https://ieeexplore.ieee.org/abstract/document/8389063

SKABAR, A., 2003. Mineral potential mapping using feed-forward neural networks. In : Proceedings of the International Joint Conference on Neural Networks, 2003. [en ligne]. Portland, OR, USA : IEEE. 2003. pp. 1814-1819. [Consulté le 24 avril 2024]. ISBN 978-0-7803-7898-8. Disponible à l'adresse : http://ieeexplore.ieee.org/document/1223683/

SKABAR, Andrew, 2007. Mineral Potential Mapping Using Bayesian Learning for Multilayer Perceptrons. Mathematical Geology. 1 juillet 2007. Vol. 39, n° 5, pp. 439-451. DOI 10.1007/s11004-007-9106-8.

SMITH, A. B. et GARDOLL, S. J., 1997. Structural analysis in mineral exploration using a Geographic Information Systems -adapted stereographic-projection plotting program. Australian Journal of Earth Sciences. août 1997. Vol. 44, n° 4, pp. 445-452. DOI 10.1080/08120099708728325.

SRI SURYANI, P, SIBARONI, Yuliant et HERIAWAN, M. Nur, 2016. SPATIAL ANALYSIS 3D GEOLOGY NICKEL USING ORDINARY KRIGING METHOD. Jurnal Teknologi (Sciences & Engineering) [en ligne]. 18 avril 2016. Vol. 78, n° 5. [Consulté le 27 février 2025]. DOI 10.11113/jt.v78.8340. Disponible à l'adresse : https://journals.utm.my/jurnalteknologi/article/view/8340

STEIGER, James H., 1980. Tests for comparing elements of a correlation matrix. Psychological Bulletin. 1980. Vol. 87, n° 2, pp. 245-251. DOI 10.1037/0033-2909.87.2.245.

SUN, Tao, CHEN, Fei, ZHONG, Lianxiang, LIU, Weiming et WANG, Yun, 2019. GIS-based mineral prospectivity mapping using machine learning methods: A case study from Tongling ore district, eastern China. Ore Geology Reviews. juin 2019. Vol. 109, pp. 26-49. DOI 10.1016/j.oregeorev.2019.04.003.

TAO, Jintao, ZHANG, Nannan, CHANG, Jinyu, CHEN, Li, ZHANG, Hao et CHI, Yujin, 2022. Unlabeled Sample Selection for Mineral Prospectivity Mapping by Semi-supervised Support Vector Machine. Natural Resources Research. 2022. Vol. 31, pp. 2247-2269. DOI 10.1007/s11053-022-10093-0.

TCHOUIKO, D et KROVIAKOV, S, 1974. Rapport sur les travaux géologiques exécutés sur le gisement polymétallique d'Achaïche avec évaluation des réserves (p. 56). 1974.

THIÉBAUT, Jean-Julien, 1951. Étude géologique des terrains métamorphiques de la Grande Kabylie, par Jean Thiébaut... É. Privat.

TIAN, Mi, WANG, Xueqiu, NIE, Lanshi et ZHANG, Chaosheng, 2018. Recognition of geochemical anomalies based on geographically weighted regression: A case study across the boundary areas of China and Mongolia. Journal of Geochemical Exploration. 1 juillet 2018. Vol. 190, pp. 381-389. DOI 10.1016/j.gexplo.2018.04.003.

TIAN, Mi, WANG, Xueqiu, WANG, Qiang, QIAO, Yu, WU, Hui et HU, Qinghai, 2023. Geographically weighted regression (GWR) and Prediction-area (P-A) plot to generate enhanced geochemical signatures for mineral exploration targeting. Applied Geochemistry. 1 mars 2023. Vol. 150, pp. 105590. DOI 10.1016/j.apgeochem.2023.105590.

TOUAHRI, B., 1987. Géochimie et métallogénie des minéralisations à Pb-Zn du Nord de l'Algérie. Th. Doct. Sc. Univ. Paris VI. 1987.

VEARNCOMBE, J. et VEARNCOMBE, S., 1999. The spatial distribution of mineralization; applications of Fry analysis. Economic Geology. 1 juillet 1999. Vol. 94, n° 4, pp. 475-486. DOI 10.2113/gsecongeo.94.4.475.

VILA, 1980. La chaine alpine de l'Algerie orientale et des confins Algero-Tunisiens. These de Doctorat-es-sciences, Universite Pierre et Marie curie [en ligne]. 1980. [Consulté le 5 novembre 2023]. Disponible à l'adresse : https://cir.nii.ac.jp/crid/1570572700876614016

WANG, Gongwen, ZHANG, Shouting, YAN, Changhai, SONG, Yaowu, SUN, Yue, LI, Dong et XU, Fengming, 2011a. Mineral potential targeting and resource assessment based on 3D geological modeling in Luanchuan region, China. Computers & Geosciences. décembre 2011. Vol. 37, n° 12, pp. 1976-1988. DOI 10.1016/j.cageo.2011.05.007.

WANG, Gongwen, ZHANG, Shouting, YAN, Changhai, SONG, Yaowu, SUN, Yue, LI, Dong et XU, Fengming, 2011b. Mineral potential targeting and resource assessment based on 3D geological modeling in Luanchuan region, China. Computers & Geosciences. décembre 2011. Vol. 37, n° 12, pp. 1976-1988. DOI 10.1016/j.cageo.2011.05.007.

WANG, Jian et ZUO, Renguang, 2019. Recognizing geochemical anomalies via stochastic simulation-based local singularity analysis. Journal of Geochemical Exploration. 1 mars 2019. Vol. 198, pp. 29-40. DOI 10.1016/j.gexplo.2018.12.012.

WANG, Jian, ZUO, Renguang et XIONG, Yihui, 2020. Mapping Mineral Prospectivity via Semi-supervised Random Forest. Natural Resources Research. 1 février 2020. Vol. 29, n° 1, pp. 189-202. DOI 10.1007/s11053-019-09510-8.

WANG, Luoqi, YANG, Jie, WU, Sensen, HU, Linshu, GE, Yunzhao et DU, Zhenhong, 2024. Enhancing mineral prospectivity mapping with geospatial artificial intelligence: A geographically neural network-weighted logistic regression approach. International Journal of Applied Earth Observation and Geoinformation. 1 avril 2024. Vol. 128, pp. 103746. DOI 10.1016/j.jag.2024.103746.

WANG, Xueqiu, CHI, Qinghua, LIU, Hongyan, NIE, Lanshi et ZHANG, Bimin, 2007. Wide-spaced sampling for delineation of geochemical provinces in desert terrains, northwestern China. Geochemistry: Exploration, Environment, Analysis. 1 mai 2007. Vol. 7, n° 2, pp. 153-161. DOI 10.1144/1467-7873/07-124.

WANG, Ziye, LI, Tong et ZUO, Renguang, 2024. Leucogranite mapping via convolutional recurrent neural networks and geochemical survey data in the Himalayan orogen. Geoscience Frontiers. 1 janvier 2024. Vol. 15, n° 1, pp. 101715. DOI 10.1016/j.gsf.2023.101715.

WANG, Ziye et ZUO, Renguang, 2022. Mineral prospectivity mapping using a joint singularity-based weighting method and long short-term memory network. Computers & Geosciences. 1 janvier 2022. Vol. 158, pp. 104974. DOI 10.1016/j.cageo.2021.104974.

WANG, Ziye, ZUO, Renguang et ZHANG, Zhenjie, 2015. Spatial analysis of Fe deposits in Fujian Province, China: Implications for mineral exploration. Journal of Earth Science. 1 décembre 2015. Vol. 26, n° 6, pp. 813-820. DOI 10.1007/s12583-015-0597-9.

WEI, Hantao, XIAO, Keyan, SHAO, Yongjun, KONG, Hua, ZHANG, Shuai, WANG, Kun, LI, Qun, CHEN, Binghan, XIANG, Jie et WEN, Chunhua, 2020. Modeling-based mineral system approach to prospectivity mapping of stratabound hydrothermal deposits: A case study of MVT Pb-Zn deposits in the Huayuan area, northwestern Hunan Province, China. Ore Geology Reviews. 1 mai 2020. Vol. 120, pp. 103368. DOI 10.1016/j.oregeorev.2020.103368.

WU, Yixiao, LIU, Bingli, GAO, Yaxin, LI, Cheng, TANG, Rui, KONG, Yunhui, XIE, Miao, LI, Kangning, DAN, Shiyao, QI, Ke, REN, Yufei et WU, Zhuo, 2023. Mineral prospecting mapping with conditional generative adversarial network augmented data. Ore Geology Reviews. décembre 2023. Vol. 163, pp. 105787. DOI 10.1016/j.oregeorev.2023.105787.

WYBORN, L.A.I., HEINRICH, C.A. et JAQUES, A.L., 1994. Australian Proterozoic Mineral Systems: Essential Ingredients and Mappable Criteria: 1994 AusIMM Annual Conference. HALLENSTEIN, C.P. (éd.), Proceedings of the 1994 AusIMM Annual Conference, Darwin, August 1994. 1994. pp. 109-115.

XIANG, Jie, XIAO, Keyan, CARRANZA, Emmanuel John M., CHEN, Jianping et LI, Shi, 2020. 3D Mineral Prospectivity Mapping with Random Forests: A Case Study of Tongling, Anhui, China. Natural Resources Research. 1 février 2020. Vol. 29, n° 1, pp. 395-414. DOI 10.1007/s11053-019-09578-2.

XIAO, Fan, CHEN, Weilin, WANG, Jun et ERTEN, Oktay, 2022. A Hybrid Logistic Regression: Gene Expression Programming Model and Its Application to Mineral Prospectivity Mapping. Natural Resources Research. 1 août 2022. Vol. 31, n° 4, pp. 2041-2064. DOI 10.1007/s11053-021-09918-1.

XIAO, Keyan, XIANG, Jie, FAN, Mingjing et XU, Yang, 2021. 3D Mineral Prospectivity Mapping Based on Deep Metallogenic Prediction Theory: A Case Study of the Lala Copper Mine, Sichuan, China. Journal of Earth Science. 1 avril 2021. Vol. 32, n° 2, pp. 348-357. DOI 10.1007/s12583-021-1437-8.

XIE, Miao, LIU, Bingli, WANG, Lu, LI, Cheng, KONG, Yunhui et TANG, Rui, 2023. Auto encoder generative adversarial networks - based mineral prospectivity mapping in Lhasa area, Tibet. Journal of Geochemical Exploration. 1 décembre 2023. Vol. 255, pp. 107326. DOI 10.1016/j.gexplo.2023.107326.

XU, Yongyang, LI, Zixuan, XIE, Zhong, CAI, Huihui, NIU, Pengfei et LIU, Hui, 2021. Mineral prospectivity mapping by deep learning method in Yawan-Daqiao area, Gansu. Ore Geology Reviews. novembre 2021. Vol. 138, pp. 104316. DOI 10.1016/j.oregeorev.2021.104316.

YANG, Fanfan et ZUO, Renguang, 2024. Geologically Constrained Convolutional Neural Network for Mineral Prospectivity Mapping. Mathematical Geosciences. 1 novembre 2024. Vol. 56, n° 8, pp. 1605-1628. DOI 10.1007/s11004-024-10141-w.

YANG, Na, ZHANG, Zhenkai, YANG, Jianhua et HONG, Zenglin, 2022. Mineral Prospectivity Prediction by Integration of Convolutional Autoencoder Network and Random Forest. Natural Resources Research. 1 juin 2022. Vol. 31, n° 3, pp. 1103-1119. DOI 10.1007/s11053-022-10038-7.

YANG, Na, ZHANG, Zhenkai, YANG, Jianhua, HONG, Zenglin et SHI, Jing, 2021. A Convolutional Neural Network of GoogLeNet Applied in Mineral Prospectivity Prediction Based on Multi-source Geoinformation. Natural Resources Research. 1 décembre 2021. Vol. 30, n° 6, pp. 3905-3923. DOI 10.1007/s11053-021-09934-1.

YIN, Bojun, ZUO, Renguang et SUN, Siquan, 2023. Mineral Prospectivity Mapping Using Deep Self-Attention Model. Natural Resources Research. 1 février 2023. Vol. 32, n° 1, pp. 37-56. DOI 10.1007/s11053-022-10142-8.

YIN, Jiangning et LI, Nan, 2022. Ensemble learning models with a Bayesian optimization algorithm for mineral prospectivity mapping. Ore Geology Reviews. juin 2022. Vol. 145, pp. 104916. DOI 10.1016/j.oregeorev.2022.104916.

YONGLIANG, Chen et WU, W., 2017. Mapping mineral prospectivity by using one-class support vector machine to identify multivariate geological anomalies from digital geological survey data. Australian journal of earth sciences. 2017. Vol. 64, n° 5, pp. 639-651. DOI 10.1080/08120099.2017.1328705.

YOUSEFI, Mahyar, CARRANZA, Emmanuel John M., KREUZER, Oliver P., NYKÄNEN, Vesa, HRONSKY, Jon M.A. et MIHALASKY, Mark J., 2021. Data analysis methods for prospectivity modelling as applied to mineral exploration targeting: State-of-the-art and outlook. Journal of Geochemical Exploration. octobre 2021. Vol. 229, pp. 106839. DOI 10.1016/j.gexplo.2021.106839.

YOUSEFI, Zeynab, ALESHEIKH, Ali Asghar, JAFARI, Ali, TORKTATARI, Sara et SHARIF, Mohammad, 2024. Stacking Ensemble Technique Using Optimized Machine Learning Models with Boruta–XGBoost Feature Selection for Landslide Susceptibility

Mapping: A Case of Kermanshah Province, Iran. Information. novembre 2024. Vol. 15, n° 11, pp. 689. DOI 10.3390/info15110689.

YSBAA, Saadia, HADDOUCHE, Omar, BOUTALEB, Abdelhak et CHEMAM, Madjid, 2020. CARBONATE-HOSTED PB-ZN-FE (CU, F, BA) DEPOSITS OF THE NORTHERN EAST ALGERIA: METALLOGENY, STRUCTURAL AND GRAVIMETRIC /AEROMAGNETIC LINEAMENTS CONTROLS. Algerian Journal of Engineering Architecture and Urbanism [en ligne]. 2020. Vol. 4. Disponible à l'adresse : https://www.semanticscholar.org/paper/CARBONATE-HOSTED-PB-ZN-FE-(CU%2C-F%2C-BA)-DEPOSITS-OF-Ysbaa-Haddouche/a29757ee9421a9e6eba7be9144d6cd0a61e237b6

YSBAA, Saadia, HADDOUCHE, Omar, BOUTALEB, Abdelhak, CHEMAM, Madjid et SADAOUI, Moussa, 2019. Mineral deposits of northeastern Algeria (southern Medjerda mounts and diapiric zone): regional-scale structural controls, spatial distribution, and importance of geophysical lineaments. Arabian Journal of Geosciences. 31 juillet 2019. Vol. 12, n° 15, pp. 482. DOI 10.1007/s12517-019-4611-x.

YSBAA, Saadia, HADDOUCHE, Omar, BOUTALEB, Abdelhak, SAMI, Lounis et KOLLI, Omar, 2021. Mineralization and fluid inclusion characteristics of Pb-Zn-Fe-Ba (Cu, F, Sr) ore-deposits in northern east of Algeria. Arabian Journal of Geosciences. 24 mai 2021. Vol. 14, n° 11, pp. 957. DOI 10.1007/s12517-021-07281-2.

YSBAA, Saadia, NEDJAI, Rachid, HADDOUCHE, O., ABDELHAK, Boutaleb et CHEMAM, Madjid, 2019. Contribution of GIS in Mineral Exploration through Mineralization Distribution Characteri- zation: Application to The Sétifien/Hodna Massifs and The Eastern Saharan Atlas (NE Algeria). Aspects in Mining & Mineral Science. 14 août 2019. Vol. 3. DOI 10.31031/AMMS.2019.03.000556.

ZADEH, L. A., 1965. Fuzzy sets. Information and Control. 1 juin 1965. Vol. 8, n° 3, pp. 338-353. DOI 10.1016/S0019-9958(65)90241-X.

ZHANG, Chunjie et ZUO, Renguang, 2021. Recognition of multivariate geochemical anomalies associated with mineralization using an improved generative adversarial network. Ore Geology Reviews. 1 septembre 2021. Vol. 136, pp. 104264. DOI 10.1016/j.oregeorev.2021.104264.

ZHANG, Nannan et ZHOU, Kefa, 2015. Mineral prospectivity mapping with weights of evidence and fuzzy logic methods. Journal of Intelligent & Fuzzy Systems. 14 novembre 2015. Vol. 29, pp. 2639-2651. DOI 10.3233/IFS-151967.

ZHANG, Quanping, CHEN, Jianping, XU, Hua, JIA, Yule, CHEN, Xuewei, JIA, Zhen et LIU, Hao, 2022. Three-Dimensional Mineral Prospectivity Mapping by XGBoost Modeling: A Case Study of the Lannigou Gold Deposit, China. Natural Resources Research. 1 juin 2022. Vol. 31, n° 3, pp. 1135-1156. DOI 10.1007/s11053-022-10054-7.

ZHANG, Shuai, CARRANZA, Emmanuel John M., WEI, Hantao, XIAO, Keyan, YANG, Fan, XIANG, Jie, ZHANG, Shihong et XU, Yang, 2021. Data-driven Mineral Prospectivity Mapping by Joint Application of Unsupervised Convolutional Auto-encoder Network and

Supervised Convolutional Neural Network. Natural Resources Research. 1 avril 2021. Vol. 30, n° 2, pp. 1011-1031. DOI 10.1007/s11053-020-09789-y.

ZHANG, Shuai, CARRANZA, Emmanuel John M., XIAO, Keyan, WEI, Hantao, YANG, Fan, CHEN, Zhenghui, LI, Nan et XIANG, Jie, 2022. Mineral Prospectivity Mapping based on Isolation Forest and Random Forest: Implication for the Existence of Spatial Signature of Mineralization in Outliers. Natural Resources Research. 1 août 2022. Vol. 31, n° 4, pp. 1981-1999. DOI 10.1007/s11053-021-09872-y.

ZHANG, Zhiqiang, WANG, Gongwen, CARRANZA, Emmanuel John M., ZHANG, JiaoJiao, TAO, Gaoshen, ZENG, Qingdong, SHA, Deming, LI, Dongtao, SHEN, Junfeng et PANG, Zong, 2019. Metallogenic model of the Wulong gold district, China, and associated assessment of exploration criteria based on multi-scale geoscience datasets. Ore Geology Reviews. 1 novembre 2019. Vol. 114, pp. 103138. DOI 10.1016/j.oregeorev.2019.103138.

ZHANG, Zhiqiang, ZHANG, Jiaojiao, WANG, Gongwen, CARRANZA, Emmanuel John M., PANG, Zong et WANG, Hao, 2020. From 2D to 3D Modeling of Mineral Prospectivity Using Multi-source Geoscience Datasets, Wulong Gold District, China. Natural Resources Research. 1 février 2020. Vol. 29, n° 1, pp. 345-364. DOI 10.1007/s11053-020-09614-6.

ZHAO, Chenyi, ZHAO, Jie, WANG, Wenlei, YUAN, Changjiang et TANG, Jie, 2024. A novel hybrid ensemble model for mineral prospectivity prediction: A case study in the Malipo W-Sn mineral district, Yunnan Province, China. Ore Geology Reviews. mai 2024. Vol. 168, pp. 106001. DOI 10.1016/j.oregeorev.2024.106001.

ZHAO, Jie, CHI, Hongqing, SHAO, Yunqing et PENG, Xiaodi, 2022. Application of AdaBoost Algorithms in Fe Mineral Prospectivity Prediction: A Case Study in Hongyuntan–Chilongfeng Mineral District, Xinjiang Province, China. Natural Resources Research. 1 août 2022. Vol. 31, n° 4, pp. 2001-2022. DOI 10.1007/s11053-022-10017-y.

ZHAO, Pengda, 1992. Theories, principles, and methods for the statistical prediction of mineral deposits. Mathematical Geology [en ligne]. 1 août 1992. Vol. 24. [Consulté le 30 novembre 2024]. DOI 10.1007/bf00894226. Disponible à l'adresse : https://discovery.researcher.life/article/theories-principles-and-methods-for-the-statistical-prediction-of-mineral-deposits/e9eeee443122331eaaa192ade563fa39?eos_user_id=4967607&expiry_in_minutes=5&usersource=paperpal&utm_source=paperpal&utm_medium=website&utm_campaign=organic

ZHENG, Dezhi, NI, Chunzhong, ZHANG, Shitao, CHEN, Zhong, ZHONG, Junwei, ZHU, Jun, LI, Yujian et YAN, Yongfeng, 2020. Significance of the spatial point pattern and Fry analysis in mineral exploration. Arabian Journal of Geosciences. septembre 2020. Vol. 13, n° 17, pp. 883. DOI 10.1007/s12517-020-05909-3.

ZHONG, Richen, DENG, Yi et YU, Chang, 2021. Multi-layer perceptron-based tectonic discrimination of basaltic rocks and an application on the Paleoproterozoic Xiong'er volcanic province in the North China Craton. Computers & Geosciences. 1 avril 2021. Vol. 149, pp. 104717. DOI 10.1016/j.cageo.2021.104717.

ZHOU, Kai, SUN, Tao, LIU, Yue, FENG, Mei, TANG, Jialiang, MAO, Luting, PU, Wenbin et HUANG, Junqi, 2023. Prospectivity Mapping of Tungsten Mineralization in Southern Jiangxi Province Using Few-Shot Learning. Minerals. mai 2023. Vol. 13, n° 5, pp. 669. DOI 10.3390/min13050669.

ZIAII, Mansour, POUYAN, Ali A. et ZIAEI, Mahdi, 2009. Neuro-fuzzy modelling in mining geochemistry: Identification of geochemical anomalies. Journal of Geochemical Exploration. 1 janvier 2009. Vol. 100, n° 1, pp. 25-36. DOI 10.1016/j.gexplo.2008.03.004.

ZUO, Renguang et CARRANZA, Emmanuel John M., 2010. Support vector machine: A tool for mapping mineral prospectivity. Computers & Geosciences [en ligne]. 11 novembre 2010. Vol. 37. [Consulté le 30 novembre 2024]. DOI 10.1016/j.cageo.2010.09.014. Disponible à l'adresse : https://discovery.researcher.life/article/support-vector-machine-a-tool-for-mapping-mineral-prospectivity/0a55b5a13a76318cae7916746104a9f2?eos_user_id=4967607&expiry_in_minutes=5&usersource=paperpal&utm_source=paperpal&utm_medium=website&utm_campaign=organic

ZUO, Renguang, KREUZER, Oliver P., WANG, Jian, XIONG, Yihui, ZHANG, Zhenjie et WANG, Ziye, 2021. Uncertainties in GIS-Based Mineral Prospectivity Mapping: Key Types, Potential Impacts and Possible Solutions. Natural Resources Research. octobre 2021. Vol. 30, n° 5, pp. 3059-3079. DOI 10.1007/s11053-021-09871-z.

ZUO, Renguang, LUO, Zijing, XIONG, Yihui et YIN, Bojun, 2022. A Geologically Constrained Variational Autoencoder for Mineral Prospectivity Mapping. Natural Resources Research. 1 juin 2022. Vol. 31, n° 3, pp. 1121-1133. DOI 10.1007/s11053-022-10050-x.